

MASTER OF SCIENCE THESIS

Optimizing the Superbus Public Transport System Through a Life Cycle Assessment

R.C. Caro B.Sc.

June 2013

Faculty of Applied Sciences · Delft University of Technology

Optimizing the Superbus Public Transport System Through a Life Cycle Assessment

MASTER OF SCIENCE THESIS

For obtaining the degree of Master of Science in Sustainable Energy
Technology at Delft University of Technology

R.C. Caro B.Sc.

June 2013



Copyright © R.C. Caro B.Sc.
All rights reserved.

DELFT UNIVERSITY OF TECHNOLOGY
DEPARTMENT OF
WIND ENERGY

The undersigned hereby certify that they have read and recommend to the Faculty of Applied Sciences for acceptance a thesis entitled “**Optimizing the Superbus Public Transport System Through a Life Cycle Assessment**” by **R.C. Caro B.Sc.** in partial fulfillment of the requirements for the degree of **Master of Science**.

Dated: June 2013

Head of department:

Prof.dr. G.J.W. van Bussel

Supervisor:

Ir. J.A. Melkert

Reader:

Dr.ir. J.G. Vogtländer

Summary

Superbus is a new system for sustainable public transport and comprises a vehicle capable of driving at high speeds, a dedicated infrastructure and a demand-driven logistic system. For the Zuiderzeelijn connection between Amsterdam-Schiphol and Groningen, Superbus was found to be superior compared to other high-speed systems with respect to costs, transport value and fitting within the landscape.

Because the Superbus system complies with the main criteria for sustainable mobility, the system is often presented as the sustainable public transport system of the future. However, current research has mainly focussed on the technical challenges, ignoring environmental impacts associated with the complete life cycle of the system. Investigating the possibilities for reducing the environmental impact of the system can be of great value as decisions in the design and development phase highly influence the environmental impacts in the other life cycle stages.

To optimize the Superbus system from an environmental point of view, a life cycle assessment is performed. Although the life cycle assessment is tailored to an evaluation of the impact reduction measures for the Superbus public transport system, many aspects also hold for (electric) transport in general. In the present study, the Superbus system characteristics are assumed to correspond with the Zuiderzeelijn design, i.e. a 39% occupancy rate and a Supertrack velocity of 180 km/h.

First, the contribution of the various life cycle components such as the vehicles, batteries, infrastructure and operational phase to the total environmental impact of the system are determined. It is found that for the current average European electricity mix, the operational and charging phase dominate the results with a total contribution of 76-87% for the different impact methods. In addition, the impact of the batteries and the vehicles range from 7-13% and 4-6% respectively. The infrastructure was found to have a relatively small impact of 2-5% including road maintenance. Interestingly, a shift to electricity from sustainable electricity sources reduces the total impact with 44-76% for photovoltaics and 51-84% for wind energy. In addition, the shift in electricity source brings about a change in the relative importance of the different life cycle components.

The environmental consequences of utilizing alternative powertrain operated on diesel and

compressed natural gas are also investigated. It is found that the electric powertrain has favourable properties with an environmental impact that is 38-92% smaller for diesel and 32-69% smaller for CNG. Remarkably, in spite of the lower CO₂ emissions during CNG combustion, the environmental impact of the CNG powertrain is higher than the impact of the diesel alternative.

To benchmark the performance of the Superbus system, the environmental impact is compared with alternative high-speed transport modes. Compared to the high-speed train and magnetic levitation train, the environmental impact of the Superbus system in terms of carbon footprint is 2 and 2.6 times larger respectively. The difference is mainly caused by the large ratio of $C_D A/S$ for Superbus. In addition, the batteries add a considerable amount of impact.

The effectiveness of the opportunities for environmental impact reduction are highly dependent on the electricity source. Evaluated reduction measures include among others material choice, recycling and regenerative braking. For the current average European electricity mix, a total environmental reduction of 19% can be achieved. The most effective measures are affecting the operational phase and the battery type. The latter has the largest potential with a total achievable reduction of about 8% of the total impact. For electricity from sustainable sources, a total reduction of 28% can be achieved. Especially recycling of the batteries by reusing has large potential. In addition, recycling and reuse of the vehicle components is worth considering as these measures bring about a total environmental impact reduction of 7%.

Acknowledgements

As a student with a natural interest in a broad range of topics, I was very happy with the enthusiastic way Joris Melkert reacted on my research proposal. Not only did Joris give me the opportunity to work on my own research, he also helped me to find the required exam committee and to obtain the necessary input data. Moreover, his constructive feedback has been very inspiring to me in the preceding year.

I would also acknowledge Joost Vogtländer for the support during the various challenges I encountered in my research. His extensive knowledge on the LCA methodology and critical view on the Superbus system helped me to reflect on the chosen approach and research outcomes.

Moreover, I would like to thank Wubbo Ockels and Antonia Terzi for making the Superbus a reality and Gerard van Bussel for taking the time to read my thesis and for taking part in the exam committee.

Finally, I would like to thank my friends and family for the great support they gave me throughout all the years of my study in Delft.

Delft, The Netherlands
June 2013

R.C. Caro

Contents

Summary	v
Acknowledgements	vii
List of Figures	xiv
List of Tables	xv
Nomenclature	xvii
1 Introduction	1
1.1 Superbus system	2
1.2 Sustainable transport	3
2 Problem definition	7
3 Introduction to life cycle assessment	9
3.1 Methodological framework	10
3.2 Approaches for life cycle inventory	11
3.3 Impact methods	12
4 Recent developments in LCA - a literature review	15
4.1 Scope and completeness	15
4.2 Results specific to batteries	17
4.2.1 Requirements for electric vehicles	17
4.2.2 Environmental impacts	18
4.3 Electricity generation, transmission and distribution	20
4.4 Lightweight materials	20
4.5 Infrastructure	22
4.6 Contributions to current body of knowledge	22

5	Methodology	23
5.1	Definition of aim and scope	23
5.2	Life cycle inventory	24
5.3	Impact assessment	25
5.4	Interpretation	26
6	Life cycle assessment Superbus	27
6.1	Superbus vehicle	27
6.1.1	Glider	27
6.1.2	Powertrain	30
6.1.3	Environmental impact electric vehicles	32
6.2	Battery	33
6.3	Infrastructure	36
6.3.1	Dedicated infrastructure: Supertrack	36
6.3.2	Environmental impact of Supertrack	37
6.3.3	Existing infrastructural network	38
6.3.4	Maintenance	41
6.4	Operation	42
6.5	Environmental impact Superbus system	44
6.6	Sensitivity analysis	44
6.6.1	Passenger occupancy	46
6.6.2	Supertrack velocity	47
6.7	Comparison with other studies	48
7	Comparison of powertrain alternatives	51
7.1	Diesel	53
7.1.1	Diesel powertrain	53
7.1.2	Environmental impact diesel vehicles	54
7.1.3	Operational phase	55
7.1.4	Fuelling	55
7.2	Compressed natural gas	56
7.2.1	CNG powertrain	56
7.2.2	Environmental impact CNG vehicles	56
7.2.3	Operational phase	56
7.2.4	Fuelling	57
7.3	Environmental impact powertrain alternatives	57

8	Alternative transport modes	61
8.1	High-speed train	62
8.1.1	Train manufacturing	62
8.1.2	Infrastructure	63
8.1.3	Operation	64
8.2	Magnetic levitation train	66
8.2.1	Train manufacturing	66
8.2.2	Infrastructure	67
8.2.3	Operation	68
8.3	Environmental impact alternative transport modes	68
9	Optimizing the Superbus public transport system	73
9.1	Opportunities vehicle manufacturing	73
9.1.1	Chassis material	73
9.1.2	Recycling	79
9.1.3	Vehicle length	80
9.2	Opportunities batteries	82
9.2.1	Recycling	82
9.2.2	Battery type	83
9.3	Opportunities infrastructure	85
9.4	Opportunities operation	85
9.4.1	Decrease operational energy consumption	85
9.4.2	Regenerative braking	86
9.4.3	Battery swap schedule	89
9.5	Opportunities transport efficiency	90
9.5.1	Supertrack velocity	90
9.6	Summary environmental impact reduction opportunities	93
10	Conclusion and recommendations	95
	References	97
A	Impact database	103
B	Battery specifications	105

List of Figures

1.1	Superbus side view	2
3.1	Schematic representation of a generic life cycle of a product	10
4.1	Summary model environmental performance (I)	16
5.1	Superbus product system	23
5.2	System boundary	25
5.3	Methodology	25
6.1	Vehicle component impact	32
6.2	Average number of commuting trips per person per day	35
6.3	Supertrack cross-section	36
6.4	Supertrack component impact	38
6.5	Schematic speed profile	40
6.6	Tank-to-wheel energy efficiency of electric vehicles	43
6.7	Environmental performance Superbus system	45
6.8	Sensitivity to passenger occupancy	46
6.9	Sensitivity to Supertrack velocity	47
6.10	Summary modal environmental performance (II)	48
7.1	Diesel and CNG vehicle component impact	55
7.2	Environmental performance alternative powertrains	59
8.1	Primary specific energy consumption Thalys	64
8.2	Maglev main infrastructure bodies	68
8.3	Primary specific energy consumption Maglev	69

8.4	Environmental performance alternative transport modes	70
9.1	Design options tree	74
9.2	Thin-walled beam loaded in torsion	75
9.3	Quality factor for torsion and bending scenario	76
9.4	Effect of various lightweight materials on environmental impact chassis . .	77
9.5	Additional CO ₂ emissions due to increased chassis mass	78
9.6	Achievable vehicle recycling credit	80
9.7	Pressure and shear stress distribution Superbus body	80
9.8	Effect of train length on drag coefficient	81
9.9	Decrease in battery capacity as function of cycles number and temperature	83
9.10	Practical specific energy of rechargeable batteries	84
9.11	Sensivity of specific energy battery	85
9.12	Comparison of carbon footprint road top layers	85
9.13	Effect drag coefficient on carbon footprint	86
9.14	Development of drag coefficient	87
9.15	Superbus FBD and KD	87
9.16	Travel distance distribution	89
9.17	Effect of Supertrack velocity	92
9.18	Environmental performance including impact reduction measures	94

List of Tables

4.1	Electric vehicle energy storage requirements	18
4.2	Carbon footprint battery manufacturing	20
6.1	Mass balance Superbus vehicle	28
6.2	Intensity and occurrence of different traffic types	34
6.3	Daily battery (dis)charge cycle	35
6.4	PCE, VKT and distribution of vehicle kilometres by vehicle type	39
6.5	Total road length per road type	40
6.6	Design load comparison of the Supertrack and A13 highway	42
7.1	Alternative fuel properties	52
7.2	Mass balance of diesel and compressed natural gas powertrains	53
8.1	Mass balance of ICE high-speed train	62
8.2	Mass balance high-speed train infrastructure	63
8.3	High-speed train specific energy consumption	65
8.4	Train pre and post transport	67
8.5	CO ₂ emissions of Maglev infrastructure bodies	68
8.6	Superbus, HST and Maglev system characteristics	70
9.1	Physical properties of various lightweight materials	75
9.2	Acceleration/deceleration distance and energy requirements	89
9.3	Superbus trip characteristics	90
9.4	Adapted results of the LMS model for different Supertrack speeds	91
9.5	Overview of achievable system impact reductions	93
A.1	Impact database life cycle assessment data on products and services	104
B.1	SE100AHA battery specifications	105

Nomenclature

Latin Symbols

A	beam cross-sectional area	[m ²]
A	average number of axles per truck	[-]
A_m	mean enclosed area	[m ²]
b	beam width	[m]
C	battery capacity	[Ah]
c	distance of neutral axis to cross-sectional point	[m]
C_B	drag coefficient vehicle tail	[-]
C_D	drag coefficient	[-]
C_i	initial battery capacity	[Ah]
C_{DL}	drag coefficient leading car	[-]
D	transport demand	[-]
D	distribution of VKT along different road types	[%]
d_y	distance from neutral axis to centre cross-sectional area	[m]
h	beam height	[m]
E	elasticity	[-]
E_{batt}	battery energy capacity	[MJ]
$E_{batt,req}$	required battery energy capacity	[MJ]
f	axle load frequency distribution	[%]
$F_{aerodyn.}$	aerodynamic drag	[N]
FE_{diesel}	diesel powertrain fuel economy	[MJ/km]
$FE_{electric}$	electric powertrain fuel economy	[MJ/km]

FE_{gas}	gas powertrain fuel economy	[MJ/km]
F_{motor}	motor force	[N]
$F_{rolling}$	rolling drag	[N]
G	shear modulus	[Pa]
g	gravitational acceleration	[m/s ²]
I	moment of inertia	[m ⁴]
$I_{bending}$	chassis impact bending	[€, kg CO ₂ , MJ, Pts]
$I_{specific}$	specific material impact	[€, kg CO ₂ , MJ, Pts/kg]
$I_{torsion}$	chassis impact torsion	[€, kg CO ₂ , MJ, Pts]
k_l	linear battery capacity constant	[-]
k_p	parabolic battery capacity constant	[-]
L	average axle load	[N]
L	beam length	[m]
l_e	load equivalence factor	[-]
l_L	train leading car length	[m]
l_{seat}	seat length	[m]
l_T	train length	[m]
M	internal moment	[Nm]
m	mass Superbus vehicle	[kg]
$m_{bending}$	beam mass bending	[kg]
m_{empty}	empty vehicle mass	[ton]
$m_{payload}$	payload mass	[ton]
$m_{torsion}$	beam mass torsion	[kg]
N	battery cycle number	[-]
N	number of cities	[-]
n	amount of substance of gas	[mol]
N_{eq}	design load	[-]
$n_{parallel}$	number of cells in parallel	[-]
n_{series}	number of cells in series	[-]
p	pressure	[N/m ²]
$P_{auxiliaries}$	auxiliary power consumption	[W]
$P_{vehicle}$	vehicle power consumption	[W]
Q	cell nominal capacity	[Ah]
$Q_{bending}$	quality factor bending	[-]
$Q_{torsion}$	quality factor torsion	[-]
R	ideal gas constant	[J/molK]
R_{type}	road space	[-]
S	frontal area Superbus vehicle	[m ²]

S	number of seats	[-]
s	length beam circumference	[m]
S_{avg}	average city road length	[m]
S_{tot}	total road length in the Netherlands	[m]
S_{train}	frontal area train	[m ²]
s_{trip}	trip distance	[km]
T	internal torque	[Nm]
t	beam thickness	[m]
t_h	time in one hour	[s]
u	cell float voltage	[V]
V	number of trucks per direction during structural lifetime	[-]
V	tank volume	[m ³]
v	driving velocity	[m/s]

Greek Symbols

θ	angle of twist	[rad]
λ_T	friction coefficient along the train	[-]
μ	friction coefficient	[-]
ρ	material density	[kg/m ³]
ρ_{air}	air density	[kg/m ³]
σ_{allow}	allowable material stress	[N/m ²]
σ_{yield}	yield stress stress	[N/m ²]

Abbreviations

ADP	abiotic depletion potential
BEV	battery electric vehicle
CED	cumulative energy demand
CFRE	carbon fibre reinforced epoxy
CNG	compressed natural gas
DoD	depth of discharge
D	day
EMU	electric multiple unit
EP	evening peak
FBD	free body diagram
FVF	fibre volume fraction

GMT	glass mat thermoplastic
GWP	global warming potential
HC	hydrocarbon
HEV	hybrid electric vehicle
HSL	high-speed train
HSS	high-strength steel
ICE	internal combustion engine
IO-LCA	input/output-LCA
ISO	International Standard Organisation
KD	kinetic diagram
KT	kilometres travelled
LCA	life cycle assessment
LCIA	life cycle impact assessment
LCI	life cycle inventory
LFP	lithium-iron phosphate
LHV	lower heating value
Li-ion	lithium-ion
Li-po	lithium-polymer
LMO	lithium-manganese spinel
LMS	Landelijk Model Systeem
Maglev	magnetic levitation train
MP	morning peak
NCM	lithium-nickel-cobalt-manganese oxide
NiMH	nickel-metal hydride
PCE	passenger car equivalent
PHEV	plug-in hybrid electric vehicle
PKT	passenger-kilometres travelled
PLC	programmable logic component
PM	particulate matter
POS	project objective statement
PVC	polyvinylchloride
RES	road energy system
SMC	sheet moulding compound
SRIM	structural reaction injection moulding
T	through
UCTE	Union for the Co-ordination of Transmission of Electricity
VARTM	vacuum assisted resin transfer moulding
VOC	volatile organic compound

Chapter 1

Introduction

On average, each person in the Netherlands travels about 29 kilometres on daily basis. 74% of this distance is travelled by car (as driver or passenger), 8% by train and 18% by bus, tram, metro, bicycle or by foot [Centraal Bureau voor de Statistiek (CBS), 2011d]. The travelling distance, as well as the ease with which we travel from one place to another, has increased drastically over time. Originally, goods were mainly transported via the extensive water network in the Netherlands using ships. However, the increased need for mobility in the nineteenth century, triggered the search for new means of transport with increased reliability and speed. The railway which was introduced in the Netherlands in 1837 should be placed directly into this perspective. In general, the railway gave people the power over both time and space and enabled mass mobility [van der Woud, 2010]. The railway also redefined the economic, cultural and political relations between cities and regions, i.e. the railway literally induced the development of both social and economic prosperity.

Reliable and fast transport still has an important role in modern society. For example, consider the construction of the Betuweroute which was completed in 2007. This railway was build to enable fast transport of freight from and to the harbour of Rotterdam and Germany. Planbureau [1995] estimated the associated benefits of the Betuweroute in the order of 3.2 - 4.3 billion Euro in twenty years. The Zuiderzeelijn which aimed at facilitating economic development of the northern provinces by enabling fast commuter transport is another example of the important role that transportation might fulfil.

Although the Betuweroute is still subject of an ongoing political discussion and the Zuiderzeelijn was cancelled for several reasons, both examples illustrate that in spite all recent developments in electronic communication, the need for transportation is still present. Moreover, requirements for reliability, speed, quality, energy consumption, sustainability, costs, etc. have become even more important compared to the nineteenth century. Researchers in the field of transportation are therefore continuously in search for new modes of transport that better comply with the current requirements and/or exploring optimization possibilities of existing transport modes. In last decades, this has led to the development of several new modes of transport that are already in use today

or still in development. Well known examples are the high-speed train (HSL) and the magnetic levitation train (Maglev). Another example is Superbus: an innovative public transport system that is currently being developed at the Delft University of Technology.

1.1 Superbus system

Superbus is a new system for sustainable high speed public transport. The system comprises a vehicle which is capable of driving at high speeds, a dedicated infrastructure and a demand driven scheduling system. Due to the unique integration of these three components, Superbus is able to compete with existing high-speed public transport modes and to entice car owners to shift to public transportation [Ministerie van Infrastructuur en Milieu, 2009].

The aerodynamically shaped Superbus is fifteen meters long and provides seating for 23 passengers, see Figure 1.1. The vehicle mass including driver, passengers and luggage, is foreseen to be 10,500 kg and is relatively low compared to similar sized transit buses. At cruising speed, Superbus is envisioned to reach speeds up to 250 km/h on a dedicated infrastructure. To secure safety at these speeds, the vehicle is equipped with a proactive suspension system, driver assisted control, autopilot and advanced measurement and control systems. The power train of Superbus consists of four electric motors which are powered by a lithium-ion battery.



Figure 1.1: Superbus side view with opened top hinging doors. Due to the aerodynamic shape of the vehicle, Superbus' appearance greatly differs from traditional buses seen in dense urban areas.

Superbus is able to drive on existing roads to collect passengers with similar destination. This demand-driven scheduling is very different compared to the more traditional supply-driven scheduling and offers higher service levels and quality and reduces overall travel time. The logistic system of Superbus incorporates the advantages of both a taxi and a high-speed train. Once all passengers are collected or all seats are occupied, Superbus enters its dedicated infrastructure. Once the vehicle is close to its destination, it exits the dedicated infrastructure and seamlessly integrates with the existing roads. Subsequently, all passengers are dropped off at their preferred destination.

The Superbus system was first investigated during the Structuurvisie Zuiderzeelijn. This research aimed at investigating the usefulness and necessity of the Zuiderzee connection between Amsterdam and Groningen. In the Structuurvisie, Superbus was compared with three alternatives for a fast connection between the economically developed west and the less developed northern provinces. The alternatives included a normal railway, a high-speed train and a magnetic levitation train. Moreover, the public transit alternatives were compared with region-specific investments for stimulating the immature economic situation in the North.

Although region-specific investments were found to be more effective for this specific situation, Superbus was proven to be superior compared to its competitors with respect to cost-benefits ratio, placement within the landscape and transport value. For this reason, the Dutch cabinet positively assessed the Superbus as an innovative concept for future mass transit in the Netherlands and as a possible export product and decided to invest in a research and development trajectory for further development of the concept [Ministerie van Infrastructuur en Milieu, 2009]. At the moment of writing, the first prototype of Superbus has been built and the first test runs have been completed. The current phase of development is characterized by the possibilities to improve the concept using new insights obtained by research results and tests.

1.2 Sustainable transport

The above elaboration illustrates that transportation is essential in our society. Superbus is designed to comply with the high requirements imposed on modern high-speed transport, i.e. Superbus is not only able to deliver the same service, it can also entice people to make use of sustainable mobility [Ministerie van Infrastructuur en Milieu, 2009]. With sustainable mobility, one refers to the ability to meet the needs of society to move freely, gain access, communicate, trade and establish relationships without sacrificing essential human or ecological values today or in the future [Dr. Ing. A. Terzi, 2010]. The main criteria for sustainable mobility include:

- Fossil fuel independent;
- High well-to-wheel efficiency;
- Low vehicle weight;
- High safety and reliability;
- Efficient use of resources (i.e. high occupancy rates);
- Infrastructure with low environmental impact.

The transition to sustainable mobility is induced by the increasing awareness for sustainability in a broader sense and is reflected in the continuous efforts of politicians and scientists to support sustainable development via funding bodies for market incentives and technological developments. The subsidies for the research and the construction of the prototype of Superbus is a direct consequence.

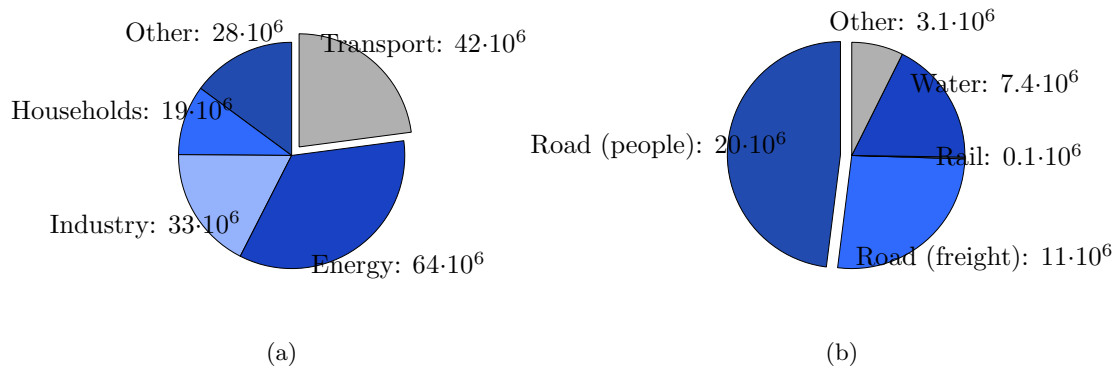


Figure 1.2: Dutch annual CO₂ emissions by sector (left) and mode of transport (right) for 2011 in tons CO₂ [Centraal Bureau voor de Statistiek (CBS), 2011c].

It is important to involve the transport sector in the pursuit of a more sustainable way of living as many environmental impacts are strongly linked to the energy consumption processes associated with transportation.

The necessity of reducing the ecological footprint and energy consumption of our public transport modes are reflected in the statistics on energy use and environmental harmful emissions of the sector. On annual basis, transport accounts for an energy consumption of about 15% of the total annual energy consumption in the Netherlands [Centraal Bureau voor de Statistiek (CBS), 2011a]. Moreover, transportation produces 42 million tons of carbon dioxide on annual basis: equal to 23% of the total Dutch annual CO₂ emissions [Centraal Bureau voor de Statistiek (CBS), 2011c].

A large part of the CO₂ emissions of transportation are directly related to passenger road traffic, see Figure 1.2b. The actual amount of emissions are however even higher because the emissions associated with vehicle production, infrastructure provision and fuel production are not included in the sector 'Transport', but in 'Energy' and 'Industry' in Figure 1.2a. For example, the emissions for railway transport are relatively small compared to road traffic and water because the CO₂ emissions caused by electricity production are not included in this figure. Hence, the real contribution of transportation to the total CO₂ emissions is even larger than shown in Figure 1.2.

Appropriately mitigating the impacts from transportation through a reduction in resource consumption and emissions requires an analysis of the energy consumption and associated emissions during the production, operation and depreciation of each mode. An analysis of this type is called a life cycle assessment (LCA) because the complete life cycle of a product is elaborated. Scientists have developed a complete methodological framework for performing LCAs.

The environmental impacts of the Superbus life cycle consist of the extraction of raw materials, manufacturing, operation and depreciation is yet unclear. Hence, this thesis focuses specifically on a LCA of Superbus. The assessment is used to improve the Superbus system as decisions in the design and development phase highly influence the environmental impacts in the other life cycle stages. The main goal of the present study is to optimize the design of the Superbus public transport system through a life cycle assessment, see Chapter 2.

The outline of this thesis report is as follows. Chapter 2 elaborates the problem definition and defines the research (sub)question(s). The general theory on LCA and a literature review is given in Chapter 3 and 4 respectively. Consequently, Chapter 5 describes the applied methodology. In Chapter 6, a life cycle assessment of the Superbus system is carried out, followed by a comparison of alternative powertrains in Chapter 7. The environmental impact of Superbus is compared with competing modes of transport in Chapter 8. The Superbus transport system is optimized in Chapter 9, followed by the conclusion and recommendations in Chapter 10.

Chapter 2

Problem definition

From the introduction it became clear that transport nowadays involves more than an easy means for transporting as much people as possible. Due to the growing pressure on the earth's natural systems and resources that arise from an increased demand for goods and services, sustainable (public) transport has become more and more important. Superbus is designed to meet the demand for a sustainable, high-speed public transport system with short pre- and aft transport. The present study will investigate whether Superbus can live up to this goal. This chapter elaborates the research question(s) in more detail and also defines the project objective statement (POS).

The main research question of this thesis is defined as:

Through which design changes can the environmental impact of the Superbus public transport system be reduced?

This research question is answered using the following four sub-questions:

1. How can the environmental impact of the Superbus public transport system be determined and quantified?
2. What is the environmental impact of the Superbus public transport system and what is the contribution of the different life cycle components?
3. How does the environmental impact of the Superbus public transport system compare to alternative high-speed systems?
4. How does the electrical powertrain compare to alternative powertrains utilizing natural gas or diesel?

The project objective statement of this thesis is defined as:

Optimise the design of the Superbus public transport system through a life cycle assessment within nine months and by one master student

Introduction to life cycle assessment

In sustainable development, it is important to identify the opportunities for reduction of resource consumption and pollution prevention. An evaluation of these opportunities requires a methodological framework or, as stated by [Rebitzer et al. \[2004\]](#): "sustainable development requires methods and tools to help quantify and compare the environmental impacts of providing goods and services ("products") to our society".

A powerful tool is life cycle assessment because it provides a framework to estimate and assess the environmental impacts associated with the life cycle of a product. The results of a life cycle assessment are considered as a measure for the sustainability of a product and can contribute to underpin statements regarding sustainability. According to the International Standard Organisation (ISO), life cycle assessment is a "compilation and evaluation of the inputs and outputs and the potential environmental impacts of a product system throughout its life cycle" [[Guinee et al.](#)]. Here, a product system is the collection of small portions of the product that are connected by flows of intermediate products. These small portions are called unit processes in LCA. Moreover, 'life cycle' refers to the 'life' of the product system. This life covers resource extraction, material production, material processing and use of the product, to waste processing of the discarded product. A schematic overview of the life cycle of a product can be seen in [Figure 3.1](#).

The starting point of a life cycle assessment is to define the function that is fulfilled by the product system. In LCA, this function is referred to as the functional unit and is used as the important basis that enables the comparison and analysis of different products. The functional unit needs to be defined from an aggregated point of view because the function can involve material products that are closely related to the potential function they fulfil. For example, the product 'bus' is equivalent to the function 'transport X people from A to B'. However, the bus only embodies part of that function because other products like gasoline and a road are also required. Moreover, the bus itself is produced from certain materials, as well as ancillary goods (electricity, etc.) and capital goods (factories, etc.). The environmental impact of several orders of these upstream products should therefore be included in the analysis.

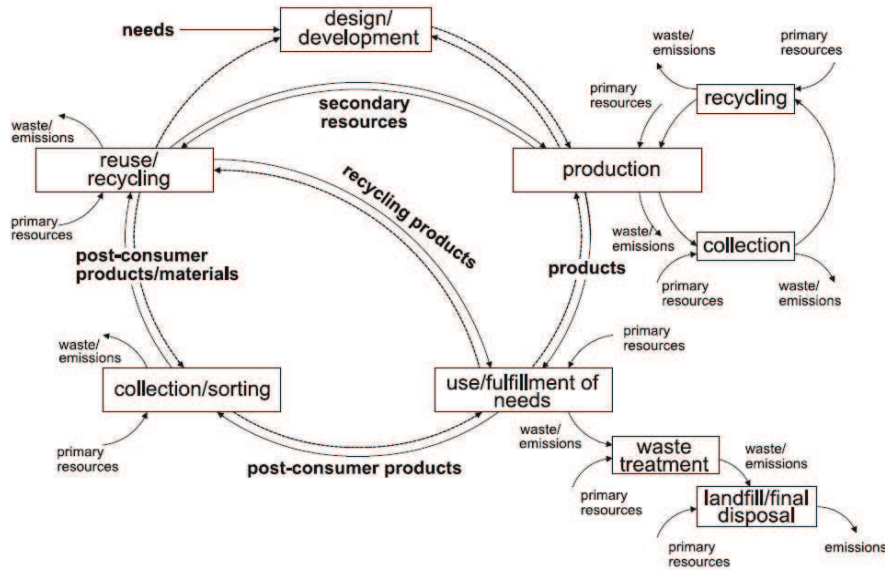


Figure 3.1: Schematic representation of a generic life cycle of a product [Rebitzer et al., 2000].

The methodological framework of life cycle assessment is elaborated in this chapter. The first section provides an overview of the different phases that should be completed in a LCA. In the second section, process based LCA and input-output LCA is elaborated. The last section will discuss how the impact for several impact methods is obtained from the category indicators.

3.1 Methodological framework

The ISO has established a methodological framework that distinguishes three phases in a LCA: goal and scope definition, inventory analysis and impact assessment. In addition, the ISO states that interpretation should take place throughout the LCA. A brief description of these phases is given below.

Goal and scope definition

The goal and scope definition provides a description of the product system and associated boundaries and functional unit. Moreover, it includes a definition of the impact categories that are assessed during the LCA. The system boundaries are chosen such that only those components having a clear contribution to the environmental performance of the product are evaluated. For example, an environmental comparison of internal combustion engine cars and electric vehicles comes down to an evaluation of the differences between the powertrains and operational phase. The supporting structure (chassis, wheels, etc.) can thus be excluded from the analysis. The product system and system boundaries are displayed using a process tree. The system boundaries of the Superbus transport system can be seen in Figure 5.2.

The functional unit defines with respect to which property a product system is analysed. Usually, the functional unit is related to the service that is provided by the product(s). For example, alternative types of public transport may be compared on the basis of the number of kilometres travelled, the amount of passengers transported or on the basis of the amount of passenger-kilometres.

Inventory analysis

The most critical step in a LCA is the life cycle inventory analysis (LCI). During the LCI, the resource use, waste flows and emissions that are caused by the product system are determined. Generally, the inventory analysis is considered as the most time consuming because the analysis aims at obtaining a comprehensive model of the product system. This model is a static simulation model composed of unit processes that each represent one or several activities, such as production processes, transport or retail. The unit processes are the 'building blocks' of the product system. All flows within the economic system and the environmental interventions should be recorded for each unit process.

Overall, the challenges that may arise during this phase include little or no previous experience of the LCA practitioner or the owner of the product/service, lack of measurement points, and companies refusing to share data because an inventory analysis is often considered as the 'environmental parallel' to a cost statement. Because the choices and assumptions made in the inventory analysis influence the outcomes to a large extent, they should be accurately tracked and recorded.

Impact assessment

During the life cycle impact assessment (LCIA), the product system is evaluated in terms of several impact categories. For example, a product system can be evaluated in terms of its contribution to climate change by considering the amount of carbon dioxide that is emitted or in terms of the energy that consumed during the life cycle of the product system. Indicators for each impact category can be calculated using Equation 3.1.

$$\text{Category indicator} = \sum \text{Characterisation Factor}(s) \cdot \text{Inventory Data} \quad (3.1)$$

The inventory data resembles the amount of 'flow' per functional unit, i.e. kg of material or MJ of energy per functional unit. The characterisation factors express the contribution of a certain amount of flow to an impact category. For example, the CO₂ and CH₄ emissions both contribute to the category 'climate change'. As such, the characterisation factors of both substances determines their relative importance to this category. Characterisation factors can be readily obtained from databases. The outcome of the impact assessment is the environmental impact of the system aggregated in the different impact categories.

3.2 Approaches for life cycle inventory

As was stated in the previous section, the inventory analysis is the most critical step during a LCA. In general, three different ways of modelling the product system can be

used, namely 1) process oriented modelling, 2) economic input-output modelling and 3) a combination of both approaches. A brief summary of the first two modelling approaches is given below. Moreover, it is discussed which approach should be used for which situation.

During process based LCA, the product system is evaluated in terms of unit processes. Because the product system can be broken into a very large number of unit processes, this approach is characterised by a high level of detail. A good overview of the product system is required to ensure that all important processes are included in the evaluation. If the contribution of certain processes is only little, the process is said to be cut-off and excluded from the inventory analysis.

Input-output-LCA (IO-LCA) is based on the impact intensity of different economic sectors in a country (e.g. the Netherlands). The impact intensity is obtained by combining economic input-output matrices which describe the amount of money that each industrial sector spends on its commodities with impact data of the same economic sectors. The environmental impact of a product system with value X is obtained by multiplying the value with the impact intensity of the economic sector. The main advantage of IO-LCA is the overall comprehensiveness of the modelled product system. However, the level of detail provided by IO-LCA is limited and the approach is therefore only suitable for questions where the overall environmental impact of a system are the focus.

Specific comparisons within one industrial sector can usually not be answered by the IO-LCA approach. In general, process analysis is used to assess an atypical product system that cannot be represented by an aggregated industry sector and thus requires process-specific data [Rebitzer et al., 2004].

3.3 Impact methods

As was elaborated in Section 3.1, the performance of a product system is determined on the basis of several impact categories, for example acidification, eutrophication, land use and climate change. Most product systems contribute to these different effects in a variety of ways.

An optional step in LCA is to quantify the relative importance of the various impact categories, or midpoint indicators. If weights are assigned to the impact categories, the impact scores can be multiplied with the weight and added to give an impact score at endpoint level. These endpoint impacts are easier to interpret and may even be combined to form a single impact score.

The primary objective of weighing is to transform the long list of inventory results into a small number of impact categories at endpoint level, for example human health, material depletion and biodiversity. Different methods are developed to weigh the environmental effects in LCAs. Some include single issue methods like the carbon footprint and cumulative energy demand (CED). Both methods have received a lot of attention due to the increasing awareness for global warming. Other methods include a weighing based on prevention costs or the ReCiPe method. In the present study, the environmental impact of Superbus is determined using four different methods. The weighed impact of all materials and processes used in this study, are tabulated in Table A.1. All methods will be shortly introduced below.

Carbon footprint

The carbon footprint is a single issue method that utilizes the amount of emitted carbon dioxide during the life cycle of a product as a measure for the environmental performance. Because of the well known effects of carbon dioxide on global warming, the carbon footprint is used in many studies. However, although the carbon footprint can be used to reduce the amount of greenhouse gas emission during a life cycle, the method is too restricted when it is used as a proxy for the environmental impact of a product where other impacts are non-negligible.

Cumulative energy demand

The cumulative energy demand of a product system is the total energy that is consumed during the life cycle of the system. Because the CED is based on a statistical correlation between the energy consumption of a process and corresponding impact categories, it remains uncertain whether the CED is a real indicator of impact categories that are not related to energy. The CED should therefore be considered as an overall measure of depletion of fossil fuels and climate change or as a first indicator of the environmental impact of products where land use is not important.

Eco-costs

The eco-costs of a product is a measure of the environmental burden that is caused by the product life cycle and is based on the prevention measures that are required to bring back the environmental burden to a sustainable level by either end of pipe measures or by system integrated solutions. The total eco-costs is the sum of the prevention costs of toxic emissions, materials depletion and energy consumption.

ReCiPe

The ReCiPe method uses an environmental mechanism as the basis for the weighing. This environmental mechanism should be seen as a series of effects that together create a certain level of damage to for instance, human health or ecosystems. The ReCiPe method provides both robust midpoints and more uncertain endpoints. In the present study, these endpoint are aggregated into a single impact score.

Overall, LCA studies on transportation most often use the carbon footprint and cumulative energy demand methods as they grasp the most essential environmental interactions associated with transportation. In the present study, all the above described methods will be used to verify whether this also holds true for the Superbus system.

Recent developments in LCA - a literature review

The increasing concerns for global warming and depleting oil reserves, caused a large and active group of researchers to work on the transition to sustainable mobility. The research that is carried out in this perspective, aims at a broad spectrum of topics ranging from the development of a hydrogen fuel infrastructure to improving battery characteristics and reducing mass and drag of vehicles.

This chapter provides a review of recent developments of LCA in relation to sustainable mobility and also benchmarks industries best practice. Moreover, this chapter provides a statement about what this master thesis is adding to the current body of knowledge.

Many LCA studies deal with a large variety of topics related to the technical, social and environmental aspects of sustainable mobility. Because of the broad range of topics, and because not all aspects are equally important to the present study, the study is limited to a discussion about batteries, lightweight materials, electricity generation and infrastructural considerations.

The outline of this chapter is as follows. In the Section 4.1, the scope and completeness of the literature is elaborated. The environmental results specific to batteries are elaborated in Section 4.2. Sections 4.3 and Section 4.4 are about the impacts of electricity generation and lightweight materials. The chapter is concluded with the environmental effects of the infrastructure and, finally, a statement about what this master thesis is adding to the current body of knowledge.

4.1 Scope and completeness

Most LCA studies have originally focused on passenger cars as they dominate the passenger transport market. Especially hybrid electric vehicles have been studied in many different forms [Hawkins et al., 2012a].

A comprehensive analysis of the environmental performance of road, rail and air transport modes in the United States is performed by Chester [2008]. An overview of the main conclusions of his dissertation can be found in Figure 4.1. The figure shows the carbon footprint of various transport modes for stated occupancy rates. The results were published in two articles [Chester and Horvath, 2009a, 2010] and supplemented with a working paper with additional findings and a related publication [Chester and Horvath, 2009b, Chester et al., 2010].

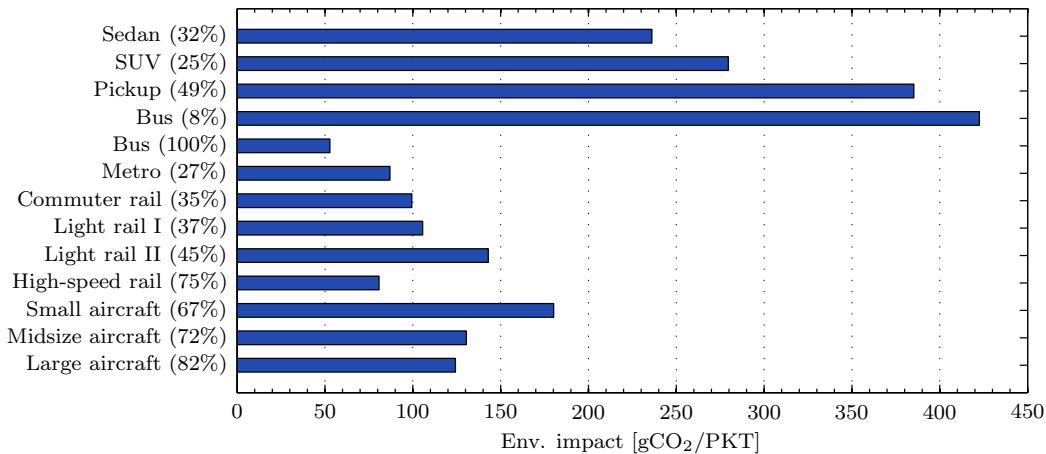


Figure 4.1: Summary modal environmental performance [Chester, 2008].

A second study of interest is Hawkins et al. [2012b]. Hawkins et al. [2012b] compared the environmental performance of conventional and electric vehicles after performing an extensive literature study [Hawkins et al., 2012a].

Other studies are McKenzie and Durango-Cohen [2012] about the environmental impacts of transit buses with alternative fuel technology, Ally and Pryor [2007] who assessed the life-cycle of diesel, natural gas and hydrogen fuel cell buses and Cooney [2011] who compared the environmental burden of diesel and electric public transportation buses.

The functional units of preceding studies are defined as kilometres travelled (KT) during vehicle lifetime or passenger-kilometres travelled (PKT) during vehicle lifetime. The latter also normalizes the results with respect to the passenger occupancy, an important variable during the LCA of passenger transportation [Chester and Horvath, 2009a].

Although Chester [2008] used broad systems boundaries by evaluating the construction, operation, maintenance and insurance of the vehicle and the infrastructure required for road and fuel, large variations are observed in the boundaries applied in literature. The operational phase of each mode has been assessed predominantly, usually by assuming an average consumption per distance travelled. More recent studies include the fuel infrastructure and Chester and Horvath [2009a] emphasizes the importance of also including the road infrastructure. The end-of-life phase is usually omitted during most LCAs. Chester and Horvath [2009a], Schmidt et al. [2004] argue that this phase is not expected to have a large contribution to the total inventory. Moreover, evaluating the waste management options and material reuse is considered as a difficult matter. As such, literature results

indicate a conservative scenario as recycling of materials cause a decrease in environmental impact.

In terms of impact categories, the most popular for quantifying the environmental impact is, either CO₂ and/or GWP. NO_x emissions are the second most reported, followed by CO. SO₂, PM, N₂O, HC, VOC and CH₄ emissions are assessed less frequently. Energy use is most popular regarding the consumption of resources [Hawkins et al., 2012a].

The majority of studies apply a hybrid approach combining IO-LCA and process based LCA. Specifically, IO-LCA is used for the manufacturing stage of the vehicle and the construction of the supporting fuel and road infrastructure. Process based LCA is used most often for the operational phase and, if included, the end-of-life phases.

The aggregated nature of IO-LCA causes difficulties to place products in appropriate economic sectors. For example, Chester [2008], Cooney [2011] assume the production of a bus to match the 'Heavy Duty Truck Manufacturing', whereas McKenzie and Durango-Cohen [2012] assume a model where manufacturing of a bus is composed of 'Motor Vehicle Body Manufacturing' and 'Motor Vehicle Parts Manufacturing'. These inconsistencies, combined with the revolutionary character of Superbus, raises questions about the applicability of IO-LCA for assessing the environmental impact of Superbus.

4.2 Results specific to batteries

The batteries are an important component as they provide the energy for the propulsion of the vehicle. The implications of the batteries for the environmental impact of electric vehicles are elaborated in this section. The review is based on the results of three studies that currently provide the most complete LCIs of batteries [Hawkins et al., 2012a].

4.2.1 Requirements for electric vehicles

Previously, electric vehicles were equipped with lead-acid, nickel-metal hydride (NiMH), or sodium-nickel-chloride batteries. New electric cars typically use lithium-ion (Li-ion) batteries because they offer a high power and energy density, require little maintenance, are not affected by memory effect, have only little self-discharge and no scheduled cycling is required to prolong the cycle life [Notter et al., 2010]. The preferred battery technology is prescribed by the requirements for energy and power density of HEVs, PHEVs and BEVs. While batteries in HEVs are mostly used to enhance vehicle performance and therefore require higher power densities, PHEVs and BEVs use batteries as their primary energy source and require optimal energy densities [Majeau-Bettez et al., 2011]. The requirement differences that exist for the electric vehicle types is shown in Table 4.1.

Li-ion batteries comprise a family of battery chemistries that employ various combinations of anode and cathode materials. The general working principle of batteries is based on the difference in electrochemical potential of the reactions taking place at the anode and cathode materials. The chemistries for Li-ion as well as lithium-polymer (Li-po) batteries that are most mature and receive the most attention among developers are lithium-nickel-cobalt-manganese oxide (NCM), lithium-manganese spinel (LMO), and lithium-iron phosphate (LFP) [Notter et al., 2010, Majeau-Bettez et al., 2011, A.Dinger et al.,

Table 4.1: Electric vehicle energy storage requirements [Kalhammer et al., 2007].

Type	Power density [W/kg]	Energy density [Wh/kg]	Cycles [-]
HEV	800-1200	30-60	n/a
PHEV	540-400	50-75	2300-2400
BEV	200-400	100-160	1000

2010]. Superbus is equipped with a Li-ion battery pack based on a LiFePO₄ chemistry. Notter et al. [2010] concluded that the effects of the different active materials in Li-ion batteries on the environmental performance can be neglected in a general LCA.

The shift to battery-powered vehicles like Superbus, largely depends on the way current limiting factors related to driving range, cycle life and charging time are solved. Although Li-ion batteries offer the highest energy densities of all battery technologies currently available, the driving range of electric vehicles is still relatively small. Moreover, the battery packs cause a reduction in passenger and cargo space [Chan, 2007]. The issue of limited driving range is enhanced by long charging, i.e. refuelling, times of the batteries, especially compared to ICE vehicles. Efforts to enable fast charging of batteries shows potential but still requires much research. The battery swap stations of Better Place are developed to overcome the problem of battery charging by replacing depleted batteries using an automated mechanical system. The stations are able to replace the battery in less than five minutes [Better Place, 2012]. At the time of writing, however, this part of Better Place was declared bankrupt.

Cycle life refers to the ability of batteries to handle large amounts of charge-discharge cycles as batteries deteriorate due to the cumulative changes of the structure and composition of the key battery cell components. The number of required cycles for a 80% depth of discharge (DoD) for HEVs, PHEVs and BEVs is shown in Table 4.1. The indicated cycle life is developed from analysing representative vehicle driving patterns. From this input, the required number of 80% discharge cycles are calculated by dividing the required total electric energy over the vehicle lifetime by the battery capacity (i.e. 80% of total capacity). The current status of Li-ion cell and battery technology indicate that more than 3000 deep cycles can be achieved [Kalhammer et al., 2007].

4.2.2 Environmental impacts

The environmental impacts of batteries are the result of manufacturing, use and recycling. The life cycle impacts during manufacturing are caused by the construction of the different components of the battery, i.e. cathode, anode, electrolyte, separator, cell packaging and electronics. Moreover, module and battery assembly, as well as transport of raw materials to the cell manufacturer, transport of the cell to the battery manufacturer and transport of the battery to the car assembly plants should also be considered. The use phase of the battery comprises the electricity losses in the battery during the lifetime use of the battery in the vehicle and the extra energy needed to carry the mass of the battery. This

way of modelling the use phase of the battery has been used in several LCAs [Matheys et al., 2008].

Notter et al. [2010] evaluated the environmental impacts of LMO batteries and compared his results with the total impacts of an electric vehicle. The results indicated that the environmental impact caused by the battery is between 7% (CED) and 15% (ReCiPe) of the total vehicle impact. Moreover, it was found that the production of the Li-ion battery itself is dominated by the production of the anode, cathode, and the battery pack. The anode was found to have the highest impact for ReCiPe, while CED, GWP and ADP show the highest impact for the production of the cathode (between 28-36%). The latter is mainly caused by the collector which is made from aluminium. The production of the battery pack accounted for a relatively large share of more than 20%.

Preceding results are in accordance with those presented by Majeau-Bettez et al. [2011] who focused on the environmental impacts of NiMH, NCM and LFP batteries. The impacts were expressed in terms of thirteen midpoint categories. In the study, it was shown that the production of the cathode is responsible for more than 35% of the Li-ion GWP impacts. Moreover, the polytetrafluorethylene binder in the electrode is responsible for more than 97% of the ozone depletion along with 14-15% of the GWP. The influence of the binder was also demonstrated by Notter et al. [2010]. The results of Majeau-Bettez et al. [2011] also show that the electronic components for the battery management system have non-negligible contributions in all impact categories.

The environmental impacts of the battery components were also assessed by Zackrisson et al. [2010]. However, since the impacts as a consequence of the energy consumption during manufacturing are not part of the impacts of each component, comparing the results is not possible. For example, the production of the cathode accounts for only 10% of the GWP. The general conclusions of Zackrisson et al. [2010] are however very consistent with Notter et al. [2010] and Majeau-Bettez et al. [2011], i.e. the most dominating sources of global warming impacts results from battery manufacturing, electronics and the cathode. Especially the electronic components at both module and cell level add 30% to the total GWP of the battery. Moreover, because a transport-dependent battery industry was assumed, the transportation of raw materials and components was found to be responsible for 3% of the total CO₂ emissions.

From literature, it can be concluded that there is a general consensus about the influence of the different battery components on the environmental impact of batteries. The differences in total environmental impact shown in Table 4.2 are the result of system boundary differences and estimations of material and energy use. For example, the estimates for manufacturing energy requirements in Notter et al. [2010] and Majeau-Bettez et al. [2011] cause the impacts of Majeau-Bettez et al. [2011] to be 3.6 times higher [Majeau-Bettez et al., 2011]. Moreover, a key source of variability is battery lifetime [Hawkins et al., 2012a].

The system boundary of all studies does not include the end-of-life phase of the battery. The results therefore represent a worst case scenario, as no benefits were derived from the recycling potential or possibilities for a second-life use as stationary electric storage.

Table 4.2: Carbon footprint battery manufacturing.

Source	Carbon footprint [kg CO ₂]
[Zackrisson et al., 2010]	1.7
[Notter et al., 2010]	6
Ecoinvent v2.2	8
[Majeau-Bettez et al., 2011]	22

4.3 Electricity generation, transmission and distribution

The electricity supply chain consist of the exploration, extraction, transportation, processing and delivery steps. Additionally, an infrastructure is required for fast charging and/or replacing depleted batteries. The impact of different supply chains is tabulated in Table A.1. The impact differences originate from the way the electricity is obtained and processed.

Because of the non-negligible impacts for on road transport modes [Chester and Horvath, 2009a], the supply chain is part of many studies. For example, [Held, 2011] studied the influence of the supply chain for mini and compact class cars. It was found that the carbon footprint of battery electric vehicles fuelled with a German electricity mix is similar to the carbon footprint of fossil fuel vehicles. Primarily utilizing wind energy would on the other hand reduce the carbon footprint to levels far below those for fossil fuel cars. Similar results were obtained during a study performed by [Frischknecht, 2011]. This study considered the Swiss grid mix, certified renewable electricity, nuclear power and gas combined cycle-based electricity, among other, and found carbon footprint differences of a factor 2.5-3 for photovoltaics and wind energy with respect to electricity from hard coal.

As a shift to electric driving causes an increase in electricity demand, it is expected that batteries are charged via a fossil fuel dominate electricity mix. This effect was demonstrated by an energy model for heat pumps in Jakob [2011]. The model revealed that the additional electricity demand for an increase in heat pump applications is likely to be covered by fossil power plants. Although these results are not directly transferable to the situation for electric cars due to the significant different temporal demand pattern, it will be likely that electric cars will not, or only to a limited extent, reduce the environmental impacts of mobility right after implementation due to the influence of the energy mix. In the present study, it is assumed that Superbus is operated by an UCTE electricity mix.

4.4 Lightweight materials

As a result of more stringent requirements for improved fuel economy and consumption, there is growing trend to substitute aluminium and magnesium for conventional steels and cast irons in vehicles. In addition, increasing interest exist for the use of composites within the automotive industry. Next to weight reduction, other causes for the increasing interest of lightweight materials are the superior mechanical properties (both physical

properties and properties related to formability) and enhanced safety of vehicle occupants and pedestrians.

The change in impact induced by replacing conventional steels with lightweight materials is elaborated by several studies. For example, [Witik et al. \[2011\]](#) considered a bulkhead component of a car for mass reduction through materials substitution. The goal of the study was to compare the lightweight materials with a steel baseline in terms of cost and environmental performance and evaluated the extraction, production, use and end-of-life phases. The study considered steel, magnesium, glass mat thermoplastic (GMT), sheet moulding compound (SMC) and structural reaction injection moulding (SRIM) of glass and carbon fibres. The operational phase was represented by the required amount of fuel for transporting the bulkhead through the life cycle of the vehicle.

It was found that the reduction in component masses led to reduced CO₂ emission between 57% for SMC to 70% for carbon fibre. However, all components had increased emissions for the material and manufacturing phases with the exception of SMC. Overall, SRIM, GMT and SMC caused a reduction in GWP of 52%, 44%, and 56% respectively, while the carbon fibre only achieved a 12% reduction despite having the largest weight saving. The relatively minor reduction for carbon fibre was attributed to the high energy requirements for the production of the carbon fibre. The environmental burdens associated with the end-of-life phase of the composites were very small and contributed less than 1% of the life cycle. This figure is based on incineration of the composites. In general it can be stated that the use of higher performance materials resulted in increase in environmental burden coming from earlier life cycle phases for components from composites. Moreover, the increased impact from these early phases limited the effectiveness of the lightweight materials to varying degree.

Another study of interest is [Duflou et al. \[2009\]](#) who compared the environmental impacts of manufacturing the structural components of a Volkswagen Lupo from steel and carbon fibre. The results of the study are very similar to those presented by [Witik et al. \[2011\]](#). The study used the Eco-Indicator 99 for weighing purposes. An impact reduction was observed during the operational phase for the carbon fibre situation. Moreover, also [Duflou et al. \[2009\]](#) conclude that the production of the carbon fibres, especially with respect to the use of fossil fuels, dominates the life cycle. Incineration of the automotive parts was assumed for the end-of-life phase.

The end-of-life phase of lightweight materials is considered as one of the main problems. Especially composites do not excel in terms of recyclability. While currently landfill is the most popular and least expensive option, the proportion of a vehicle that can be disposed of in this way in the future is limited by the EU's End-of-Life Directive [[End of Life Vehicle Directive, 2000](#)]. It requires that 95% of the vehicles manufactured after January 2015 should be reused or recovered. As a consequence, the use of composites in the transportation sector is only possible if valid recycling options exist. This is the main reason that the industry that uses the most carbon fibers today, the aerospace industry, takes the initiative to establish best practices for dealing with end-of-life composites. Because the recycling related problems are recognized by the aerospace and automotive industry, industry expects that they can be solved relatively fast, i.e. within a time frame of about ten years.

4.5 Infrastructure

Traditionally, different transport modes are compared on the basis of their tailpipe emissions. With this approach, the environmental impacts caused by vehicle production and maintenance, infrastructure provision and fuel production requirements to support these modes are neglected [Chester and Horvath, 2009a]. Ignoring these indirect processes and services corresponding to transportation, gives rise to an incomplete overview of the actual impacts. For this reason, Chester [2008] argues that the environmental assessment of passenger transportation should include infrastructure and supply chain.

The conclusions of Chester [2008] are based on an extensive assessment of many transport modes, i.e. on road, rail and air travel. Results show that although the operational phase dominates modal life cycle energy consumption, auto and bus non-operational components have non-negligible results, i.e. non-active operation accounts for 25-35% of the total life-cycle energy for on road and 76-61% for rail. Infrastructure construction for road transportation was found to account between 1% and 11% for the energy demand and 1% and 12% for GWP. The lower values relate to urban bus diesel modes operating at peak occupancy.

4.6 Contributions to current body of knowledge

In the present chapter, a review was presented of several topics related to the LCA of the present study. This section is used to summarize the current research and to put the current study into a conceptual and theoretical context. The main question to be answered is what this study adds to the current body of knowledge.

Generally, a life cycle assessment is considered as a valuable and important tool for assessing the environmental performance of products and services. The results of LCA studies are therefore often used for decision-making within governmental bodies and companies, especially in recent years. Concerning mobility, many studies can be identified that elaborate on the burden of different transport modes and the effects of different powertrains. The current research as such fits perfectly into the existing field of research. Yet, some important contributions to the current body of knowledge can be identified. For example, no LCA has been performed on a public transport system that is completely build from advanced lightweight materials. In addition, the majority of studies do not come up with environmental reduction measures, but only determine the relative contribution to the total impact of the different life cycle stages.

Methodology

Preceding chapters provided a thorough introduction to sustainable transportation, the methods and tools that can be used to assess the environmental impacts of a product system and the state of the art of current LCA studies on transportation. This chapter will elaborate the methodology that will be applied in the present study.

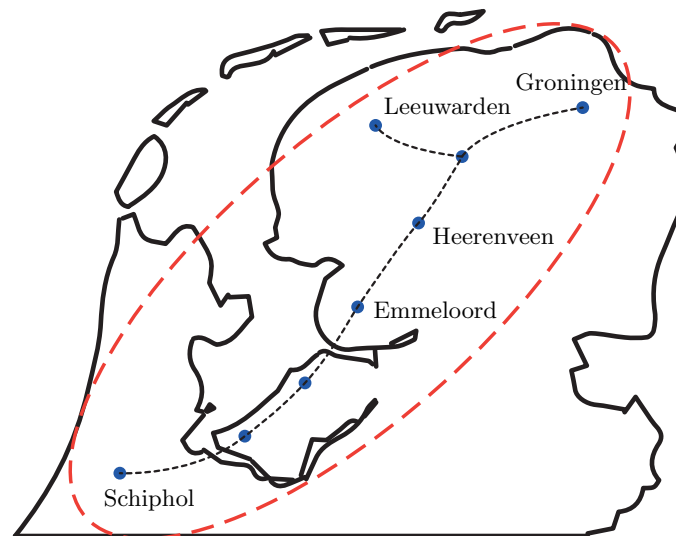


Figure 5.1: Superbus product system.

5.1 Definition of aim and scope

The life cycle assessment that is conducted in the present study, deals with the environmental impacts of the Superbus product system, i.e. financial, political, social and other factors will be ignored. As such, the study complements the 'Strategische Milieubeoordeling' performed by [Ministerie van Verkeer en Waterstaat \[2006\]](#). An overview of the

evaluated product system can be found in Figure 5.1. The figure shows the route of the Zuiderzeelijn from Schiphol to Leeuwarden and Groningen. The red dashed line represents the boundary of the product system, i.e. all Superbus components within the boundary are part of the life cycle assessment of the present study. This implies that the product system comprises all buses, infrastructure and other components that are required for the Zuiderzeelijn.

The basic point of departure is the strategic research question: *"Through which design changes can the environmental impact of the Superbus public transport system be reduced?"*. As presented in Chapter 2, this research question is answered following several consecutive sub-questions. The mode of interpretation is both descriptive and change-oriented [Guinee et al.].

The functional unit is defined as the transportation of 70,510 passengers in 24 hours over an average distance of 90.6 kilometres. The functional unit is obtained from the study by Melkert and Ockels [2006] where the performance of the Superbus product system for the Zuiderzeelijn was calculated using the 'Landelijk Model Systeem' (LMS). The results of this study correspond with a Supertrack velocity of 180 km/h and an average Superbus passenger occupancy of 39%.

The scope of the study can be observed in Figure 5.2 which illustrates the system boundary of the Superbus system. It can be seen that the boundary includes the manufacturing of the vehicles, the batteries, the 210 kilometre Supertrack and the existing infrastructure. Moreover, vehicle maintenance in the form of replacement tyres and infrastructural maintenance is also included. Although the recycling phase is present in the lower part of the figure, it will not be discussed until Chapter 9.

The system boundary is in accordance with Hawkins et al. [2012a] which details the compulsory life cycle components of conventional and electric vehicles. Moreover, the scope has large similarities with Chester [2008], although some non-critical components have been excluded in the present study (for example: insurance).

5.2 Life cycle inventory

The required resources for manufacturing, use and maintenance of the various life cycle components of the Superbus public transport system are determined in the life cycle inventory phase, see Figure 5.3. According to the ISO, LCI also includes an assessment of associated environmental emissions. However, due to the characteristics of the provided impact database, inventory of associated emissions, characterization and weighing will not explicitly be carried out, see also Section 5.3. The life cycle inventory consists of tabulating the material and energy flows to and from all unit processes of the Superbus product system. The static simulation model is made in Microsoft Excel and is composed of >100 unit processes.

The material content of the vehicles is determined from the mass balance of the prototype. In case of a lack of data, surrogate materials and processes are used to determine the use of resources. Furthermore, the transport scenario for production is based on the scenario that is applicable to the prototype to avoid unsubstantiated assumptions. The required number of vehicles to fulfil the function is obtained from Melkert and Ockels [2006].

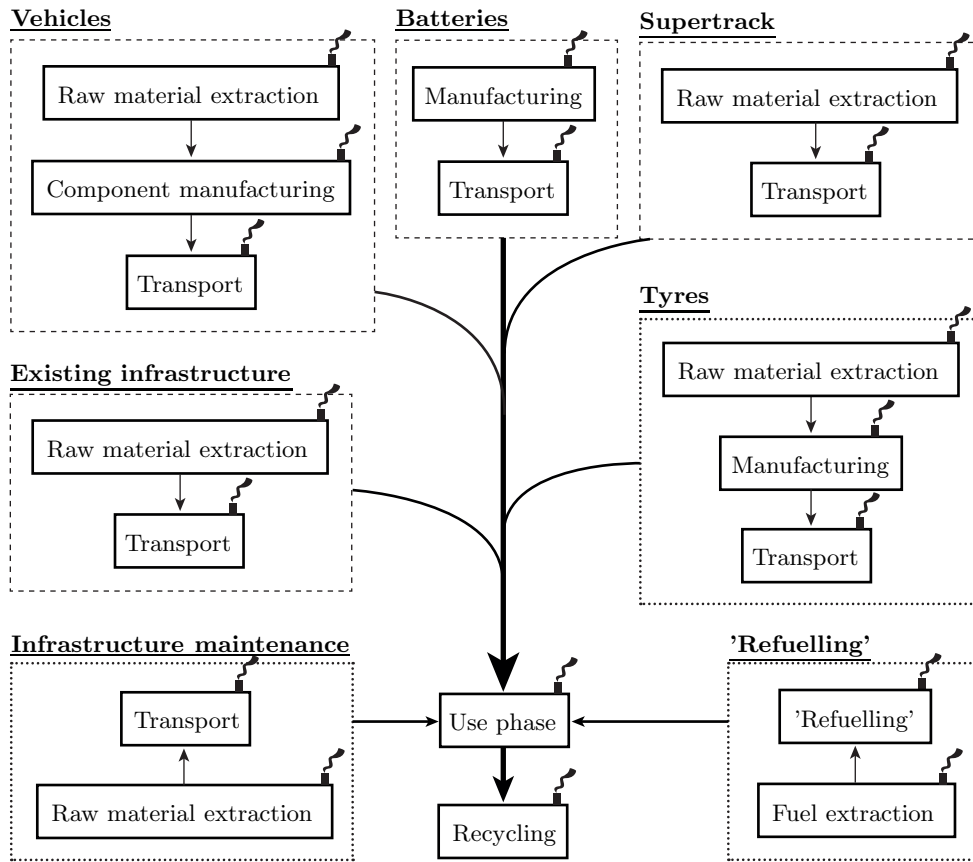


Figure 5.2: System boundary.

The energy consumption during the operational phase is determined from an analysis of the forces acting on the vehicle during operation and follows the procedure adopted by Verduyck et al. [2006]. Here, the speed profile of the vehicles is assumed to correspond with an average speed profile defined by Figure 6.5. Infrastructural details are mainly obtained from Kartanegara [2011].

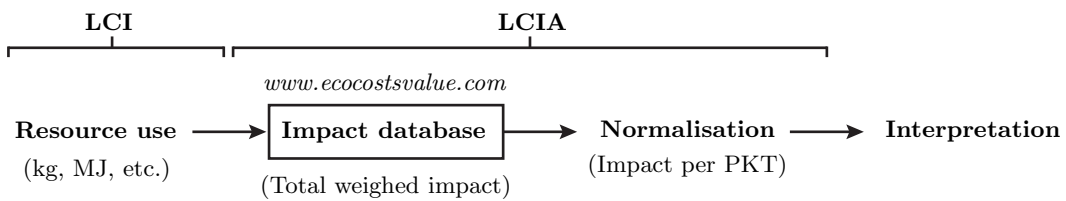


Figure 5.3: Methodology.

5.3 Impact assessment

The environmental impact assessment comprises the steps shown in figure 5.3. Firstly, the LCI tables with material and energy use are fed into the impact database. This database

contains specific weighed impact data of about 5,000 substances, materials, processes, transport and processing scenarios, and can be accessed via <http://www.ecocostsvalue.com/>. The database contains values for eco-costs, carbon footprint, cumulative energy demand and ReCiPe weighing methods and is based on the Ecoinvent database v2.2. The characteristics of these weighing methods were discussed in Chapter 3. The outcome of the database is the total weighed environmental impact of the Superbus product system.

Secondly, normalisation will be carried out with respect to the functional unit which was defined in the previous section. From normalisation, the effect of occupancy rates and transport value of Superbus can be examined.

5.4 Interpretation

Although interpretation occurs at every stage in the LCA, the interpretation step shown in Figure 5.3 refers to processing of the results after normalisation. In analogy with Heijungs and Kleijn [2001], several approaches have been used towards interpretation of these results. The approaches include a contribution analysis, uncertainty analysis, perturbation analysis and the comparative analysis. The outcomes of the different methods have been visualized and discussed using tables, bar charts and graphs.

Life cycle assessment Superbus

In the present chapter, the Superbus public transport system is evaluated in terms of its environmental performance. The model that is developed for this purpose contains the life cycle components shown in Figure 5.2.

The outline of this chapter is as follows. The calculations and assumptions for modelling the various components are elaborated in Section 6.1 to 6.4. The environmental impact of the Superbus public transport system is presented in Section 6.5 and a sensitivity analysis is performed in Section 6.6. A comparison of the results with literature is performed in Section 6.7.

6.1 Superbus vehicle

The environmental impact associated with manufacturing the Superbus vehicles is elaborated in this section. The various components of the vehicle are divided into two main groups, i.e. components belonging to the powertrain and those belonging to the glider. The powertrain is considered as the group of components that generate power and deliver it to the road surface. The glider contains all other components. A mass balance and overview of the manufacturers of the various components of the powertrain and glider can be found in Table 6.1.

6.1.1 Glider

This section elaborates the material content and the resource requirements for manufacturing the different components of Superbus' glider. Moreover, it is discussed how the impact database is used to obtain the environmental impact of component manufacturing. If possible, the material impact is assumed to be equal to the market mix impact.

Table 6.1: Mass balance Superbus vehicle.

Category	Component	Total mass [kg]	Manufacturer, location
Glider	Chassis, bodywork	1,536	Rep-air, Ypenburg (fibers, epoxy); Superbus, Delft (moulding)
	Glazing	324	Sabic, Bergen op Zoom (PC) Weiss, Hofolding, DE (forming)
	Hydraulics	1,500	Various
	Electrical components	600	Wago, Minden, DE
	Seats (24x)	492	Fiberworx, Ypenburg (CFRP); Recticel, Kesteren (foam); Hulshof, Lichtenvoorde (leather)
	Furniture	100	Bolon AB, Ulriceham, SE (carpet) Hulshof, Lichtenvoorde (leather)
Powertrain	Motors (4x)	440	E2M Technologies, Amsterdam
	Motor drives (4x)	92	Genova, IT (components) Superbus, Delft (assembly)
	Power electronics	30	Various
	Supsension frames	1,824	MFK, Vessem
	Tyres (6x)	132	Vredestein, Enschede
	Rims (6x)	96	Dymac, Slough, GB
Battery	LiFePO ₄ battery	1,600	CALB, Luoyang, CH
Total		8,766	

Chassis and bodywork

The chassis and bodywork are made from carbon fibre reinforced epoxy (CFRE). Next to the properties of the fibres, resin and geometry/orientation of the fibres in the composite, the strength of CFREs is greatly determined by the fibre volume fraction (FVF). The FVF that can be achieved is determined by the manufacturing process used to combine the fibre with the resin. For example, the hand lay-up process typically has a FVF limit of 30-40%. The CFRE components of Superbus are manufactured using vacuum assisted resin transfer moulding (VARTM) with which a FVF of 0.7 can be achieved. In general the strength of the material increases with increasing FVF.

The mass fraction of the fibres and the resin can be found using the FVF and the density of carbon fibre and epoxy which are given as $\rho_{cf} = 1.8 \text{ g/cm}^3$ and $\rho_{epoxy} = 0.60 \text{ g/cm}^3$. It is determined that 68% of the total laminate weight can be allocated to the fibres.

Because the database only contains impact data of a reinforced polymer with a carbon fibre mass fraction of 25%, the impact of the chassis and bodywork is determined by considering the material composition and manufacturing process of the specific CFRE. Because no data is available for VARTM, 'injection moulding, plastics' was used as a

surrogate process. It is obtained that the impact of the CFRE is 112-134% higher than the impact of the CFRE with a carbon fibre mass fraction of 25%. This increase is caused by the relatively high production impact of the carbon fibre.

Glazing

The production and forming of the polycarbonate glazing is done by two different companies. The forming process is assumed to correspond with the database process 'thermoforming, plastics'. The transport from Bergen op Zoom to Hofolding, Germany and back to Delft in total concerns 1,710 km of truck transport.

Hydraulics

The hydraulic system contains the various components for the power steering and the elevation system that is used to change the height of the vehicle. The different components considered in the analysis are: one hydraulic pump unit, tens of meters of stainless steel pipes, six stainless steel cylinders and hydraulic fluid. The mass percentages of these components with respect to the total mass of the hydraulic system of 1500 kg is assumed as 20%, 40%, 30% and 10% respectively. The hydraulic pump consist of 20% aluminium, 29% steel, 35% iron, 7% copper and 6% rubber [ITT, 2009, Xylem, 2009, Grindex, 2009]. The tubes and cylinders are assumed to consist entirely of stainless steel and the hydraulic fluid of mineral oil. Due to a lack of data, the required energy for production of the various components is not taken into account. Moreover, transportation of the components from the manufacturer to Delft is not included for the same reason.

Electrical components

Superbus is controlled by many different programmable logic components (PLC) which are connected to the various actuators throughout the vehicle. The total aggregated mass of the electrical components is 600 kg. It is assumed that 10% of this mass can be attributed to the PLCs, 10% to the supporting steel rail system, and the remainder, i.e. 80%, to the interconnecting cables. Because the cables do not transport high currents, the core area was assumed to be 0.5 mm² with a 1 mm thick polyvinylchloride (PVC) insulation. The environmental impact of the PLCs was considered to be similar to the impact database product group 'electronics for control units'. The underlying material composition of this product group (i.e 46% steel, 32% plastics, 14% printed wiring boards and 8% cables) was found to be very similar to the composition stated in the environmental product declaration of the ABB AC800M controller [ABB, 2005]. A total of 360 km of truck transport was taken into account.

Seats

In total 24 seats are installed in Superbus for the passengers and driver. Twelve seats are designed by TU Delft and comprise a CFRE bottom box and an inner shell of 4 and 14 kg respectively. Moreover, the seats contain 1.5 kg of leather and foam. The

other twelve seats are made by RECARO and attached to similar CFRE bottom boxes. Because of a lack of data on the RECARO seats, all seats are assumed to be build by TU Delft. Because the production process of the bottom box and inner shell from pre-impregnated fibres, or pre-pregs, is not available in the impact database, the surrogate process 'injection moulding, plastics' is used. In total, 286 km of truck transport was taken into account for the transport of the various component, i.e. CFRE, foam and leather.

Furniture

The furniture comprises the carpet and leather that is used to cover (parts of) the walls and roof. In the calculations the weight distribution ratio of the carpet and leather was assumed as 60% and 40%. The carpet consists of woven Nylon 6 fibres. The transport of the carpet from Ulriceham to Delft in total involves 1,200 kilometres of truck transport. The leather requires 174 km of transport.

6.1.2 Powertrain

The composition of Superbus' powertrain is elaborated in this section. The material content and the resource requirements for manufacturing are assessed for all different components. Moreover, it is discussed how the impact database is used to obtain the environmental impact of component manufacturing. It is assumed that no replacement parts are required during the lifetime of Superbus. If possible, the material impact is assumed to be equal to the market mix impact.

Motors

The four motors of Superbus, each with a mass of 110 kg, are fabricated by E2M Technologies and able to deliver a continuous power of 100 kW with an efficiency of 97%. An electric engine consist of 56% steel, 35% cast iron, 7% copper and 2% aluminium [ABB, 2002b, CEMEP, 2011]; the energy requirements for manufacturing the motors are 3.78 kWh/kW of electricity and 3.19 kWh/kW of heat [ABB, 2002b]. The transport distance from Oude Meer to Delft is 50 km.

Motor drives

Each of the four motors is connected to a 100 kW frequency controller that is operated by the main control unit. The mass of the individual motor drives and the iron casing amounts to 17 kg and 6 kg respectively. The material composition of the drives was assumed to be similar to the composition of the ACS600 and ACS800 frequency converters build by ABB. These drives consist of 59% steel, 15% iron, 18% copper and 8% aluminium [ABB, 2001, 2002a]. The comprehensive environmental product declarations that are available for both drives have been used in the recent study by Hawkins et al. [2012b] on the comparative LCA of conventional and electric vehicles. The manufacturing energy of the motor drives amount to 0.23 kWh/kW of electricity and 0.43 MJ/kW of heat. A distance of 1200 km was assumed for the truck transport from Genova to Delft.

Power electronics

The main current from the batteries to the motor (drives) is controlled by the power electronics. The total aggregated mass of the power electronics is 30 kg. It is assumed that 30% of the mass can be attributed to the controlling unit and the remainder to the cables connecting the batteries to the motor(s) (drives). In analogy with the electrical components elaborated above, the main controlling unit is assumed to correspond with the database product group 'electronics for control units'. Because the cables are used for high current transport, the core area is assumed to be 500 mm² with an insulation thickness of 5 mm. Because no data was available on the manufacturing location of the various components of the power electronics, transport was not taken into account.

Suspension frames

The suspension of Superbus consists of two frames located at the front and rear of the vehicle. The frames contain various components such as springs, brakes, attachment bolts for the wheels, etc. Because of a lack of data, it is assumed that the frames are built entirely from aluminium. The machining of the aluminium frames is assumed to correspond with the impact database process 'aluminium machining'. The transport from manufacturer MFK to Delft in total concerns 120 km of truck transport.

Tyres and rims

The tyres and rims are designed to cope with the exceptional conditions that arise from the high travelling speed of Superbus. The material tyre composition of a generic tyre is 27% natural rubber, 14% synthetic rubber, 28% carbon black, 14% steel and 17% nylon fabric. Due to a lack of data, fillers, accelerators, and anti-ozonants are not accounted for. The manufacturing energy of tyres is reported by Stankevičiūtė [2000] and Kromer et al. [1999] and amounts to 3.2 and 4.4 kWh of electricity and heat per kg tyre respectively. Because calendaring (coating of textile fabric or steel cords with thin rubber layers) is not included in the first figure, the manufacturing energy is assumed to be 4.4 kWh per kg tyre. This number consists for 26% of electricity and 74% of heat [Stankevičiūtė, 2000].

The assumption for the lifetime of tyres is 65,000 kilometres for tyres connected to a driven axle and 200,000 kilometres for other tyres [Bos, 1998]. The consequences of this assumption will be elaborated at the end of this chapter. It is assumed that tyres are completely replaced when they reach the end of their lifetime. Although retreaded tyres are found to offer similar levels of safety and are currently used for school buses, fire trucks, ambulances, and on approximately 80% of all aircraft tyres in service in the United States [Lindquist and Wendt, 2009], it is unclear if retreaded tyres can also be used for Superbus. As such, the results indicate a worst case scenario. A distance of 210 km was assumed for the truck transport from Enschede to Delft.

The rims consist of an aluminium spoke system and a CFRE rim. The spoke system is assumed to comprise 60% of the total mass. The carbon fibre and epoxy resin masses are obtained using the same procedure as for the chassis. The fabrication process of the aluminium spokes are assumed to correspond with the database process 'aluminium machining'. The truck transport from Slough to Delft was considered to be 540 km.

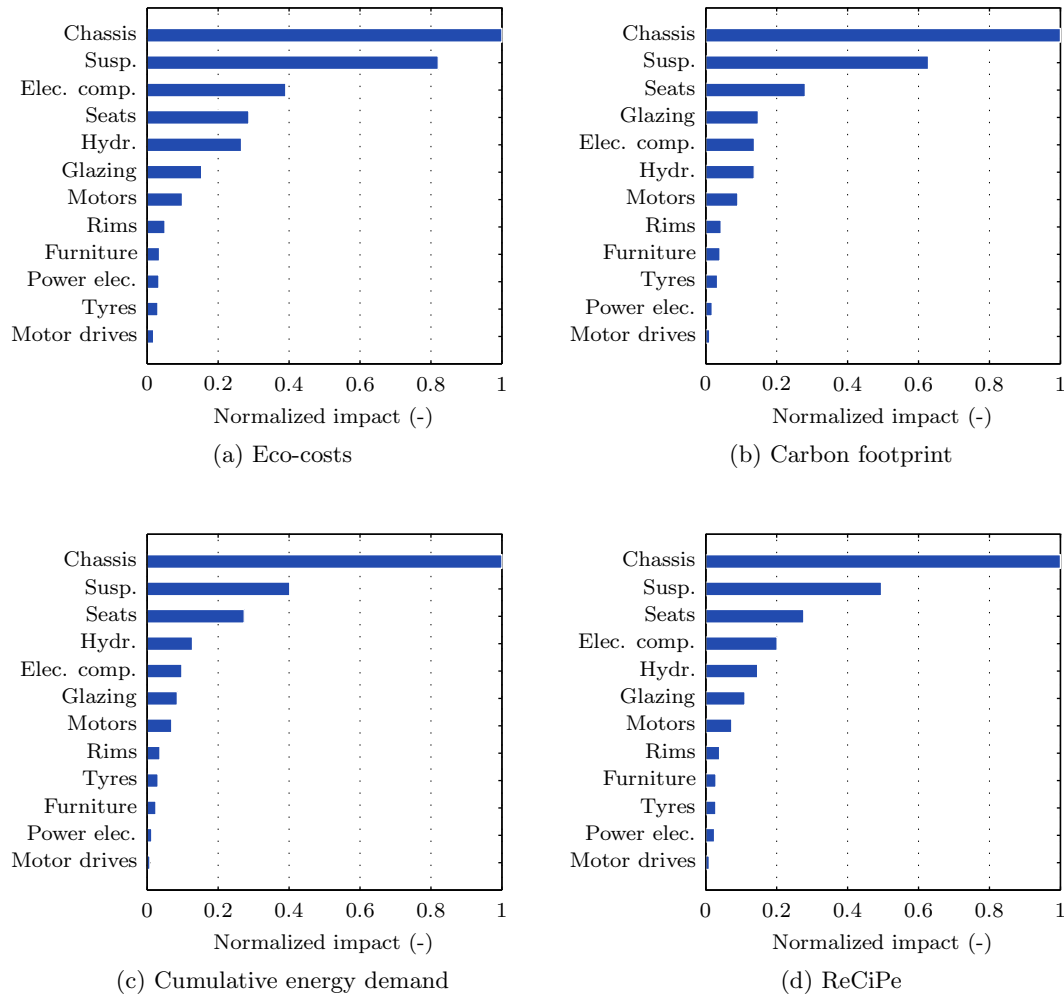


Figure 6.1: Impact of vehicle components normalized to highest impact in category.

6.1.3 Environmental impact electric vehicles

The environmental impact of the Superbus vehicle is presented in this section. The eco-costs associated with manufacturing of the vehicle are 15.2 k€. Moreover, the carbon footprint, cumulative energy demand and ReCiPe are 47.4 tons of CO₂, 1,005 GJ and 5.30 kPts respectively. The impact per passenger seat is €659, 2,060 kg CO₂, 43.7 GJ and 230 Pts for the different impact methods.

For all impact methods, the impact is dominated by the chassis and the suspension frames, see Figure 6.1. The chassis has the largest impact for all impact methods, in particular the cumulative energy demand. The combined impact of the chassis and suspension frames amount to 57-65% of the vehicle impact.

Given the mass balance of Table 6.1 and the results of Figure 6.1, it can be concluded that the environmental impact of the vehicles is dominated by the heaviest components. Remarkably, the impact of the hydraulic system is relatively low given its mass of 1,500 kg.

An explanation for this can be found in the material composition of the hydraulic system which mainly consist of steel. Steel has a relatively low impact compared to aluminium and CFRE.

Transportation of the different components increases the environmental impact with about 0.2%. It can be expected that the effect of transport will be reduced even further if the vehicles are produced in large numbers, i.e. during mass production.

6.2 Battery

From Chapter 5 it became clear that the batteries are treated as a separate component of the transport system. This approach is very different to the way batteries are treated in environmental studies on electric passenger cars where the battery is seen as part of the vehicle, for example in the analysis of Hawkins et al. [2012b]. The reason for this distinct approach is found in the way the batteries are used in both vehicles. Passenger cars have fixed batteries that can be charged during several occasions a day, for example during work or overnight. Ideal for an average passenger car because these cars travel a distance of about 80 km, i.e. an equivalent of one battery charge. Superbus on the other hand, is used almost non-stop throughout the day. Intermediate charging of the batteries is therefore impossible. This problem can be solved in two possible ways. A solution might be to use batteries with a very high capacity that will last a whole day. However, the energy density of current generation batteries will cause the batteries to become too heavy and large. The other option is to replace the batteries once empty. This is called battery swapping and is currently used by Better Place to increase the driving range of their electric vehicles. By adopting such system, batteries will become a separate component of the transport concept. Not only because the batteries are not fixed to the bus, but also because each battery can be used by several buses during a day.

The characteristics of the battery in the prototype are used as a starting point for determining the environmental impact of the batteries. The battery consists of two packs connected in parallel with 210 individual LiFePO_4 cells per pack. The maximum amount of energy, E_{batt} , that can be stored in these batteries is calculated from Equation 6.1 and equals 514.1 MJ. Here, Δu is the cell float voltage in volts, Q is the cell nominal capacity in ampere-hours (cf. Appendix B), t_h is the time in one hour and n_{series} and $n_{parallel}$ are the number of cells in series and parallel.

$$E_{batt} = \Delta u Q t_h n_{series} n_{parallel} \quad (6.1)$$

However, this energy is not completely available to power the vehicle because fully discharging a battery will reduce its cycle life. According to the manufacturer, the battery cells have a cycle life of 3000 cycles for a 70% DoD (cf. Appendix B). This means that the current battery can provide 359.9 MJ per cycle.

From the average fuel economy at 180 km/h, it can be calculated that the driving range is 90 kilometres. Hence, the prototype cannot transport passengers over a distance larger than 90 km, for example from Schiphol to Groningen.

Superbus should be able to travel large distances up to 210 kilometres on a single charge. The battery is therefore scaled up to the required capacity. It is assumed that the new

battery can be fitted in the current chassis. The required energy capacity of the battery, $E_{batt,req}$, can be calculated from Equation 6.2. Here, s_{trip} is the trip distance and $FE_{electric}$ is the fuel economy which depends on the Supertrack velocity. The required battery capacity increases with increasing velocity.

$$E_{batt,req} = \frac{s_{trip} \cdot FE_v}{DoD} \quad (6.2)$$

The battery mass can be found from the specific energy of the current battery. Dividing the available energy of the prototype battery by its mass yields $E_{specific} = 0.32$ MJ/kg. Note that the specific energy is calculated using the total available energy of the prototype battery.

The next step is to determine the amount of batteries that are required for the Zuiderzeelijn. This can be calculated by evaluating the daily production of a bus. In the calculations, it is assumed that transport takes place during 18 consecutive hours from 6 AM to 12 PM.

Because the amount of travelling people is not constant, a total of four different traffic intensities are distinguished. The main difference between these intensities is the amount of vehicle kilometres that are travelled per hour. In addition, the intensities only occur for several hours a day. An overview of the intensities with corresponding occurrence can be found in Table 6.2. In addition, the table shows the amount of charge that is required per hour per traffic type.

Table 6.2: Intensity and occurrence of different traffic types and associated required battery charge [lr. J.A. Melkert, 2013].

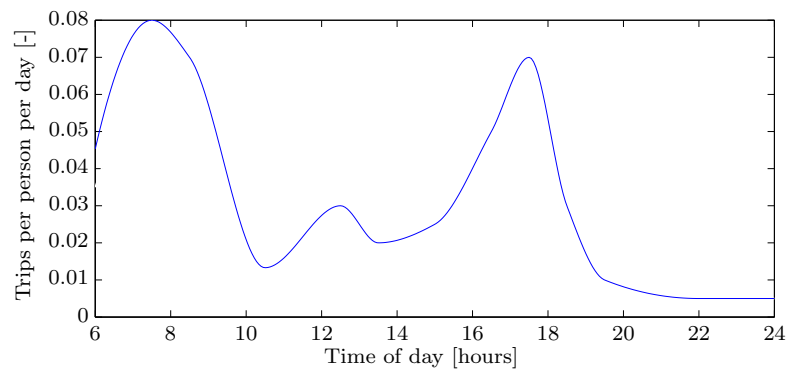
Type	Intensity [% daily VKT per hour]	Occurrence [hour]	Charge used [% per hour]
Peak, morning (MP)	10	3	35
Peak, evening (EP)	10	3	35
Day (D)	4	7	14
Through (T)	2	5	7

If the state of charge of the batteries is now calculated as a function of the time of the day, the result as shown in Table 6.3 can be obtained. From Table 6.3, it can be concluded that for a charge rate of 0.3C, three different batteries are required throughout the day. The required number of batteries can be decreased applying fast charging. Note that the traffic intensities in the table are distributed by considering the variation in the amount of commuting trips per person, see Figure 6.2.

Next to the required number of batteries for constant operation, the minimum number of batteries is determined by the cycle life of the battery in relation to the lifetime of the bus. By considering the amount of energy that can be stored in the batteries during 3000 cycles and comparing the result with the consumed energy during the lifetime of the bus, it is found that 2.4 batteries are required during the operational phase of the Superbus vehicle. The number is calculated given the fact that the battery capacity depends on the Supertrack velocity.

Table 6.3: Daily (dis)charge cycle of the batteries for a charge rate of 0.3C.

Time	Traffic	Discharging [SoC]			Charging [SoC]		
		1	2	3	1	2	3
5	-	100%					
6	MP	65%	100%				
7	MP	30%	100%		30%		
8	MP		64%		60%		
9	D		50%		90%		
10	T	100%	43%		100%		
11	D	99%	30%				32%
12	D	85%					62%
13	T	78%					92%
14	D	64%					100%
15	D	50%	100%				
16	EP	30%	85%		43%		
17	EP		50%	100%	73%		
18	EP		30%	85%	100%	43%	
19	T			77%		73%	
20	T			70%		100%	
21	T			63%			
22	T			56%			
23	T			49%			

**Figure 6.2:** Average number of commuting trips per person per day [Centraal Bureau voor de Statistiek (CBS), 2007].

In the present study, the impact database product 'Li-ion battery (99 Wh/kg)' was used to calculate the environmental impact of the battery. Although this battery utilizes a LiC_6 anode and LiMn_2O_4 cathode, it was concluded from Notter et al. [2010] that the chemistry does not change the impact results in a general LCA. Moreover, the difference in energy density (90 Wh/kg versus 99 Wh/kg) is neglected. A total of 700 km of truck transport from the manufacturer in Luoyang to the harbor of Lianyngang, 19,700 km of ship transport to the Harbour of Rotterdam, and 30 km truck transport to Delft is included in the calculations.

6.3 Infrastructure

The infrastructural network for Superbus comprises a dedicated Supertrack and (parts of the) existing road network. An important difference exist in the way the construction impact of these infrastructures should be allocated to Superbus. The environmental impact of the Supertrack should be allocated entirely to the transport concept. Because the existing road network is also used by other traffic, only a part of the construction impact should be allocated to Superbus. The impact of both infrastructure types, as well as the required road maintenance, is elaborated in this section.

6.3.1 Deditated infrastructure: Supertrack

The Supertrack is envisioned to be integrated with the existing infrastructure on the route from Schiphol to Groningen which covers a total distance of about 180 kilometres. As stated by Verduyckt et al. [2006], its construction is relatively lightweight compared to infrastructures of competitive transport modes due to the low axle loads of Superbus of about 40 kN.

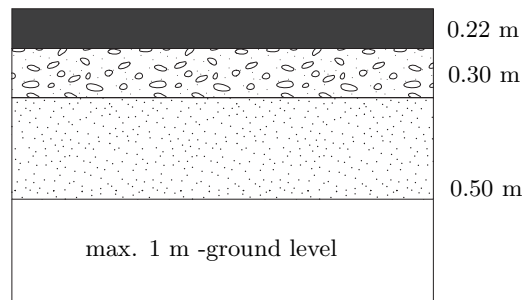


Figure 6.3: Cross-section of the Supertrack structure with from top to bottom: asphalt, aggregate mix, sand and subsoil improvement.

A design proposal for a smaller portion of the track was developed by Kartanegara [2011]. Based on functionality, operation and costs, a road construction on ground level utilizing an embankment foundation was found as the favourable option. Embankment foundations are a traditionally proven concept that are relatively cheap compared to road structures located under or above ground level. A cross section of the proposed design can be found in Figure 6.3. As can be seen in the figure, the track consists of four consecutive layers, i.e. a top layer of asphalt that is supported by an aggregate mix layer, a sand layer and a bottom layer used for subsoil improvements.

The top layer comprises different asphalt layers that enable the use of a Road Energy System (RES) or WinnerWay system. These systems are used to control the temperature of the road surface by pumping water through the pipes located in the asphalt layer. The 0.02 m diameter polyethylene tubes of the Winnerway system have a 0.1 m spacing and longitudinal orientation [Kartanegara, 2011]. It is assumed that the wall thickness of the tubes is about 3 millimetres.

Subsoil improvements are required to enhance the load carrying properties of sediments that have little load carrying capacity. Along the route from Schiphol to Groningen via

the Flevoland province, the major part of the soil consist of clay or thin sand layers on top of peat. It is assumed that subsoil improvements are required on the entire track from Schiphol to Groningen.

Concrete step barriers are used to ensure safety of the passengers of Superbus, as well as that of the road users of the adjacent highway. The frontal area of the edge and middle step barriers are 0.32 m^2 and 0.37 m^2 respectively [Kartanegara, 2011].

Although bridges, overpasses and other special constructions are likely to have a non-negligible effect on the environmental impact of the infrastructure, their impact is not taken into account due to a lack of data. It should be noted that during the initial phases of implementation, Superbus will most likely use existing bridges, overpasses, etc.

From Vogtländer et al. [2010], it can be concluded that the impact of road construction is dominated by the impact caused by the extraction of materials and the transport of these materials to the construction site. The impacts due to the use of shovels and asphalt spreading machines are therefore neglected in the present study. In calculations of the construction impact of the infrastructure, the material impacts used are those as listed in Table A.1. Asphalt is assumed to consist of coarse aggregate, fine aggregate, bitumen and air pores. The mass percentages of these components is 65%, 30% and 5% respectively [Molenaar and Houben, 2011]. The transport distance for sand and aggregate is 20 kilometres [van den Berg et al., 1995]. For asphalt and concrete it is assumed to be 50 and 24 kilometres [Jorritsma, 2010, van Ooijen B.V., 2012, Connel et al., 2008]. A relatively high transport distance of 100 km was assumed for the Winnerway system due to a lack of data.

6.3.2 Environmental impact of Supertrack

An overview of the relative impact of the different Supertrack components can be found in Figure 6.4. The per kilometre eco-costs associated with construction are 297 k€. Moreover, the carbon footprint, cumulative energy demand and ReCiPe are 524 tons of CO_2 , 14.3 TJ and 65.9 kPt per kilometre respectively. Taking into account the lifetime of the infrastructure, the impact is found as 5.95 €, 10.5 kg CO_2 , 285 MJ and 1.32 Pt per meter per year.

For all impact methods, the impact is dominated by the asphalt and the concrete step barriers. Asphalt has the highest impact in all impact categories except carbon footprint. It is observed that the effects of transport in road manufacturing cannot be neglected. In fact, transport has the third highest impact for carbon footprint and the fourth highest impact in the other methods.

Interestingly, the impact of the step barrier and aggregate layer which are both made from concrete, is very different. In spite of the much larger amount of aggregate, its environmental impact is smaller for all different methods. The reason for this originates from the fact that aggregate is a residual product, i.e. its impact is only caused by crushing the aggregate and not by material extraction.

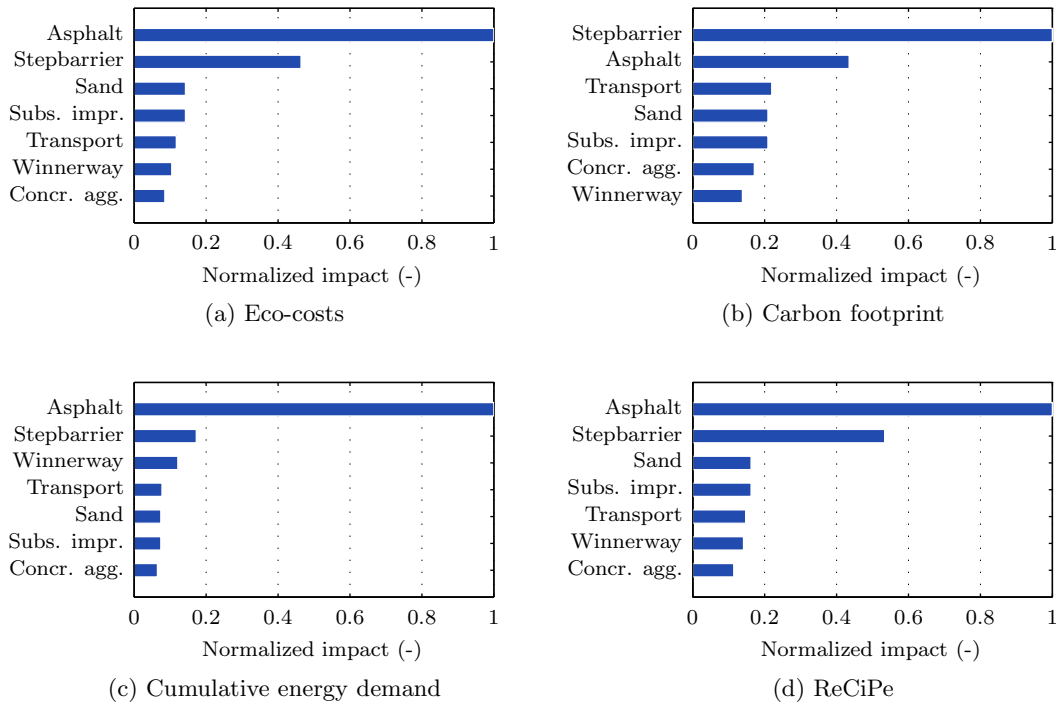


Figure 6.4: Impact of Supertrack components normalized to highest impact in category.

6.3.3 Existing infrastructural network

To enable point to point transportation, Superbus makes use of the existing road network to drop off passengers close to their destination. Part of the embodied construction impact of the existing infrastructure should therefore be allocated to Superbus. This can be done by considering the relative amount of road space that is used by Superbus.

Given the annual vehicle kilometres of the different vehicles on the Dutch road network (see Table 6.4), it is expected that only a small part of the construction impact can be attributed to Superbus. However, the analysis in this section shows that the allocated impact is non-negligible compared to the construction impact of the Supertrack.

According to their behaviour in traffic, different vehicles are considered to be equivalent to several passenger cars, i.e. they are supposed to use as much space as an equivalent number of passenger cars (PCE). For example, the passenger car equivalent of a van and a bus is equal to 1.8 and 2.25 respectively. Table 6.4 gives an overview of the PCE for other types of vehicles. Because the dimensions of Superbus are very similar to a normal bus, the PCE of Superbus is assumed to be equal to a normal bus.

The embodied construction impact of the existing infrastructure can be allocated by comparing the PCE-kilometres of Superbus with the PCE-kilometres of other traffic types. The PCE-kilometres can be determined by considering the road use in the cities where people can use the Superbus transport concept, i.e. Amsterdam, Almere, Lelystad, Emmeloord, Heerenveen, Drachten, Leeuwarden, and Groningen [Melkert and Ockels, 2006]. If it is assumed that all roads in the Netherlands equally contribute to the total annual

VKT, the amount of road space that used is by the different vehicle types can be found by multiplying the annual PCE-kilometres with the fraction of average city road length, S_{avg} , and the total road length in the Netherlands, S_{tot} , per vehicle type and road type. The numerator of this fraction is determined by calculating the average road distance for different road types in the cities given in Table 6.5 and multiplying with the number of cities N^1 . The fractions for state, provincial and municipal roads are found to be 0.07, 0.04 and 0.06 respectively. Because it is assumed that all roads equally contribute to the VKT, the contribution of vehicle kilometres of urban areas is overestimated and the contribution of vehicle kilometres of rural areas is underestimated. These effects are however neglected in the present study.

Table 6.4: Overview of PCE, VKT and distribution of vehicle kilometres over road type by vehicle type [Centraal Bureau voor de Statistiek (CBS), 2011e].

Vehicle type	PCE	Annual VKT (10^6 km)	Distribution		
			State	Provincial	Municipal
Passenger cars	1	103,450	44%	36%	21%
Vans	1.8	17,386	51%	32 %	16%
Trucks	3	2,517	70%	20%	10%
Tractors	1.75	4,659	70%	20%	10%
Buses	2.25	652	37%	25%	38%
Superbus	2.25	231	10%	20%	5%

The annual vehicle kilometres travelled by different vehicle types in the year 2011 is given by Table 6.4. The given numbers are the sum of the distances travelled on state roads, provincial roads and municipal roads. The distribution of VKT along these different road types, D , is also shown in the table.

The annual VKT of Superbus are calculated by assuming a daily travel distance of 1055.3 km for all 673 buses and a factor of 325 to convert the daily distance to a yearly distance. These numbers were obtained from the model in the Landelijk Model Systeem that was made in the context of the Structuurvisie Zuiderzeelijn [Melkert and Ockels, 2006]. In the LMS, people's movements are modelled for a 24 hours time period to predict the use of cars, trains and urban transport modes (buses, trams, metros, etcetera) in the Netherlands. For the Structuurvisie, Superbus was modelled as a train and the demand driven scheduling was approximated with a strand of stops in eight different cities. The model resulted in approximations for the required number of vehicles, the amount of passengers, the average kilometres travelled per passenger and the average velocity of Superbus. An average velocity of 105 km/h was obtained for a speed profile with three different velocities, i.e. 30 km/h in cities, 90 km/h around Amsterdam and 180 km/h on the Supertrack.

In the present study, the distribution of VKT along the different road types is adapted to include state and provincial roads. Figure 6.5 shows a schematic overview of the distribution of the VKT in terms of the maximum speeds that apply to the different road types in the Netherlands. The distribution of the VKT of Superbus are obtained

¹For the cities of Emmeloord and Drachten no data was available

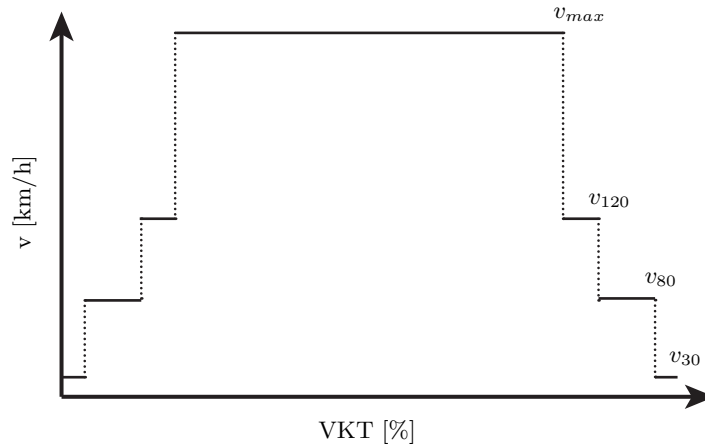


Figure 6.5: Schematic speed profile for the Supertrack.

by considering three typical trips of Superbus: from Schiphol to Groningen Zernike, from Almere Muziekwijk to Lelystad Centrum and from Amsterdam CS to Almere Muziekwijk. Provincial roads were found to have a relatively large share compared to state and municipal roads. State roads are used to enter and exit the Supertrack and for trips from and to Amsterdam CS and Leeuwarden. Municipal roads are used to collect and drop off passengers.

Because the average speed of Superbus is determined by the speed profile given by Figure 6.5 and the total stop time, the distribution of VKT along the different road types can be validated by considering the stop time per hour that is required to obtain an average speed of 105 km/h. It is determined that six minutes per hour are available for stops at the given average speed. This corresponds to about three stops per hour assuming a stop time of two minutes per stop. The profile can therefore be considered as a reasonable estimation of the distribution of the VKT during Superbus' life.

Table 6.5: Total road length per road type [Centraal Bureau voor de Statistiek (CBS), 2011b].

Location	Road length [km]		
	State	Provincial	Municipal
Netherlands	5,121	7,863	117,637
Amsterdam	94	9	1,723
Almere	47	51	1,014
Lelystad	39	84	579
Heerenveen	29	23	448
Leeuwarden	18	9	495
Groningen	39	31	634

By combining all data, the road space of the different vehicles, R_{type} , can be calculated from Equation 6.3. For Superbus, the relative share of space occupied corresponds to 1.0%, 5.2%, and 1.5% for state roads, provincial roads and municipal roads respectively.

This corresponds to road lengths of 3.6 km, 15.3 km and 104 km.

$$R_{type} = (VKT \cdot PCE \cdot D)_{vehicletype} \cdot N \cdot \left(\frac{S_{avg}}{S_{tot}} \right)_{roadtype} \quad (6.3)$$

Above results demonstrate that the amount of existing infrastructure that should be allocated to Superbus is relatively large compared to the length of the dedicated infrastructure, i.e. an extra 123 km of road should be considered in the infrastructural impact of Superbus. However, the figures are somewhat distorted due to the relatively long distance of municipal roads, see Table 6.5. It is not expected that Superbus will use all the municipal roads in the cities, i.e. it is only used to exit the provincial road and to make a quick stop. It is therefore assumed that only 10% of the municipal roads is used by Superbus. The total road impact of the existing infrastructure that should be allocated to Superbus thus becomes 30 km, which is 14% of the length of the Supertrack.

An assessment of the embodied construction of state roads, provincial roads and municipal roads is out of scope of the current study. Therefore, the embodied impact of the Supertrack is increased with 14%. Hence, the existing infrastructure is treated as if it was part of the Supertrack.

6.3.4 Maintenance

Regular road maintenance is determined by the amount and size of the loads that are exerted on the road surface. In particular, the axle loads of the traffic are crucial for the maintenance requirements and the expected structural lifetime of the road. During the design of a road, it is therefore common practice to use the number of equivalent axle loads of 100 kN as a measure of the expected traffic induced loads. The so called design load N_{eq} , is calculated using Equation 6.4. In this equation, L is the average axle load in a given load class, f the axle load frequency distribution, V the number of trucks per direction, A the average number of axles per truck and l_e the load equivalence factor [Molenaar and Houben, 2011].

On Dutch highways, the average number of axles per truck is 3.5. Moreover, the load frequency distribution is usually considered to correspond with the three reference distributions that are determined by Rijkswaterstaat, i.e. 'light', 'medium' and 'heavy' [Dienst Weg- en Waterbouwkunde, 1994].

$$N_{eq} = LfVA l_e = LfVA \left(\frac{l}{l_{st}} \right)^4 \quad (6.4)$$

The design load can be used to compare the traffic intensity of the Supertrack with the intensity of a Dutch highway, for example the A13. By doing the math, the results as presented in Table 6.6 can be obtained.

The loads for the A13 are obtained by considering 4,750 trucks in eastern direction per working day with a total of 275 working days per year. Moreover, it was assumed that the axle load frequency distribution corresponds with the reference distribution 'light' of Rijkswaterstaat. The traffic growth was set at 0%. The design load of the Supertrack is calculated assuming the vehicle kilometres are achieved by driving back and forth on the track and using data from Section 6.3.3.

Table 6.6: Design load comparison of the Supertrack and A13 highway.

L [kN]	f_{A13} [%]	$f_{Sprtrck}$ [%]	l_e [-]	$N_{eq,A13}$ [-]	$N_{eq,Sprtrck}$ [-]
10	7.6	-	0.001	693	-
30	25	-	0.0081	184,771	-
40	-	100	0.0256	-	1,609,909
50	30	-	0.0625	1,710,844	-
70	18	-	0.2401	3,943,426	-
90	11	-	0.6561	6,585,243	-
110	6.1	-	1.4641	8,149,100	-
130	1.8	-	2.2861	4,690,887	-
150	0.41	-	5.0625	1,893,904	-
170	0.07	-	8.3521	533,461	-
Total	100	100	-	27,930,153	1,609,909

From Table 6.6 it can be concluded that the number of equivalent axle loads of the Supertrack is only 6% of the equivalent axle loads of the A13. It is thus demonstrated that the infrastructure for Superbus can indeed be relatively lightweight. Moreover, regular road maintenance will be required less often compared to a normal highway. In the Netherlands, regular maintenance is supposed to take place beyond the age of about twelve years. The need for asphalt is 70 tons per kilometre of infrastructure which needs to be maintained [VBW Asphalt, 1989]. This number is calculated assuming a road lifetime of 50 years. Hence, each road requires 38 years of maintenance. Moreover, it is an average value for the requirements of all asphalt roads in the Netherlands, i.e. for smaller and larger roads. In the present study, this value is used to calculate the required material for maintenance.

6.4 Operation

The environmental impact during operation of Superbus is caused by the consumption of raw materials and the emissions that are associated with the production of electricity that is consumed during the operational phase. The electricity consumption of Superbus is determined by the energy that is consumed by the motors and the auxiliary systems, as well as the tank-to-wheel efficiency.

The consumption of the motors is induced by the aerodynamic and rolling forces that act on the vehicle during driving. For a steady state ($dv/dt = 0$) and a horizontal road, the required force at the wheels, F_{motor} , is given by Equation 6.5. In the equation, C_D is the drag coefficient equal to 0.3, ρ_{air} is the air density, v is the driving velocity, S is the frontal area equal to 4.2, μ is the friction coefficient between the tyres and the road equal to 0.01, m is the mass of the vehicle and payload and g is the gravitational acceleration. The effect of crosswinds is neglected in the calculations.

$$F_{motor} = F_{aerodyn.} + F_{rolling} = 0.5C_D\rho_{air}v^2S + \mu mg \quad (6.5)$$

The total power consumption of the vehicle, $P_{vehicle}$ is obtained by multiplying Equation

6.5 with the driving velocity v and adding the power that is consumed by the auxiliary systems $P_{auxiliaries}$, see Equation 6.6.

$$P_{vehicle} = 0.5C_D\rho_{air}v^3S + \mu mgv + P_{auxiliaries} \quad (6.6)$$

The total electricity consumption during Superbus' lifetime can be calculated by multiplying the power consumption at velocity v with the operation time t at that speed for the different sections of the speed profile given by Figure 6.5 and adding the results. Moreover, the tank-to-wheel efficiency should be taken into consideration. An overview of the different efficiencies that make up the tank-to-wheel efficiency can be found in Figure 6.6. From the figure, it can be calculated that the overall tank-to-wheel efficiency is about 72%.

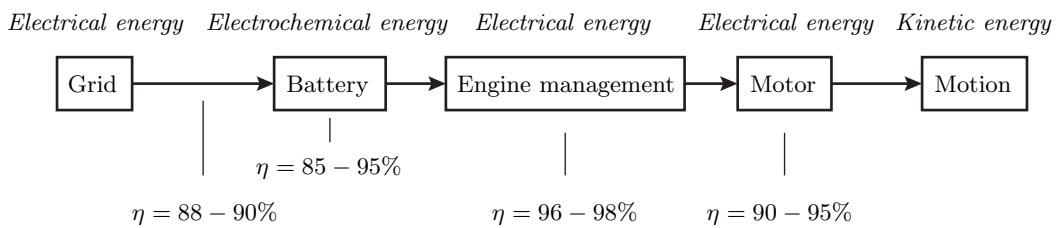


Figure 6.6: Tank-to-wheel energy efficiency of electric vehicles [van Mierlo and Marenne, 2009].

The average fuel economy can be determined by dividing the total electricity consumption by the total vehicle kilometres travelled during Superbus' lifetime. The average fuel economy including a tank-to-wheel efficiency of 72% for a Supertrack speed of 180 km/h is given by Equation 6.7.

$$FE_{avg} = 4.50MJ/km \equiv 54.3Wh/seat - km \quad (6.7)$$

It should be stated that the fuel economy is a function of the battery mass. Moreover, the required battery capacity and thus the battery mass depends on the fuel economy. The calculated fuel economy of Equation 6.7 is therefore obtained by iteration.

The difference between the fuel economy given by Equation 6.7 and the fuel economy calculated by Verduyckt et al. [2006] (2.4 MJ/km and 26.5 Wh/seat-km, long trajectory), is caused by the difference in drag coefficient ($C_D = 0.3$ versus $C_D = 0.2$), the larger battery mass that is assumed in the present study (3751 kg versus 1100 kg) and the difference in vehicle capacity (23 seats versus 25 seats). Moreover, a difference exist in the tank-to-wheel efficiency and the foreseen speed profile. The calculated fuel economy of Superbus is about 17% smaller than the fuel economy of an electric passenger bus: 5.4 MJ/km [X.O. et al., 2010], and about 7 times higher than the efficiency of a small electric passenger car: 0.63 MJ/km [Nissan Europe - France, 2012].

An overview of the impacts associated with the production of electricity can be found in Table A.1. The difference between the electricity impacts of different countries is caused by differences in the electricity mix. For example, the Dutch electricity mix relies on natural gas (46%) and hard coal (17%), whereas the Belgian electricity mix relies on nuclear power (45%) and natural gas (23%). Because the impact of electricity from

nuclear is smaller than the impact of electricity from natural gas (mainly due to the differences in carbon dioxide emissions), the overall impact of the Belgian electricity is smaller. The environmental impact during operation is determined using the impact values that correspond to 'Electricity, UCTE mix'. Moreover, the impact of the electricity from photovoltaics and wind energy is assumed as 'Electricity, PV' and 'Electricity, wind' respectively, see Table A.1.

Next to the use of electricity, there is a non-negligible additional demand for materials. In the present study, only replacement tyres are taken into account, see also Figure 5.2. The assumption for the lifetime of tyres was given in Section 6.1.2. It is calculated that in total 106 tyres are needed during the vehicle lifetime.

6.5 Environmental impact Superbus system

Figure 6.7 shows the environmental impact of the Superbus public transport system for the four impact methods. All results are normalized with respect to the amount of passenger-kilometres transported as given by Melkert and Ockels [2006].

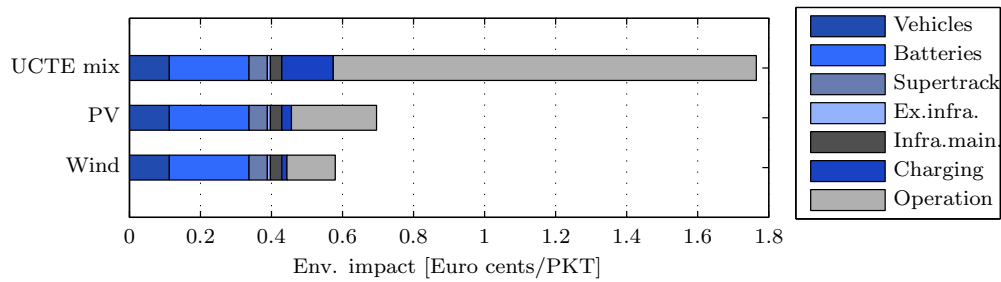
The first case, labelled with 'UCTE mix', is the reference situation where Superbus is operated with the current electricity mix of the UCTE countries. This mix is dominated by electricity from fossil fuels (49%) and thermal nuclear power plants (27%). The remainder is produced via hydro generation and other renewable energy sources such as wind, solar, geothermal, waste, etc. The eco-costs and carbon footprint of the Superbus transport concept are 1.76 €cents and 81.84 gCO₂ per PKT respectively. Moreover, the cumulative energy demand and ReCiPe are 1.88 MJ and 7.54 mPts per passenger-kilometre.

It can be seen that for an UCTE electricity mix, the 'tailpipe' component account for the largest portion of the life-cycle impact for all impact methods, i.e. its contribution ranges from 67-78%. The impact of the batteries is the second largest for all impact methods. The impact of the batteries ranges from 7-13%. The other main contributor is the vehicle which has an impact that varies between 4-6% for the different impact methods. The impact of the infrastructure and its maintenance has a combined impact of 2-5% in the different impact categories. Interestingly, the impact due to road maintenance takes between 22-68% for the different impact methods. In this number, the higher figure corresponds to the cumulative energy demand.

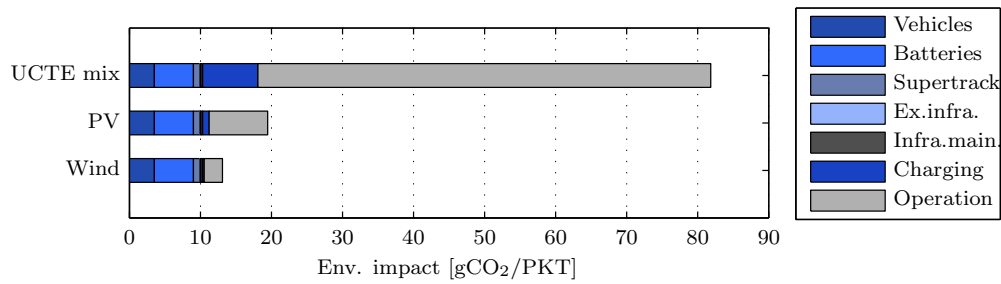
The second and third case corresponds to a situation where it is assumed that the electricity is obtained directly from solar panels or wind turbines. In reality, this is not possible because the electricity will always be a mix of different type of sources. It is found that the environmental impact is reduced to a large extent when utilizing renewable energy. Compared to the UCTE electricity mix, the obtained impact reduction varies between 44-76% for photovoltaic and 51-84% for wind energy.

6.6 Sensitivity analysis

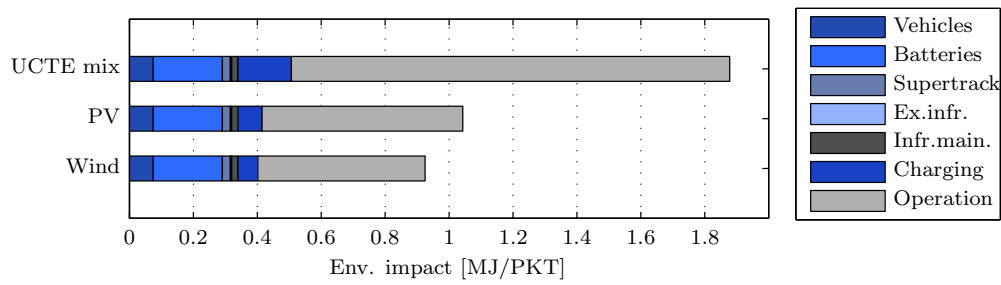
In this section, a sensitivity analysis is performed to determine the effects of changes in key parameters. The sensitivity analysis confines itself to an examination of the effects



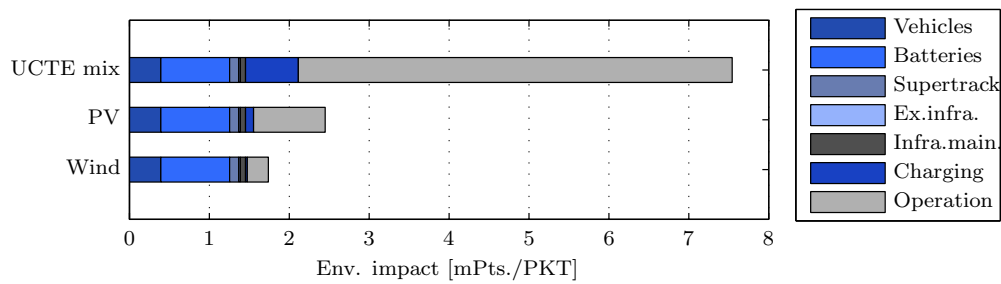
(a) Eco-costs



(b) Carbon footprint



(c) Cumulative energy demand



(d) ReCiPe

Figure 6.7: Environmental performance Superbus public transport system.

of changes in passenger occupancy and Supertrack velocity. Investigating the effects of passenger numbers corresponds to examining the effects of changes in the functional unit as was defined in Chapter 5.

6.6.1 Passenger occupancy

The importance of considering the effects of passenger occupancy in relation to the environmental impact of different transport modes is given by [Chester and Horvath \[2009a\]](#): "While the per-VKT performance of any mode can potentially be improved through technological advancements, the per-PKT performance, which captures the energy and emissions intensity of moving passengers, is the result of occupancy rates". An evaluation of the occupancy rates with realistic variations in ridership, will thus illustrate both the potential environmental performance of the mode, as well as the passenger conditions when modes are equivalent. The latter point will be discussed in Chapter 8. In addition, the discussion of the environmental performance of transit modes often focuses on the ranking of vehicles assuming average occupancy. This approach does not acknowledge that there are many conditions under which passenger transport modes can perform equally in terms of environmental impact.

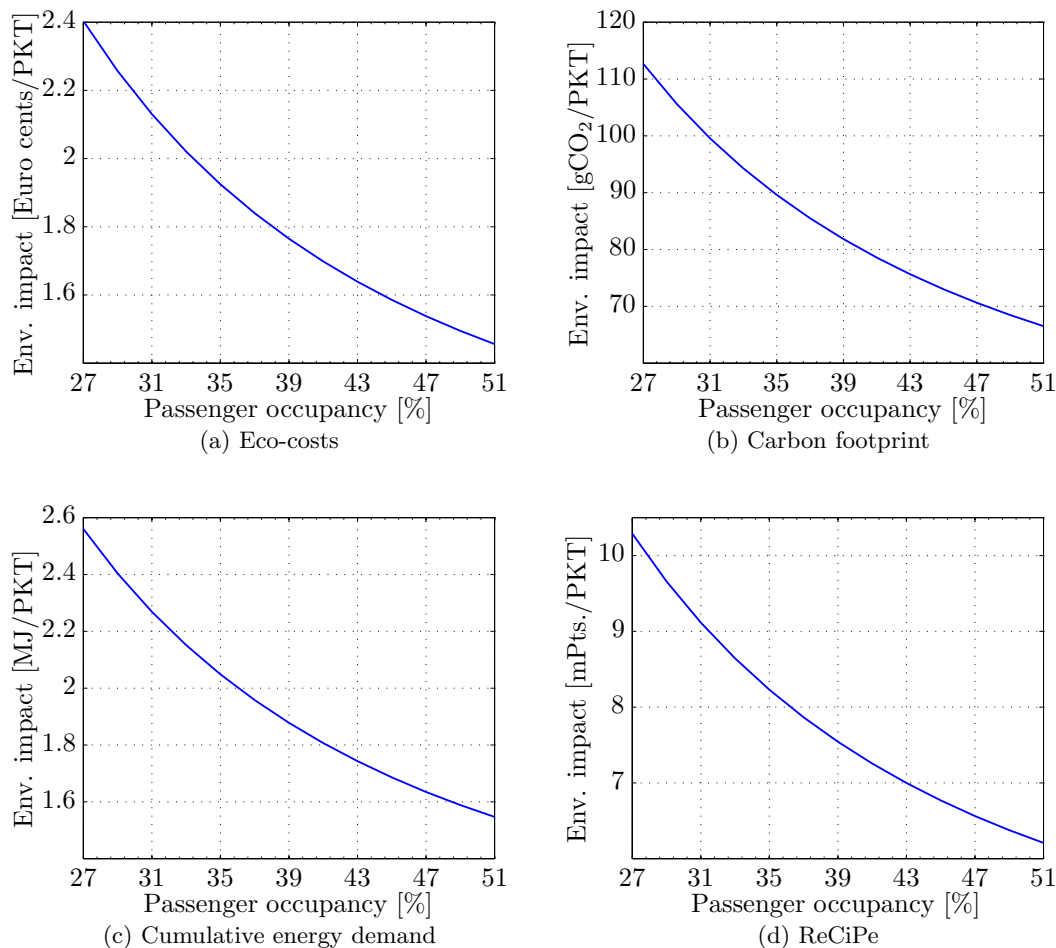


Figure 6.8: Sensitivity to passenger occupancy.

The environmental impact of the Superbus transport system for passenger occupancies ranging from 27% to 51% can be found in Figure 6.8. From the figure, it can be seen that the environmental impact is inversely proportional to the passenger occupancy. A 30%

decrease in passenger occupancy results in about 31% increase in environmental impact. A 30% increase in passenger occupancy results in about 20% decrease in environmental impact.

6.6.2 Supertrack velocity

By recalling Equation 6.6, it can be seen that the power consumption of the Superbus vehicle during the operational phase is determined by the driving speed. At the same time, it is known that the operational phase of the Superbus system has the largest contribution to the environmental impact of the transport system. This section will therefore examine the effect of driving speed on the environmental performance.

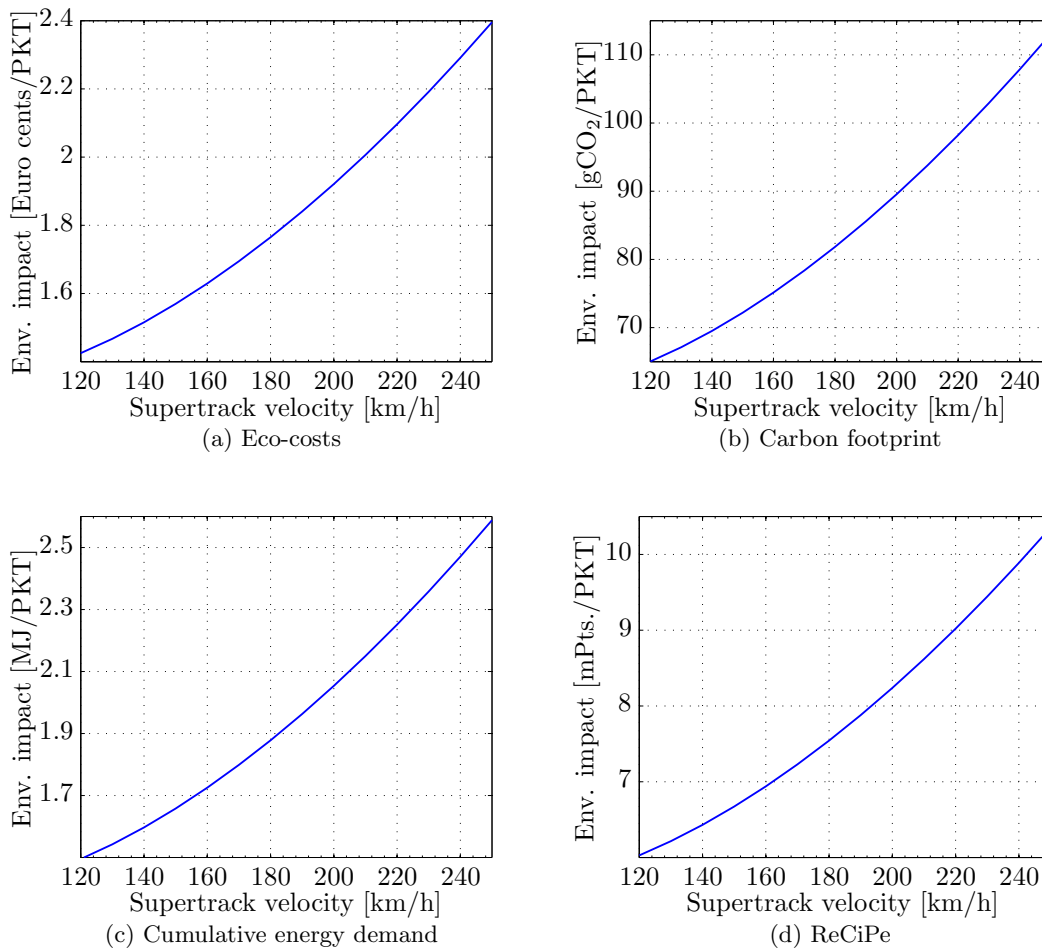


Figure 6.9: Sensitivity to Supertrack velocity.

The total environmental impact of the Superbus system for a speed range of 120 to 250 km/h can be found in Figure 6.9. The shape of the figure is induced by the cube of velocity in Equation 6.6. It can be seen that the environmental performance is highly influenced by the Supertrack velocity. For example, an increase in velocity from 180 to 250 km/h, will increase the environmental impact by 35-38% for the different impact methods.

6.7 Comparison with other studies

Finally, the results can be compared with results of others studies. Of special interest is a Dutch study in which the indirect energy requirements of road transport are calculated from an IO-LCA and a process-LCA perspective [Bos, 1998]. According to the study, the indirect energy requirements of a 40-tons truck with an empty weight of 14.3 tons are 946 GJ. The embodied energy of Superbus with an empty weight of 7.2 tons excluding battery is 1005 GJ. The weight of the truck in the Dutch study is 63% higher, the embodied energy is 6% lower. The indirect energy requirements of Superbus are comparable to that of a 40-tons truck. It should be mentioned that the battery is not included in this figure for embodied energy of Superbus. Moreover, in the Dutch study, the energy requirements connected to manufacturing of an *average* Dutch road are calculated as 33.1 TJ per kilometre for IO-LCA and 25.2 TJ per kilometre for process based LCA. The difference of 7.9 TJ between both approaches is caused by the fact that small bridges and other constructions are included in the first number. The embodied energy of the Supertrack including maintenance is 21.6 TJ. Hence, the indirect energy requirements for construction of the Supertrack are 14% lower than an average Dutch road.

Another relevant study is a study by Chester and Horvath [2009b]. The study concerns a life cycle assessment of an electric bus with an empty weight of 11.3 tons. According to Chester and Horvath [2009b], the manufacturing energy of the electric bus is 1900 GJ. If the embodied energy of the battery is included in the present study, an indirect energy requirement of 2231 GJ can be found. The difference is mainly caused by the relatively large battery of Superbus of 3751 kg. It is worth noting that the operating characteristics of the electric bus where set at a vehicle life of 12 years during which $0.67 \cdot 10^6$ passenger-kilometres are transported annually. Superbus, on the other hand, has an expected lifetime of 4.4 years with an annual PKT of $2079 \cdot 10^6$.

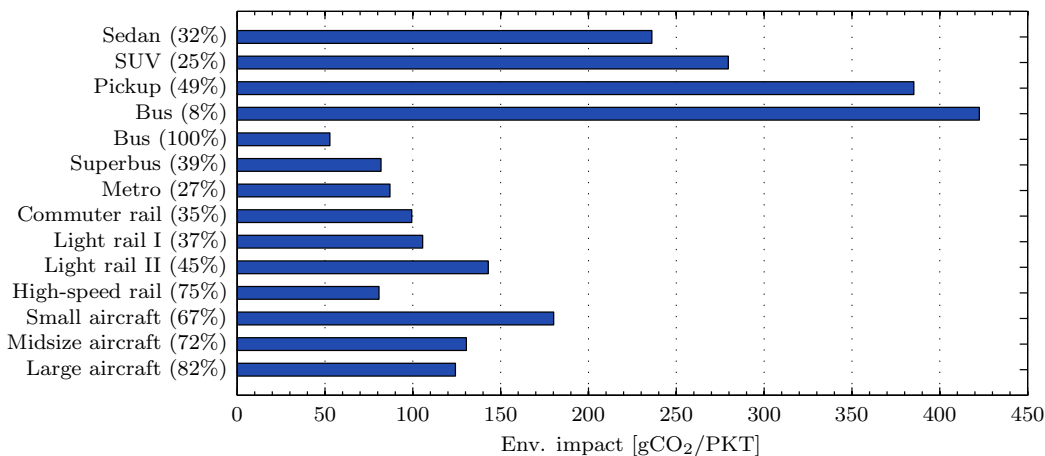


Figure 6.10: Summary modal environmental performance [Chester, 2008].

A third relevant study concerns the life cycle analysis of the construction of a road with a 165 mm thick asphalt layer and 250 mm concrete aggregate [Vogtländer et al., 2010]. According to the study, the associated eco-costs for this road are €21.7 for the construction of 1 m² road. In the present study, an impact of about €22.2 euro is found if the sand

layers, Winnerway and step barrier are excluded from the calculations. Thus, the results by [Vogtländer et al. \[2010\]](#) and the present study are comparable.

If the environmental performance of Superbus from [Figure 6.7](#) is compared with [Chester and Horvath \[2009a\]](#), it can be seen that the CO₂ emissions of the Superbus system are comparable with the emissions of commuter and light rail systems, see [Figure 6.10](#). Moreover, similar contributions of the different life cycle phases are found. [Chester and Horvath \[2009a\]](#) derives that the contribution of the operational phase for on road modes is 65-75%. The share of the operational phase in the present study is about 73%. Also, [Chester and Horvath \[2009a\]](#) determined that infrastructure construction was found to have major energy implications in terms of absolute values, the share with respect to the use phase is negligible. Similar conclusions can be drawn from the results in the present study.

Comparison of powertrain alternatives

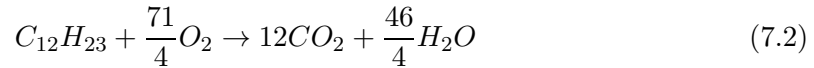
In Chapter 4, a study was conducted about the environmental life cycle impacts of an electrically powered Superbus. The results of this study revealed some important advantages and disadvantages of the electric propulsion system. For example, it was found that due to the electric powertrain, the transport system holds great potential for significant reduction in the environmental impact by switching to alternative, sustainable sources of electricity like photovoltaics and/or wind energy (see Figure 6.7). This advantage is of particular importance in view of the depletion of fossil fuels which in recent years became an important incentive to develop new ways to produce energy and meet societies transport needs. Main disadvantages were found in the large impact associated with the batteries that are required to support the transport system. The limited specific density of the current generation batteries add additional challenges regarding driving range and volumetric limitations. Moreover, charging of such large batteries is still in its infancy, particularly in relation to quick charging and its impact on cycle life.

Because of the disadvantages that are associated with electric driving, the question arises as to how other forms of propulsion compare with the electric powertrain of Superbus. In particular, it is important to evaluate diesel and natural gas because these fuels are currently the most commonly used for public road transport. Of these two fuels, natural gas is often considered as the sustainable alternative because of the smaller amount of carbon dioxide that is emitted during combustion. This can be demonstrated by calculating the amount of carbon dioxide that is produced for the production of one MJ of energy.

Since natural gas contains about 80% methane [van Vlijmen, 2011], its combustion can be approximated with the combustion equation of methane, see Equation 7.1. It can be seen that one mole of carbon dioxide is produced during the combustion of one mole of methane. Using the molar mass, density and specific energy of methane (see Table 7.1), it is calculated that 54.6 g CO₂ is produced to obtain one MJ of energy from combustion.



A similar calculation can be done for diesel fuel which is composed of about 75% saturated hydrocarbons with an average chemical formula of $C_{12}H_{23}$. From the combustion equation of diesel fuel, see Equation 7.2, it is determined that the combustion of one mole of diesel produces twelve moles of carbon dioxide. From the molar mass, density and specific energy of diesel fuel (see Table 7.1), it is calculated that 75.6 g of CO_2 is emitted to obtain one MJ of energy from combustion.



Above results show that there is about 25% less CO_2 produced during the combustion of natural gas. However, the calculations also reveal a major shortcoming of natural gas, i.e. its specific energy is about 1000 times smaller than the energy density of diesel fuel. Obtaining a similar amount of energy from natural gas will therefore require a volume which is approximately 1000 times larger than the volume of diesel fuel. Therefore, natural gas is usually compressed and stored in large cylindrical storage tanks. When compressed, natural gas is usually referred to as compressed natural gas (CNG). The molar mass, density and specific energy of CNG assuming a final pressure of 200 bar are shown in Table 7.1.

Table 7.1: Alternative fuel properties [van Vlijmen, 2011].

Fuel	Molar mass [kg/mol]	Density [kg/m ³]	Calorific value [MJ/m ³]	CO₂ emissions [g/MJ]
Diesel	0.167	837	35916	75.6
Methane	0.016	0.717	36	54.6
Natural gas	0.019	0.833	31.65	63.9
CNG (200 bar)	0.019	167	6330	63.9

In addition to diesel and natural gas, there is an increasing interest for biofuels. The main advantage of biofuels is the carbon neutral character during combustion. Disadvantages relate to the high land use for cultivation and the limited supply. For this reason, biofuels are currently not considered as a viable alternative to diesel, natural gas or electricity. It should be stated that current advances made in next generation biofuels have the potential to overcome these barriers as they utilize agricultural waste. However, the present study will not look into the impact associated with biofuels. Moreover, also fuel cells will not be considered due to time constraints.

A comparison of the electric, diesel and CNG powertrain requires a similar analysis as performed in Chapter 6. This chapter will again evaluate the alternative powertrains for a Supertrack velocity of 180 km/h. The different components of the diesel and natural gas powertrains and consequences for the operational phase will be elaborated in Section 7.1 and 7.2. Both sections will also address the contribution of refuelling of the diesel tanks and compression of the natural gas. The results of the analysis will be presented in Section 7.3.

7.1 Diesel

The environmental impact associated with the different life cycle components of a diesel operated Superbus is elaborated in this section. Consecutively, the impacts associated with powertrain manufacturing, the operational phase and refuelling are discussed in Section 7.1.1, 7.1.3 and 7.1.4.

7.1.1 Diesel powertrain

The material content and the resource requirements for manufacturing the diesel powertrain are elaborated in this section. Moreover, it is discussed how the impact database is used to obtain the environmental impact of component manufacturing. If possible, the material impact is assumed to be equal to the market mix impact.

Table 7.2: Mass balance of diesel and compressed natural gas powertrains.

Category	Component	Total mass (kg)
Powertrain, diesel	Engine	670
	Fuel storage system	80
	Exhaust	100
	Electrical components, powertrain	10
	Emission control electronics	10
	Transmission	293
Powertrain, CNG	Engine	450
	Fuel storage system (125 L) (4x)	160
	Exhaust	100
	Electrical components, powertrain	10
	Emission control electronics	10
	Transmission	293

Determining the material content of the diesel powertrain was found to be very challenging due to a lack of data. The mass balance that is shown in Table 7.2 is compiled using data of passenger cars, medium-sized trucks and own assumptions.

Engine

The diesel engine has a total mass of 670 kg. This corresponds to a power-to-weight ratio of 0.6 kW/kg [Weiss et al., 2000]. The material composition of an internal combustion engine is 50% cast iron, 30% cast aluminium, 10% steel, 4.5% plastic, 4.5% rubber and 1% copper [Burnham et al., 2006]. The energy requirements for manufacturing are 3 kWh per kg engine [G. W. Schweimer and M. Levin, 2000].

Fuel storage system

The mass of the fuel storage system depends on the capacity of the fuel tank and the length of the filling and supply piping. Based on the mass of similar systems in conventional passenger cars (55 kg) [Burnham et al., 2006] and own assumptions, the mass of the fuel storage system is estimated at 80 kg. The fuel storage system is made entirely from steel [Burnham et al., 2006] and the manufacturing is assumed to correspond with the database process 'rolling steel'.

Exhaust

The exhaust comprises a catalytic converter, muffler, heat shields and exhaust piping. The mass of the exhaust system is set at 100 kg based on the weight of the system in passenger cars (45 kg) and taking into account the additional required exhaust piping. The exhaust consist of steel and contains 2 grams of platinum to reduce the exhaust emission of volatile organic compounds, CO and NO_x [Burnham et al., 2006]. The manufacturing process of the exhaust system is assumed to correspond with the database process 'deep drawing' as this process resembles the manufacturing process of the exhaust piping.

Electrical components, powertrain

The electrical components of the powertrain have a total aggregated mass of 10 kg and contain the control wiring, sensors, switches and micro controllers required for operating the engine. The material composition is similar to the electronics for emission control and power regulation, i.e. 59% plastic and 41% copper [Burnham et al., 2006].

Electronics for emission control and power regulation

The system for emission control consist of sensors, micro controllers and engine emission feedback equipment. The system is manufactured from 59% plastic and 41% copper and has a total mass of 10 kg [Burnham et al., 2006].

Transmission

The total mass of the transmission is 293 kg [Detroit, 2008]. A transmission consist of 30% steel, 30% wrought aluminium, 30% cast iron, 5% plastic and 5% rubber [Burnham et al., 2006]. The energy requirements for manufacturing are 2.4 kWh/kg of electricity and 1.8 kWh/kg of heat [G. W. Schweimer and M. Levin, 2000].

7.1.2 Environmental impact diesel vehicles

The manufacturing impact of the diesel Superbus vehicles in terms of the carbon footprint can be found in Figure 7.1a. The eco-costs associated with manufacturing are 16.6 k€per vehicle. The carbon footprint, CED and ReCiPe are 50 tons of CO₂, 1032 MJ and 5.6 kPt respectively.

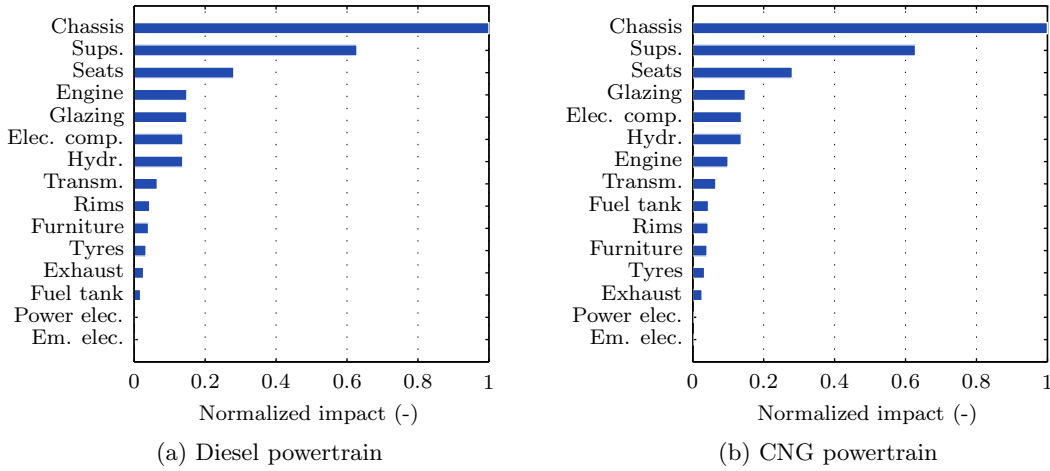


Figure 7.1: Impact of diesel and CNG vehicle components normalized to highest impact in category.

The construction impact of the diesel Superbus is about 3 to 10% higher compared to the impact of the electric vehicle excluding battery. Besides, no differences are observed in the relative importance of the different components, i.e. the chassis and suspension system still dominate the results.

7.1.3 Operational phase

The diesel energy consumption during the operational phase can be calculated using a similar approach as described in section 6.4. The overall efficiency of the diesel powertrain is hereby assumed to be 22%, which is relatively high compared to the efficiency of gasoline engines ($\eta_{thermal, gasoline} = 18\%$) [van Mierlo and Marenne, 2009]. The higher efficiency is caused by the higher compression ratio. The average fuel economy of the diesel powertrain, FE_{diesel} for a speed of 180 km/h is found as:

$$FE_{diesel} = 13.3 MJ/km \equiv 161 Wh/seat - km \quad (7.3)$$

The total fuel consumption of Superbus can be calculated by multiplying the average fuel economy with the distance travelled during the lifetime and dividing by the specific energy of the diesel fuel. The calorific value of diesel is given in Table 7.1. The total diesel consumption during the operational phase is equal to 517,141 litres.

The impact associated with the extraction and combustion of diesel is obtained from the impact database: 'Diesel incl. combustion', see Table A.1

7.1.4 Fuelling

The energy that is required for refuelling can be calculated by considering the power consumption of the fuel dispenser. The power consumption the compressor within the dispenser is 0.75 kW at a flow rate of 60 l/min [Shenzen Kaisai Electric Motor Co. Ltd.,

2010]. Using the results from Section 7.1.3, it can be calculated that 388 MJ is required for refuelling.

7.2 Compressed natural gas

7.2.1 CNG powertrain

The mass and composition of the CNG powertrain is assumed to be equal to the diesel powertrain except for the engine and fuel storage system, see Table 7.2. The material content and manufacturing energy requirements of both components are discussed below.

Engine

The CNG engine has a mass of 450 kg, which is about 33% lighter than the diesel engine due to the higher compression ratio. The power-to-weight ratio is 0.9 kW/kg [Weiss et al., 2000]. The material composition is 50% cast iron, 30% cast aluminium, 10% steel, 4.5% plastic, 4.5% rubber and 1% copper [Burnham et al., 2006]. The energy requirements for manufacturing are 3 kWh per kg engine [G. W. Schweimer and M. Levin, 2000].

Natural gas storage tank

The Hexagon Type 4 CNG cylinders with a volume of 125 L and a weight of 40 kg are assumed to resemble the storage tank of Superbus [Ragasco]. The tanks are made from a polyethylene cylinder that is contained within a carbon fibre composite that carries all the loads and an impact-absorbing foam that protects the tanks in the event of a crash. It is assumed that the storage tanks consist of 60% polyethylene, 35% carbon fibre and 5% foam. The FVF is assumed to be equal to 0.7. A total of four storage tanks are installed in the vehicle to give a total storage volume of 0.5 m³.

7.2.2 Environmental impact CNG vehicles

The manufacturing impact of the diesel Superbus vehicles in terms of the carbon footprint can be found in Figure 7.1b. The eco-costs associated with manufacturing are 16.5 k€/per vehicle. The carbon footprint, CED and Recipe are 49.5 tons of CO₂ equivalent, 1053 MJ and 5.6 kPt respectively.

7.2.3 Operational phase

Gas engines are generally less efficient than diesel engines. The typical efficiency of a gas engine is 18% [van Mierlo and Marenne, 2009]. The fuel economy for the compressed natural gas powertrain, FE_{gas} , is calculated as:

$$FE_{gas} = 16.3MJ/km \equiv 196Wh/seat - km \quad (7.4)$$

Based on the calorific value of natural gas, it can be calculated that at standard conditions, 543.4 m³ natural gas is required per vehicle per day. For isothermal conditions this corresponds to 2.72 m³ of natural gas per vehicle per day at a pressure of 200 bar. The total natural gas consumption during the operational phase is calculated as 772,352 m³.

The impact of the combustion of natural gas is obtained by considering the impact values of the database process 'Heat, natural gas', see also Table A.1.

7.2.4 Fuelling

The calorific value of natural gas is 1135 times smaller compared to the calorific value of diesel (31.65 MJ/m³ (LHV) versus 35916 MJ/m³). Usually, natural gas is therefore compressed to a pressure of about 200 bar and stored in gas tanks at the rear of the vehicle. For this purpose, a fast-fill compressor is used to rapidly fill empty gas tanks. If it is assumed that the compression takes place under isothermal conditions (gas is slowly compressed), the required work can be calculated from the ideal gas law: $pV = nRT$. The work from an initial state 1 to a final state 2 is found using Equation 7.5.

$$W_{1-2} = - \int_{V_1}^{V_2} p dV = - \int_{V_1}^{V_2} \frac{nRT}{V} = -nRT \ln \left(\frac{V_2}{V_1} \right) = -p_2 V_2 \ln \left(\frac{p_1}{p_2} \right) \quad (7.5)$$

Where p is the pressure, V the volume, n the amount of substance of gas and R the ideal gas constant. Moreover, for isothermal conditions $pV = p_1 V_1 = p_2 V_2$ and thus $\frac{V_2}{V_1} = \frac{p_1}{p_2}$.

From the main infrastructure data of the Dutch natural gas supply, it is found that the gas inlet pressure to the fuelling station is 8 bar [Energie Nederland, 2011]. Moreover, the natural gas is compressed to a pressure of 200 bar. The fast-fill compressor station uses an electrically powered gas compressors with an assumed efficiency of 96.6% [Wang and Huang, 1999].

From Equation 7.5, it is found that 64.4 MJ is required to store natural gas with an initial volume of 25 m² in a 1 m³ fuel tank at a pressure of 200 bar. The total required work for the compression of natural during the operational phase can found by considering the total gas consumption of Superbus and Equation 7.5. The total energy consumption of the compressor is 257 GJ.

7.3 Environmental impact powertrain alternatives

The environmental impact of the Superbus system utilizing diesel and CNG can be found in Figure 7.2. All results are normalized with respect to the amount of PKT transported as given by Melkert and Ockels [2006].

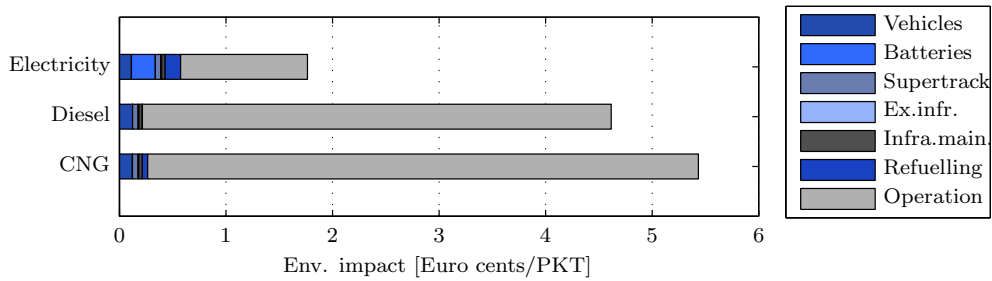
It can be seen that the diesel and CNG powertrains perform worse than the electric powertrain for all impact methods. The impact of the vehicle utilizing diesel is about 1.1 to 2.6 times larger for the different methods. For CNG, these figures increase to 1.5 to 3.1 times. The lower figures correspond with the CED method and can be explained by considering the fact that the results for electricity are based on the underlying efficiency of production, see also Table A.1. From Maclean and Lave [2003] it can be concluded that

the well-to-tank efficiency of diesel and natural gas is roughly 2.3 times higher compared to the well-to-tank efficiency of electricity. Efficiency is herein defined as: (energy in fuel delivered to consumers/energy inputs to produce and deliver the fuel).

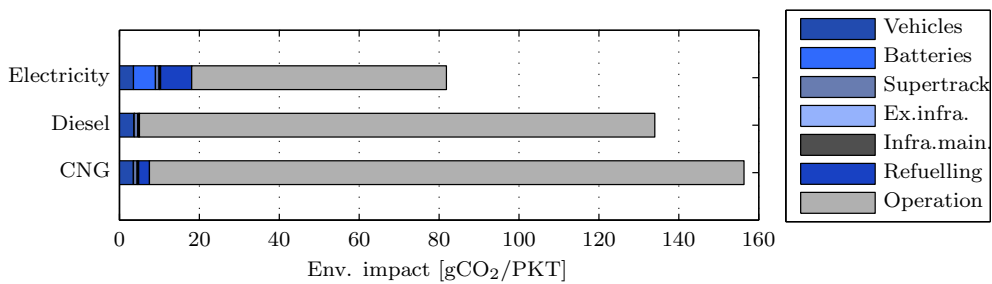
Remarkably, the normalized impact of the CNG powertrain is higher than the impact of the diesel powertrain even for the carbon footprint (recall the result the introduction of this chapter). This is caused by of the lower conversion efficiency of the natural gas powertrain which cancels the smaller amount of CO₂ per MJ.

The impact for natural gas compression is comparable to the impact caused by vehicle manufacturing. For the different impact methods, the contribution of compression is about 2%.

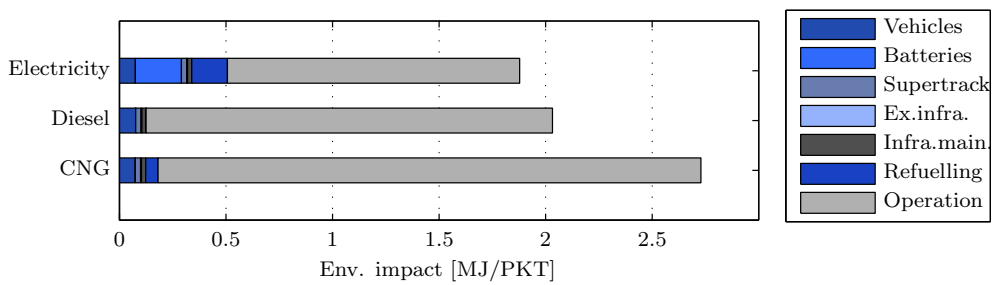
From Figure 7.2, it is found that the relative impact difference between the alternative powertrains and the electric powertrain for the eco-cost method is larger than the relative difference for the other impact methods. This is because the eco-cost method severely punishes the use of diesel and natural gas.



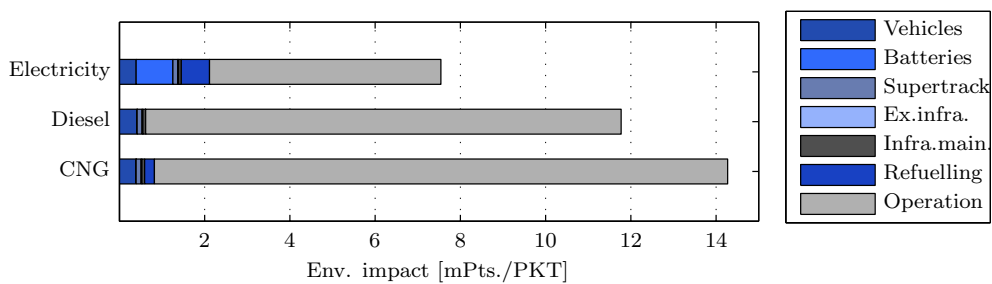
(a) Eco-costs



(b) Carbon footprint



(c) Cumulative energy demand



(d) ReCiPe

Figure 7.2: Environmental performance alternative powertrains.

Alternative transport modes

So far, the present study has dealt with the environmental performance of the Superbus transport system. Although Chapter 6 and 7 gave insight in the strong and weak points of the system, it is yet unclear how Superbus compares to other modes of transport in terms of environmental impact. This chapter will therefore elaborate the life cycle impacts of Superbus' competitors and compare the results with the findings of the previous chapters. The discussion includes the high-speed 'steel wheel on steel rail' train and the magnetic levitation train because the offered trip time savings and service level of these modes are roughly similar to Superbus.

The HST and Maglev evolved from the development of the high-speed train which spans a period of about 50 years. In general, the Japanese 'Shinkansen', which was the first modern HST in operation, is considered as the base model for both trains. The French TGV and German ICE resemble the Shinkansen in purpose but differ in design philosophy in that the most significant difference can be attributed to the ability of the TGV and ICE to run on conventional tracks. Modern high speed trains can operate at a maximum speed of 300 km/h, although the standard for new lines is even higher (350 km/h). The Maglev technology was first tested in the 1970s and is mostly associated with countries like China and Germany. The technology relies on electromagnetic forces to cause the vehicle to hover above the track and move forward at an operating speed of about 500 km/h. In China, a short Maglev line was opened with trains running at maximum speeds of 430 km/h.

As was stated in Chapter 5, the pivot of the analysis of the present study is the function and not the associated material product. Hence, comparing the environmental performance of the three transport modes comes down to comparing the way the different modes can fulfil the function. Therefore, the system characteristics of the transport modes should be chosen such that all modes move an equal amount of passenger-kilometres. This implies that all transport modes should have the same transport value for the given trajectory. Later, it will be determined for which passenger conditions the alternative transport modes are equivalent in terms of environmental performance.

To obtain a similar transport value, it is required to control several system parameters. In this study, the cruising speed, acceleration and intermediate stop distance are chosen as the controlling system parameters. Moreover, since Superbus offers point to point transport, pre and post transport is included in the analysis. The effects of transport value on the system characteristics will be elaborated in Section 8.3. It should be stated that in the present chapter, it is assumed that a maximum velocity of 250 km/h can be attained on the Supertrack. This is done because both alternative transport modes are designed to operate at a speed starting from about 250 km/h. Moreover, the analysis is confined to the carbon footprint of the alternative modes because it is observed from previous chapters that the choice of impact method does not give rise to a change in conclusions.

8.1 High-speed train

8.1.1 Train manufacturing

Train manufacturing and maintenance data is available from the impact database which is based on the study by [von Rozycki et al. \[2003\]](#). Stated values are used by [Chester and Horvath \[2010\]](#) to determine the impact of high-speed train manufacturing.

The material use for a German ICE train with a capacity of 672 seats can be found in Table 8.1. Moreover, about 2.2 TJ of electricity and 3.88 TJ of heat energy is required for manufacturing. This includes the energy that is required for enhancing the glass strength via tempering. Train manufacturing further requires 27.6 ton kilometre of transport by lorry and 110 ton kilometre of transport by rail.

[von Rozycki et al. \[2003\]](#) also provides data on high-speed train maintenance. In order to comply with the system boundaries that are presented in Figure 5.2, maintenance will only include the replacement of worn out steel wheels. As [von Rozycki et al. \[2003\]](#) does not state how much energy is required for wheel manufacturing, only material use is taken into account. The total expected mileage of the train is 8,000,000 kilometres.

Table 8.1: Mass balance of ICE high-speed train.

Material	Total mass [tons]
Steel	323
Aluminium	90
Copper	34.4
Polyethylene	155
Glass	25
Paint	12.6
Steel (maintenance)	45

The carbon footprint of high-speed train manufacturing that can be determined from Table 8.1 is 2,418 tons of CO₂. It follows that the emission per seat is 3,598 kg CO₂, which is about 75% higher than the per seat emission of Superbus.

The total carbon dioxide emissions for manufacturing are in accordance with the carbon footprint of the Shinkansen 300 series that is stated by [Miyachi and Tsujimura \[2005\]](#) and amount to 2,400 tons of CO₂. However, because the Shinkansen has a capacity of 1,323 seats, the per seat emission is about 50% lower compared to the per seat emissions of the ICE train. Although it is not clear how this large difference is caused, it is believed that a denser seat spacing of the Shinkansen plays an important role. The present study applies the impact values stated by the impact database.

8.1.2 Infrastructure

A high-speed rail track consists of the track bedding and the associated substructure. The track bedding comprises the rails (made of steel), the railroad sleepers (made of concrete reinforced with steel) and the standard gravel for the bedding. The substructure consists of bulldozed and compressed soil.

[von Rozycki et al. \[2003\]](#) analysed the life cycle material and energy use of the high speed track between Hannover and Wuerzburg. Table 8.2 summarizes the required material and energy requirements for the manufacturing of a two-way track and corresponding lifetime of the different materials. It is found that the mass balance is dominated by the large amounts of gravel that are required for the gravel bed and the concrete for the railroad sleepers. It should be noted that the overhead system, signalling infrastructure, train overtaking stations, noise screens and electric transformer stations are not included in the study of [von Rozycki et al. \[2003\]](#). The study concluded that these components do not contribute significantly to the life cycle resource consumption of the ICE transport system. The relevance of these system to the environmental can be assessed by considering the fact that only a small portion of the impact of these systems should be allocated to a single train. The reported material and energy requirements are in accordance with the system boundaries that were defined in Chapter 5.

Table 8.2: Per kilometre mass balance high-speed train infrastructure.

Material	Total mass [tons]	Lifetime (yr)
Steel (rail)	282	30
Concrete	990	30
Steel (reinforcement)	39	30
Gravel	7950	15

The transport distances of the materials to the construction site are assumed to be similar to the distances stated in Section 6.3. The transport distance of steel is assumed to be 100 kilometres [[van der Wall Bake and Spriensma, 2010](#)]. Moreover, all transport is assumed to be carried out by train [[Molenaar and Houben, 2011](#)].

The embodied per kilometre carbon dioxide emissions of the rail infrastructure is found as 780 kg. Taking into account the lifetime of the different infrastructure layers, the carbon footprint due to manufacturing is found as 30.5 kg CO₂ per meter per year. The difference with the impact database (42.1 kg CO₂ per meter per year) is due to bridges and tunnels that are included in the database, i.e. 7% tunnels and 3% bridges [[Spielman et al., 2007](#)].

Hence, referred to one year, the environmental impact of the ICE infrastructure is about three times higher than the impact of the Supertrack.

8.1.3 Operation

The environmental impact during the operational phase of the high-speed train is determined by the energy that is consumed at the level of the overhead lines. The energy consumption arises from the required traction energy, as well as the board energy that is needed for air conditioning, lighting and operating the train restaurant. Moreover, energy is lost in the motors, the on board transformers and through transport of electricity through the overhead wires and distribution system. This section analyses the energy consumption of a high-speed train as given by literature.

The energy consumption of a high-speed train is determined by a variety of parameters which include travelling speed, intermediate stop distance, acceleration, vehicle mass, shape, etcetera. Reported values on energy consumption should therefore be treated with care and underlying assumptions should be known to review the performance the train in terms of energy consumption.

It should be stated that comparing the different trains in terms of consumed energy per seat kilometre, incorporates a comparison of the specific space utilisation of a particular vehicle design and not on the actual system characteristics. It would be better compare the energy consumption per usable interior area kilometre. However, as this approach unnecessarily complicates the following analysis, all figures are normalized per seat kilometre. It should however be kept in mind that a specific seat arrangement may affect the value of the mode of transport and thus induces a different transport demand.

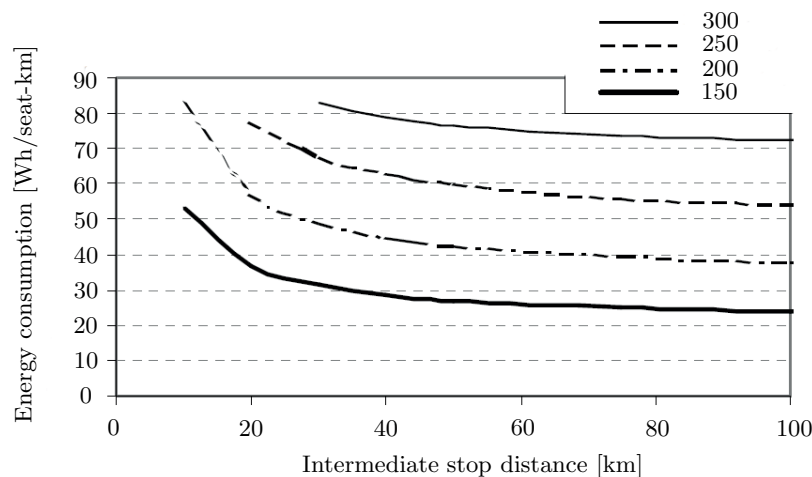


Figure 8.1: Primary specific energy consumption of Thalys as a function of intermediate stop distance for 300, 250, 200 and 150 km/h [van den Brink et al., 2001].

The specific energy consumption of the high-speed train that is reported in the strategic environmental assessment of the Zuiderzeelijn is 56 Wh/seat-km for a speed of 260 km/h and 47 kilometre between intermediate stops. The specific energy consumption is based on a study that has been conducted by the RIVM in which the characteristics of the

high-speed train are assumed to be equal to the 'Thalys', a train which is based on the French TGV [van den Brink et al., 2001]. An overview of the primary specific energy consumption for different intermediate stop distances and different speeds can be found in Figure 8.1. The primary consumption includes distribution losses and powerplant losses with an assumed overall efficiency of 85%.

The energy consumption at the overhead lines at a speed of 250 km/h and an intermediate stop distance of 50 kilometres can be derived from figure 8.1 and equals 50.2 Wh/seat-km. It should be stated that this figure does not include the potential from regenerative braking.

Another, extensive study on the energy consumption of seven high-speed trains, is conducted by Svånå [2011]. The study comprised an evaluation of the energy consumption in several scenarios, e.g. different passenger loads, track gradients, speeds, etc. An overview of the specific energy consumption for a track gradient of 0‰ at different maximum speeds including regenerative braking can be found in Table 8.3. It can be observed that the specific energy consumption of the ICE 3, ICE T and AGV trains is substantially lower compared to the other five trains. This is caused by the weight savings that are obtained by distribution of the traction system along the carriages of the train. These distributed traction systems are referred to as electric multiple unit (EMU) and enable the tractive axles to deliver the required traction without executing heavy axle loads. As a result, the power electronic components of the system can be relatively lightweight. In power-centralized systems on the other hand, the locomotive requires high axle loads to successfully pull all carriages without slipping or skidding. Lightweight power electronics can therefore not be applied.

Table 8.3: High-speed train specific energy consumption for a 0‰ track gradient and a 500 km intermediate stop distance [Svånå, 2011]

Speed [km/h]	Specific energy consumption [Wh/seat-km]						
	ICE 3	ICE T	TGV POS	Talgo 250	Talgo 350	AGV	SJ X2
220	28.76	31.70	34.85	41.96	34.46	28.06	40.47
250	32.79	33.64	40.55	48.26	39.04	31.36	n/a
280	37.64	n/a	47.41	n/a	44.66	35.47	n/a
300	41.52	n/a	52.70	n/a	49.18	38.76	n/a
330	47.31	n/a	57.92	n/a	55.99	46.68	n/a

The average specific energy consumption of trains with an EMU at a speed of 250 km/h is 32.6 Wh/seat-km, whereas trains with a centralized power system have a specific energy consumption of 42.6 Wh/seat-km. All figures include the potential from regenerative braking to recover energy from the braking phases of the trip.

Svånå [2011] also addressed the influence of intermediate stops on the specific energy consumption. The stop quantity factor that was defined in his study increases linearly with increasing number of stops for speeds below about 280 km/h. The linear increase in energy consumption for decreasing stop distance is also observed in Figure 8.1 for stop distances larger than 40 km. For an intermediate stop distance of 50 kilometre, the stop quantity factor is found as 1.035. Applying this factor to the figures stated in Table 8.3,

it can be obtained that trains with an EMU consume about 33.7 Wh/seat-km trains with a centralized power system about 44.1 Wh/seat-km.

The previously mentioned study by von Rozycki et al. [2003] also evaluated the energy consumption of the German ICE 1 and ICE 2 trains. These trains can reach speeds up to 250 km/h and are equipped with a power centralized system with regenerative braking. von Rozycki et al. [2003] report an average traction and board energy consumption of 22.5 kWh/km and 1.35 kWh/km respectively. This is equal to a specific energy consumption of 35.5 Wh/seat-km assuming 672 seats per train. Comparing this number with the specific energies of non-EMU trains given by Svåná [2011], a 19.5% difference is found. This is probably due to the efficiency of the motors and transformers that are not included in the calculations of von Rozycki et al. [2003]. Assuming a similar efficiency as Svåná [2011] ($\eta = 0.85$), the specific energy consumption of the ICE train becomes 41.8 Wh/seat-km.

Miyauchi and Tsujimura [2005] assessed the energy consumption of the Japanese Shinkansen 300 high-speed train. For a maximum speed of 270 km/h, the average energy consumption is reported as 45.5 kWh/km for non-regenerative braking. Since the Shinkansen 300 series has a passenger capacity of 1323 passengers, the specific consumption is 34.4 Wh/seat-km. This number largely differs from the values stated in the previous studies. However, it is unclear how this difference is caused. As stated previously, a possible reason might be a more dense spacing of the seats in the Shinkansen trains. For example, reducing the number of seats with 10% will increase the specific energy consumption to 38.2 Wh/seat-km.

All in all, it can be concluded that the results of the calculations performed by van den Brink et al. [2001] are relatively conservative regarding the energy consumption of the high-speed train. More recent studies show that developments in the twelve years that followed after the study have led to a decrease in specific energy consumption. Using the value from van den Brink et al. [2001] therefore result in conservative approach.

In addition to the energy consumption from station to station, an additional amount of energy is consumed during pre and post transport of passengers. This energy should be included in the calculations of the environmental impact of the high-speed train in order to comply with the function statement in Chapter 5.

In general, the average distance to an important transfer station is 10.5 km [Centraal Bureau voor de Statistiek (CBS), 2012]. An overview of the modes of transport that are used for pre and post transport and corresponding share can be found in Table 8.4. It can be seen that a large amount of passengers (61.3%) travel with a transport mode with negligible environmental impact (foot and bike). In the calculations, it is assumed that all passengers travel 10.5 km by car from and to the station as a driver. As such, pre and post transport resembles a worst case scenario.

8.2 Magnetic levitation train

8.2.1 Train manufacturing

Only few data is available with regard to train manufacturing of the Maglev. Kato et al. [2003] estimated the manufacturing impact of the Maglev train by comparing the

Table 8.4: Train pre and post transport [van Boggelen and Tijssen, 2007].

Transport mode	Share [%]
Foot	36
Bike	25.3
Bus, tram, metro	24.6
Car	11.5
Cab	0.7
Other	0.7

manufacturing costs of the Maglev with the Shinkansen high-speed train. According to the study, the carbon dioxide emissions associated with production of a 1,000 seat Maglev train is 2,100 tons CO₂. If this number is compared to the manufacturing impact of the high-speed train given in Section 8.1.1, Maglev train manufacturing impact is 13% smaller. This difference is mainly caused by the propulsion system which is not part of the Maglev train, but is rather part of the infrastructure. Because of a lack of data, the impact stated by Kato et al. [2003] is used as a reference. The lifetime of the train is assumed as 8,000,000 kilometres.

Kato et al. [2003] also report maintenance and repair impact of the Maglev trains. Reported value were determined from Shinkansen impact data. The carbon footprint due to manufacturing is estimated as 1,300 kg CO₂. It is not stated what type of maintenance is included in this figure. In general, it is expected that maintenance of the Maglev is less intensive compared to high-speed trains because the Maglev is levitated from the infrastructure. The impact due to maintenance is therefore assumed to be zero. This assumption is in accordance with the system boundaries which only considers replacement tyres (Maglev has none).

8.2.2 Infrastructure

The functional requirements of the Maglev infrastructure are very different compared to the functional requirements of the high-speed train infrastructure in that the Maglev infrastructure does not only provide a smooth interface to enable high-speed travelling, but also comprises the propulsion system of the trains. The environmental impact of this structure is therefore expected to be larger than the impact of the high-speed train infrastructure.

Kato et al. [2003] evaluated the carbon footprint of the standard sections of the Maglev test line in Yamanashi. The environmental load of the different sections was obtained from the Shinkansen infrastructural impact. An overview of the carbon footprint of the soil structure and the elevated bridge can be found in Table 8.5. The lifetime of both structure is given as 60 years.

From table 8.5 it can be seen that the carbon dioxide emissions of the elevated bridge are about 90% higher compared to the emissions associated with a soil structure. This difference can be explained by the additional amount of concrete that is required to lift the Maglev infrastructure, see Figure 8.2. It was already shown in Section 6.3.2 that concrete has a very high environmental load in terms of carbon dioxide emissions.

Table 8.5: Carbon dioxide emissions of different Maglev infrastructure bodies.

Structure type	Env. impact [tons CO ₂ /year-km]	
	Construction	Maintenance/repair
Soil structure	32.3	1.5
Elevated bridge	61.3	2



(a) Elevated bridge



(b) Soil structure

Figure 8.2: Two examples of Maglev standard main bodies.

If the environmental impact associated with the construction of the Maglev infrastructure is compared to Supertrack and high-speed train infrastructure, it is found that the impact is on par with the high-speed train. Due to a lack of data, the impact stated by [Kato et al. \[2003\]](#) is used in the present study.

8.2.3 Operation

Because the magnetic levitation train is still in its infancy, relatively little is known about the practical energy consumption during operation. Therefore, this study adopts the values given by [van den Brink et al. \[2001\]](#). An overview of the primary specific energy consumption for the Maglev as a function of intermediate stop distance can be found in [Figure 8.3](#). The primary consumption includes distribution losses and powerplant losses with an assumed overall efficiency of 85%. According to the figure, the specific energy consumption at an intermediate stop distance of 50 km equals 37.5 Wh/seat-km.

8.3 Environmental impact alternative transport modes

To compare the different transport modes using the data that was derived in the previous sections, it is necessary to determine the system characteristics of the high-speed train and Maglev. For example, it should be determined how many trains are required to enable the transport of the given amount of passenger kilometres. Moreover, the impact during the operational phase should be determined from the amount of vehicle kilometres that are travelled during operation. The system characteristics for the high-speed train and Maglev are derived from the available data given by [Melkert and Ockels \[2006\]](#). Using this data seems legitimate as Superbus was modelled as a train with a strand of stops.

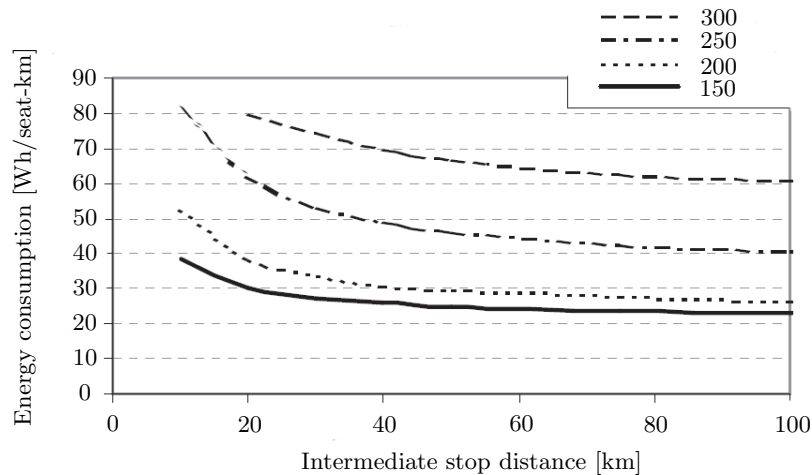


Figure 8.3: Primary specific energy consumption of Maglev as a function of intermediate stop distance for 300, 250, 200 and 150 km/h [van den Brink et al., 2001]

Melkert and Ockels [2006] determined that 4899 effective vehicle hours are required to transport the given amount of passengers. This number was increased with 28% to compensate for the empty trips that result from the demand driven scheduling to give 6764 vehicle hours. Based on the morning peak, this schedule requires a fleet of 673 vehicles. By multiplying the amount of vehicles with the number of seats per vehicle and the average daily driving distance which equals 1055 km, it can be calculated that a capacity of $1.63 \cdot 10^7$ seat-kilometres are required during operation.

Because the scheduling of the high-speed train and Maglev is supply driven, less amount of empty rides are required. If an additional 10% of train hours are assumed, the required train capacity is equal to an equivalent of 542 Superbuses, or 12466 seats. This is equal to $1.32 \cdot 10^7$ seat kilometres.

The train manufacturing impact of the high-speed train and Maglev can be calculated by multiplying the per seat impact from Section 8.1.1 and 8.2.1 with the required number of seats. Moreover, the impact due to operation can be obtained by multiplying the impact per seat kilometre with the required number of seat kilometres. Subsequently, the impact should be normalized with respect to the number of passengers kilometres given by Melkert and Ockels [2006].

Figure 8.4 shows the total carbon footprint of the different transport alternatives. The carbon footprint of Superbus corresponds to a Supertrack speed of 250 km/h utilizing an UCTE electricity mix, see Section 6.6.2.

From Figure 8.4 it can be seen that Superbus has the highest normalized carbon footprint, i.e. the CO₂ emissions associated with the high-speed train and Maglev are 50% and 62% smaller. This difference is mainly caused by the relatively large impact associated with the operational phase of Superbus, i.e. the impact of the operational phase of Superbus is 1.9 and 2.5 times larger than the impact of the operational phase of the HST and Maglev respectively. In addition, the required batteries for the Superbus public transport system have a significant contribution to the total environmental impact.

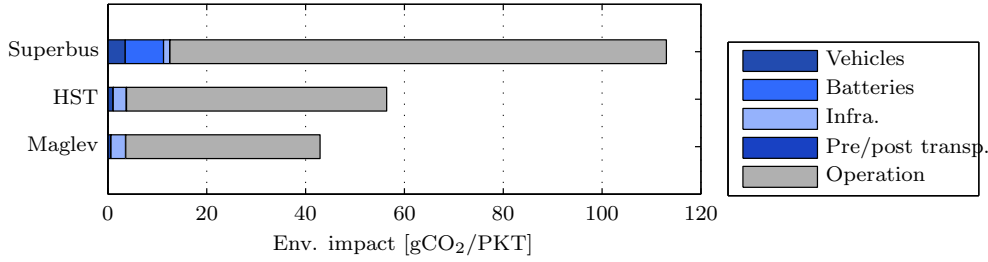


Figure 8.4: Environmental performance alternative transport modes.

The difference associated with the operational phase is mainly caused by the relatively high ratio of $C_D A$ to the number of passenger seats S of Superbus, see Table 8.6. The ratio for Superbus is about 1.5 and 3.1 times larger for the HST and Maglev respectively.

Table 8.6: Superbus, HST and Maglev system characteristics.

	Superbus	HSL	Maglev
length [m]	15	200	104
m_{empty} [tons]	13	385	198
$m_{payload}$ [tons]	1.6	26.8	23.9
$m_{empty}/m_{payload}$ [-]	8.1	14.4	8.3
C_D [-]	0.3	1.17	0.38
A [m ²]	4.2	11.8	15.5
Number of seats S [-]	23	377	336
$C_D A/S$ [m ²]	0.055	0.037	0.018
Seat area ¹ [m ²]	1.66	1.4	1.1

Given the results of Figure 8.4, it can be stated that in order for Superbus to have a competitive environmental impact, the overall passenger occupancy of the Superbus system should be higher than the passenger occupancy of the HST and Maglev. Stated differently, for an equal or lower carbon footprint, the passenger occupancy of the high-speed train and Maglev should be about 2 to 2.6 times smaller than the passenger occupancy of Superbus.

According to Melkert and Ockels [2006], the Superbus transport system creates a demand which is about 2.5-2.9 times higher compared to the demand of the HST and Maglev. In these calculations, the operating speed of the HST and Maglev is assumed as 250 and 400 km/h respectively. Hence, if these figures also hold for lower operating speeds, the higher passenger occupancy of Superbus offsets its larger environmental impact for the HST. For the Maglev, this is not so sure.

However, rebound effects might offset the beneficial effects of the Superbus system. Rebound effect refers to the behaviour or systemic responses to the introduction of new

¹Concerns a fictitious value which is calculated by dividing the outer surface (width · length) by the number of seats. The actual surface is smaller. The length of the HSL and Maglev is reduced with the length of two motor carriages.

technologies that increase the efficiency of resource use. Therefore, more accurate analysis are required to assess the effect of travelling velocity on transport demand.

Optimizing the Superbus public transport system

In this chapter, the opportunities for reducing the environmental impact of the Superbus public transport system are discussed. The discussion is based on a Supertrack speed of 250 km/h as this is the foreseen driving velocity of the system. This chapter builds on the discussion presented in Chapter 6 on the utilization of sustainable electricity sources which was found to be a very effective way of reducing the environmental impact.

Although the performed calculations enable the exploration of the effectiveness of the various reduction measures, detailed analysis should follow for almost every option. For example, reduction of the drag coefficient can only be obtained by carefully analysing the aerodynamic flow over the vehicle. Such detailed analyses are however out of the scope of the present study. The effect of all reduction measures is calculated with respect to the carbon footprint.

A design option tree for a variety of impact reduction measures can be found in Figure 9.1. The figure also shows the relative importance of the various life cycle components of the Superbus system. As was previously determined, the operational phase dominates the life cycle impact for an UCTE electricity mix. In case of electricity from wind energy, the batteries are the dominating component.

9.1 Opportunities vehicle manufacturing

9.1.1 Chassis material

From Section 6.1.3, it is known that the chassis and bodywork of the vehicle are manufactured from CFRE. Although the material properties of CFRE are superior to several properties of other lightweight materials (see Table 9.1), its environmental impact is relatively high. This raises the question whether the potentially lower impact of a chassis

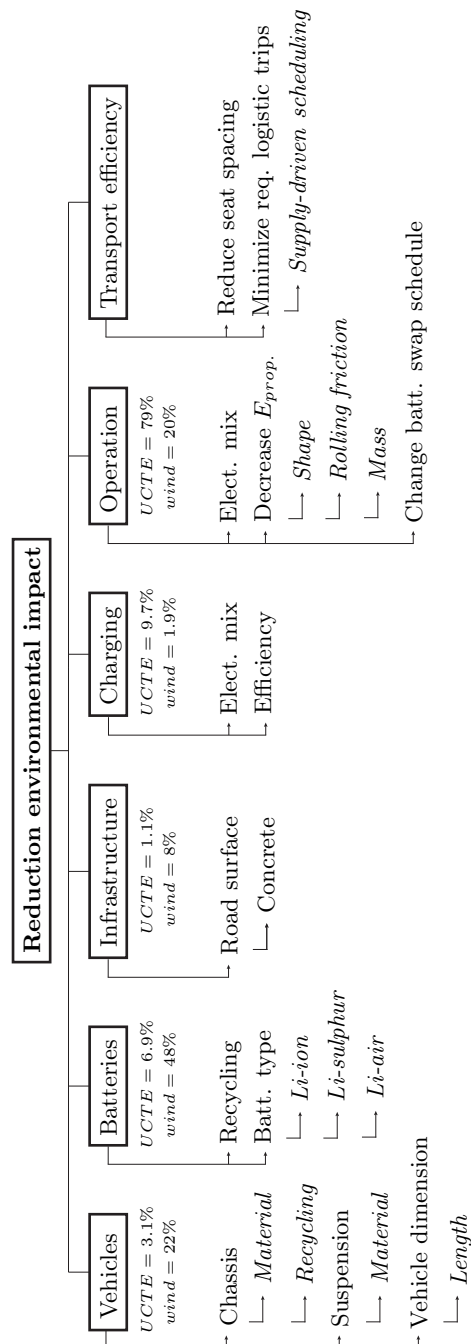


Figure 9.1: Design options tree for reduction measures.

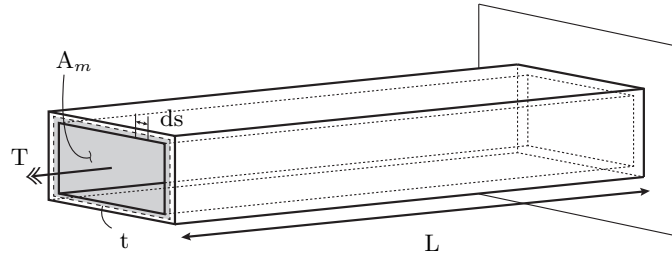
made from another (lightweight) material, offsets the increase in energy consumption during the operational phase that arises from the additional mass that should be moved. In this section, the environmental impact of the CFRE chassis is therefore compared with the impact of a chassis made from aluminium, magnesium, titanium and high-strength steel (HSS). The comparison is based on the required torsional and bending stiffness of the chassis.

Table 9.1: Physical properties of various lightweight materials.

Material	ρ [kg/m ³]	G [MPa]	σ_{yield} [MPa]
CFRP	1.8	37	1200
Aluminium	2.7	27	350
Magnesium	1.7	140	130
Titanium	4.5	44	830
High strength steel	8	80	1200

Torsion

As the torsion stiffness is one of the most important requirements, it is the first requirement that should be satisfied before evaluating and optimizing the bending stiffness and strength of the material. According to the principle of St. Venant, the torsional rigidity, $\frac{T}{\theta}$, of the thin-walled beam shown in Figure 9.2 is given by Equation 9.1. The required torsional rigidity of the chassis is 30 kNm/degree.

**Figure 9.2:** Torque T applied to a thin-walled beam.

$$\frac{T}{\theta} = \frac{4A_m^2 G t}{L} \frac{1}{\oint ds} \quad (9.1)$$

In Equation 9.1, T is the resultant internal torque at the cross section, θ is the angle of twist, A_m is the mean area enclosed within the boundary of the centreline of the beam's thickness, G is the shear modulus, t is the thickness of the beam (assumed to be constant), L is the length of the beam and s is the length of the entire boundary of the beam's cross-sectional area.

Equation 9.1 can be rearranged to give an expression for the wall thickness of the beam, see Equation 9.2.

$$t = \frac{TL}{4A_m^2 \theta G} \oint ds \quad (9.2)$$

The mass of the torsional loaded beam, $m_{torsion}$, can be found by multiplying the material volume with its density ρ , see Equation 9.3.

$$m_{torsion} = \rho t \oint ds = \frac{\rho}{G} \frac{TL}{4A_m^2 \theta} \left(\oint ds \right)^2 \quad (9.3)$$

From Equation 9.3, it can be seen that the mass of a beam that is loaded in torsion can be optimized by considering the quality factor $Q_{torsion} = \frac{\rho}{G}$, i.e. the ratio between the

material density and the shear modulus. The quality factor for torsion of the lightweight materials given in Table 9.1 can be found in Figure 9.3a. All factors are normalized with respect to CFRE. It can be seen that the quality factor of CFRE is on par with magnesium. Aluminium has a quality factor which is about 1.5 times larger compared to CFRE. High-strength steel has the highest quality factors of all materials, i.e. about 4.5 times larger than CFRE.

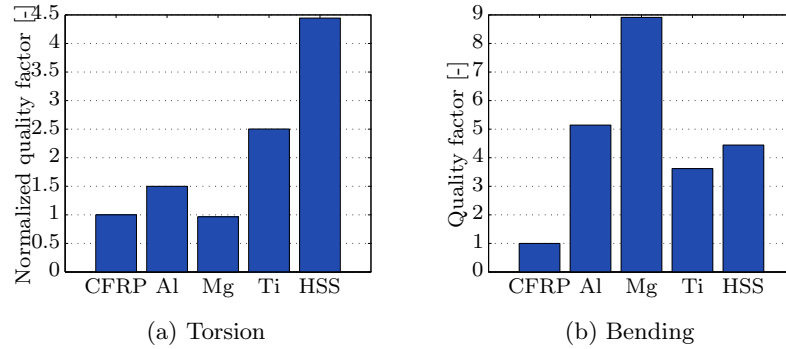


Figure 9.3: Quality factor normalized to CFRE for torsion and bending scenario.

From Figure 9.3 it can be concluded that in case of a torsional loading, a CFRE construction results in the lowest mass. However, Table A.1 shows that the environmental impact of CFRE is relatively high. For example, it is about three to nine times higher for the different impact methods compared to high-strength steel. From an environmental point of view, it is therefore required to assess the environmental impact of the different materials, $I_{torsion}$. This can be done by multiplying the quality factor of a material with its specific impact, $I_{specific}$, see Equation 9.4.

$$I_{torsion} = Q_{torsion} I_{specific} \quad (9.4)$$

Figure 9.4a shows the results which follow from equation 9.4. All numbers are normalized with respect to CFRE. It can be seen that in spite of the much larger mass of the HSS chassis, the environmental impact is the lowest of all lightweight materials for all different impact methods. CFRE has the second lowest impact for all impact methods except CED. Remarkable is the large environmental impact of magnesium and titanium for the eco-costs, carbon footprint and ReCiPe methods. The large difference is caused by the rarity of magnesium and titanium, causing 'material depletion' to have a relatively large effect on the impact scores.

Bending

A similar analysis can be performed for the bending stiffness of the chassis. In case of bending, it is required that the actual bending and shear stress in the chassis does not exceed the allowable bending and shear stress of the material. A bending design requires the determination of the chassis section modulus, which is the ratio of I and c . From the flexure formula $\sigma = \frac{M}{\sigma_{allow}}$, the section modulus is defined as:

$$S = \frac{I}{c} = \frac{M}{\sigma_{allow}} \quad (9.5)$$

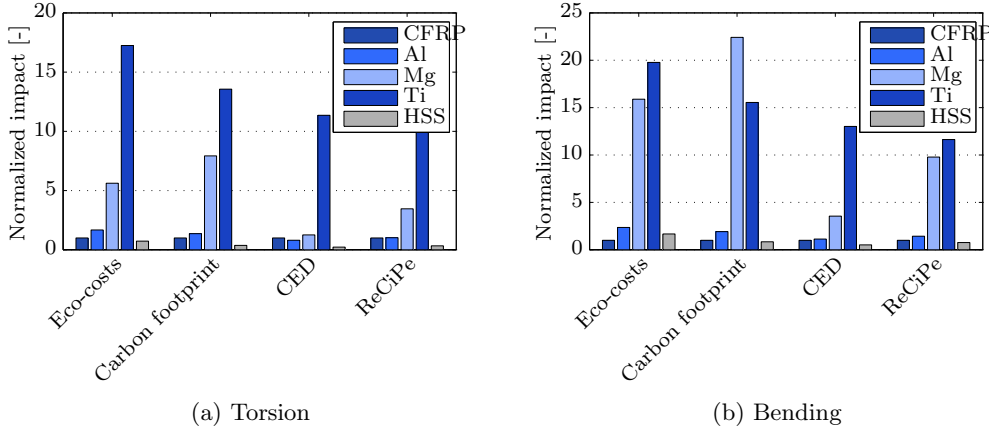


Figure 9.4: Effect of various lightweight materials on environmental impact chassis.

Where I is the moment of inertia of the cross section, c is the intermediate distance between the neutral axis and a point on the cross section, M is the internal moment determined from the beam's moment diagram and σ_{allow} is the allowable material stress, usually assumed equal to σ_{yield} .

The moment of inertia about the x axis of the thin-walled beam shown in Figure 9.2, can be determined using the parallel-axis theorem, see Equation 9.6. In this equation, A is the cross-sectional area with distance d_y from the neutral point, b is the beam width and h is the beam height. Because the beam is thin-walled, higher order terms of t are neglected.

$$I_x = \bar{I}_x + Ad_y^2 = 2 \cdot \left(\frac{1}{12}th^3 \right) + 2 \cdot \left(\frac{1}{12}bt^3 + bt \left(\frac{h}{2} \right)^2 \right) = \frac{1}{6}th^3 + \frac{1}{2}bth^2 \quad (9.6)$$

The thickness of the beam walls can be determined by substituting Equation 9.6 into 9.5, see Equation 9.7.

$$\frac{I_x}{c} = \frac{2 \left(\frac{1}{6}th^3 + \frac{1}{2}bth^2 \right)}{h} = \frac{M}{\sigma_{allow}} \rightarrow t = \frac{M}{\sigma_{allow}} \frac{1}{\frac{1}{3}h^2 + bh} \quad (9.7)$$

Consecutively, the mass of the beam, $m_{bending}$, can be found by multiplying the material volume with its density, see equation 9.8.

$$m_{bending} = \rho t \oint ds = \frac{\rho}{\sigma_{allow}} \frac{M}{\frac{1}{3}h^2 + bh} \quad (9.8)$$

From Equation 9.8 it can be seen that the mass of a (thin-walled) beam that is loaded in bending, can be optimized by considering the quality factor $Q_{bending} = \frac{\rho}{\sigma_{allow}}$, i.e. the ratio between the materials density and its allowable stress. The quality factor for bending of the lightweight materials given in Table 9.1 can be found in Figure 9.3b. All factors are normalized with respect to CFRE. It can be seen that CFRE has the lowest

quality factor. The quality factor of aluminium, titanium and high-strength steel are about equal.

Applying a similar approach as for torsion, the environmental impact of a chassis loaded in bending, $I_{bending}$, can be calculated from Equation 9.9:

$$I_{bending} = Q_{bending} I_{specific} \quad (9.9)$$

Figure 9.4b shows the environmental impact of the different lightweight materials for the different impact methods normalized to the CFRE impact. It can be seen that HSS is favourable in three of four impact methods. Moreover, the impact of magnesium and titanium is again much higher compared to CFRE, aluminium and HSS.

Effect on operational phase

From the above two sections it became clear that chassis and bodywork material has a large influence on the environmental impact. Of the five different materials considered, only high-strength steel has favourable impact characteristics. From Figure 9.3 it can be seen that the mass of a high-strength steel chassis is about 4.5 times higher than a chassis made from CFRE. Hence, does the reduced manufacturing impact of the HSS chassis offsets the increase in energy consumption during the operational phase that arises from the additional mass?

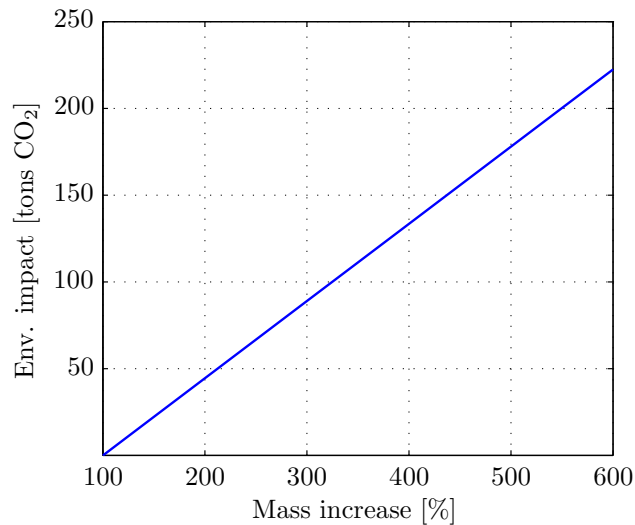


Figure 9.5: Additional CO₂ emissions caused by an increased chassis mass.

Figure 9.5 shows the additional carbon dioxide that is emitted during the operational phase as a function of an increase in chassis mass. It can be seen that a 4.5 times heavier chassis causes an increase in operational emissions of 156 tons. At the same time, it is known from Section 6.1.3 that the total carbon footprint of a Superbus vehicle is 47.4 tons of CO₂ and that the contribution of the chassis is about 39%, i.e. the CO₂ emissions associated with the chassis are 18.4 tons. By comparing this number with the increase

in emissions during the operational phase, it can be concluded that a reduction in the manufacturing impact of the chassis is negligible. Similar conclusions can be drawn for the other impact methods, i.e. Eco-costs, CED and ReCiPe.

With regard to chassis material choice, it can thus be concluded that the additional environmental impact associated with lightweight materials such as CFRP are offset by the energy reduction that are achieved during the operational phase. Hence, a CFRP chassis and bodywork is the best option from an environmental impact point of view.

9.1.2 Recycling

Up to this point, recycling has not explicitly been considered in the current study, i.e. the recycling phase has been excluded from the system boundaries given by Figure 5.2. Yet, recycling has already entered the analysis, namely via the use of the impact associated with the market mix materials. From Table A.1, it can be seen that these market mix materials offer considerable environmental impact reductions. Market mix materials are the result of open loop recycling, i.e. the waste materials of other product systems are used in the product system under consideration. As such, a portion of the benefits of recycling have already taken into account.

The basis idea of closed loop recycling is that the waste of the Superbus product system replaces the product of the normal production in the market space. This results in a reduced normal production. On global level, the Superbus waste results in the avoidance of the eco-burden which is related to the normal production. The credits associated with closed loop recycling can be calculated via: 'recycling credit' = (env. impact of recycled material) - (env. impact of virgin).

The benefits of closed loop recycling are calculated by considering the recycling credit of the materials given in the impact database, see also Table A.1. To avoid double counting, the eco-benefit is only applied to the virgin part of the market mix [Dr. Ir. J.G. Vogtländer, 2013]. The recycling benefits for the various vehicle components are shown in Figure 9.6. In the figure, the negative horizontal bars are the achievable impact reductions from recycling. It can be seen that important recycling opportunities exist for the suspension frames and the polycarbonate glazing. If all recyclable material is processed, the manufacturing impact of the vehicle can be reduced by 15%.

As was elaborated in Chapter 4, recycling of the CFRE is challenging. Currently, no recycling process exist where carbon fibres can be separated from the epoxy resin without sacrificing material quality. Besides, incineration of the CFRE is not a viable option either due to the additional impact caused by the emissions associated with combustion. It can be stated that reusing the chassis is another option for reducing the impact of vehicle manufacturing. If the chassis is reused, the vehicle manufacturing impact is reduced with 19%. This number is increased to 26% when reusing the component two times.

All in all, recycling and reusing the various components has significant potential. Although the recycling issues associated with the CFRE chassis are still to be solved, reusing the chassis can be a intermediate (final?) solution.

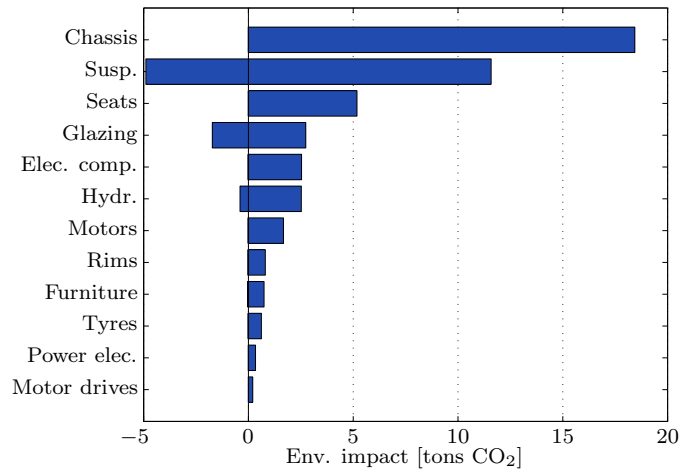


Figure 9.6: Achievable vehicle recycling credit from closed loop recycling.

9.1.3 Vehicle length

The aerodynamic drag of a vehicle is caused by the pressure and shear stress distribution on the body surface of the vehicle, see Figure 9.7. The drag of blunt bodies is dominated by pressure drag, whereas the drag of streamlined bodies is mainly due to skin friction drag. Hence, the drag of the Superbus vehicle mainly consist of skin friction drag.

Figure 9.7 also shows a schematic representation of the streamlines of the air flowing over the vehicle. It can be seen that the air at the front of the vehicle is forced up- and down; is squeezed together. Moreover, at the rear, the flow detaches from the body surface and forms a wake behind the vehicle. In between, the flow nicely follows the body surface, and, although the thickness of the boundary layer may not be constant, it remains attached to the surface.

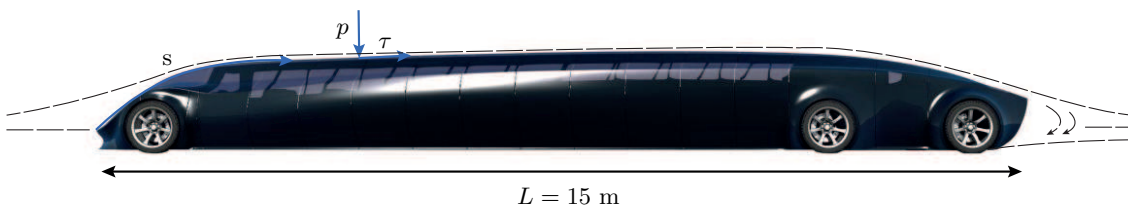


Figure 9.7: Pressure and shear stress distribution on the Superbus body surface. $p = p(s)$
 $(\tau = \tau(s))$

One might ask the question what happens in case the length of the vehicle is increased. Looking at the figure, it can be expected that the 'shape' of the streamlines does not change significantly, i.e. it only takes longer for a particle to reach the rear of the vehicle.

From experimental data on high-speed trains, a similar observation was made. For a longer train, the pressure drag resulting from the flow over the rear and front of the vehicle remains the same, whereas the skin friction drag increases linearly with increasing length. According to Sockel [1996], the drag coefficient of a high-speed train is given by

Equation 9.10.

$$C_D = C_{DL} + C_B + \frac{\lambda_T(l_T - l_L)}{S_{train}^{\frac{1}{2}}} \quad (9.10)$$

In Equation 9.10, C_{DL} is the drag coefficient of the leading car or locomotive and for the ICE equal to 0.2, C_B is the base drag at the vehicle tail and for the ICE equal to 0.12, λ_T is the friction along the train, which includes the bogies, wheels, interference, underbelly effects, etc. for the ICE equal to 0.0125, l_T and l_L are the length of the total train and the lead car respectively and S_{train} .

Equation 9.10 can be used to determine the effect of train length on the drag coefficient in relation to the number of transported passengers. For this, l_T should be expressed as a function of the number of seats and the train length required for each seat, see Equation 9.11.

$$l_T = Nl_{seat} \quad (9.11)$$

In Equation 9.11, l_{seat} is obtained from Table 8.6 and equals 0.53 metres. Consecutively, the drag per seat can be obtained by substituting Equation 9.11 into Equation 9.10 and dividing by the number of seat N , see Figure 9.8.

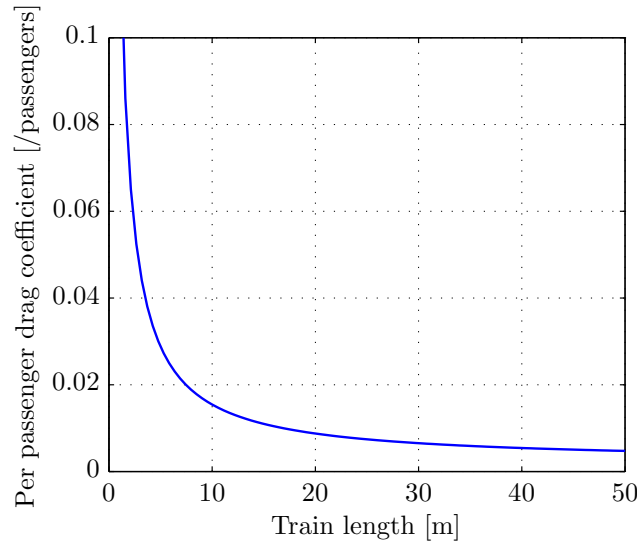


Figure 9.8: Effect of train length on the per passenger drag coefficient of a high-speed train.

From Figure 9.8, it can be derived that the drag coefficient per passenger is reduced if the length of the train is increased. According to Schetz [2001], this is one out of many strengths of the high-speed train for public transportation. The results suggest that when longer Superbus vehicles are used, the resulting drag per passenger is reduced. However, due to Dutch legislations, buses may not be larger than 18.75 metres. The potential of using longer Superbuses will therefore be small. Besides, an increased vehicle length comes at the expense of reduced manoeuvrability, increased mass, increased acceleration and deceleration distances, etcetera. For this reason, the possible benefits of using longer buses will not be examined in the remainder of this study.

9.2 Opportunities batteries

In this section, the recycling opportunities for the batteries are considered. In addition to reuse, many other possibilities exist for reducing the contribution of the batteries to the total environmental impact. For example, one might use the batteries for grid stabilization during night. The batteries can deliver a combined power of about 100 MW, i.e. an equivalent power of about 50 large wind turbines. However, in spite of the possible benefits of these scenarios, these options will not be evaluated in the present study.

9.2.1 Recycling

According to the battery manufacturer, the cycle life of the battery for a 70% depth of discharge equals ≥ 3000 times. The cycle life of the battery is defined as the number of cycles a battery can perform before its capacity drops to 80% of its initial specified capacity. The reduction in battery capacity is caused by the structural changes in the electrode and the thermodynamic instability of the electrode-electrolyte which leads to a decomposition of the electrode.

After the battery has been depreciated for use in the Superbus vehicles, the battery still contains 80% of its initial capacity, i.e. it still has the potential for use in other applications. The manufacturing impact of the battery should in these situations be allocated to both applications. In LCA, allocation should be performed on the basis of the economic value of the battery at the start of its primary and secondary use. The method of economic allocation is well described by [Guiné et al. \[2003\]](#). However, as the economic value of Li-ion batteries after its first use is currently negative [[Auto Recycling Nederland, 2010](#)], economic allocation will not give insight in the possible benefits of second life use of batteries. This section will therefore allocate the manufacturing impact of the battery on the basis of stored energy.

Due to the increasing popularity of electric vehicles, the decrease in battery capacity caused by charge-discharge cycles has been elaborated in many studies. For example, [Zhang and Wang \[2009\]](#) evaluated the cycle life of Li-ion batteries with an LiNiO_2 electrode. According to the study, the battery capacity C depends on the cycle number N as defined by Equation 9.12. In this equation, C_i is the capacity of the fresh cell, k_p and k_l are constants describing the initial parabolic behaviour and the subsequent linear behaviour.

$$C = C_i + k_p N^{0.5} + k_l N \quad (9.12)$$

In Figure 9.9, Equation 9.12 is plotted for different operating temperatures. It can be seen that the loss in capacity increases with increasing temperature.

Although Equation 9.12 and Figure 9.9 suggest that the battery capacity decreases linearly with increasing cycle number, it is unclear what happens after a very large number of charge-discharge cycles. For example, [Spotnitz \[2003\]](#) argues that the decrease in battery capacity accelerates after the constant linear part shown in Figure 9.9.

In the present study, it is assumed that the battery capacity decreases linearly with increasing cycle number. This assumption corresponds quite well with medium to high

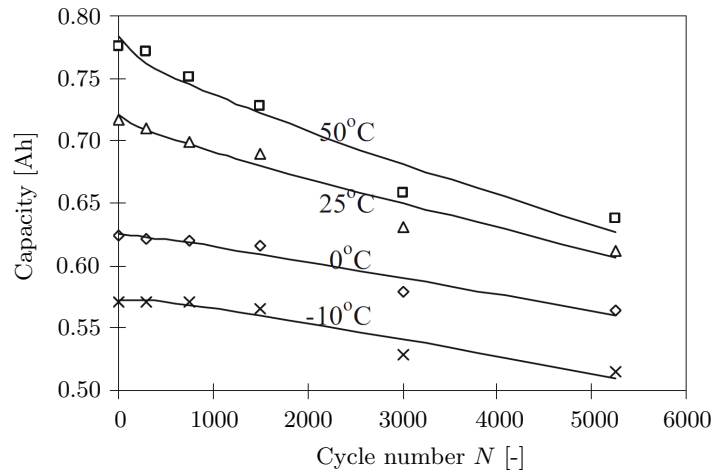


Figure 9.9: Battery capacity at different temperatures as a function of cycle number N [Zhang and Wang, 2009].

cycle numbers. An analysis of the decrease in battery capacity for very high cycle numbers is beyond the scope of the present study.

From Appendix B, it can be derived that the capacity of the battery decreases with increasing cycle number according to Equation 9.13. In this equation, C_i is the initial capacity of the battery and the slope is determined given that 80% of the initial capacity is reached after 3,000 cycles.

$$C = C_i - \frac{0.2C_i}{3000}N \quad (9.13)$$

By integrating Equation 9.13 with respect to N , it can be determined how much energy is provided during Superbus use and second-life use. Upon carrying out this integration, it is calculated that 36% of the total storable energy is used by the Superbus product system and 64% during second-life use. Hence, only 36% of the manufacturing impact of the battery should be allocated to Superbus. It should be stated that economic allocation will most probably yield a less optimistic value. Given the result, a total environmental impact reduction of about 2% can be achieved for the UCTE electricity scenario and about 17% for electricity from wind energy.

9.2.2 Battery type

As was elaborated in Section 6.2, the current prototype is equipped with a battery pack based on a LiFePO_4 chemistry. This battery is relatively heavy due to the combination of the required driving range and the relatively low energy density of 90 Wh/kg. This resulted in a large energy consumption during the operational phase. It would be interesting to determine the effect of utilizing a battery with a higher energy density, for example Li-sulphur or Li-air. An overview of the practical specific energies of rechargeable batteries along with their expected costs can be found in Figure 9.10. It can be seen that new technology batteries allow much higher energy densities at an expected price that is lower than current technology batteries.

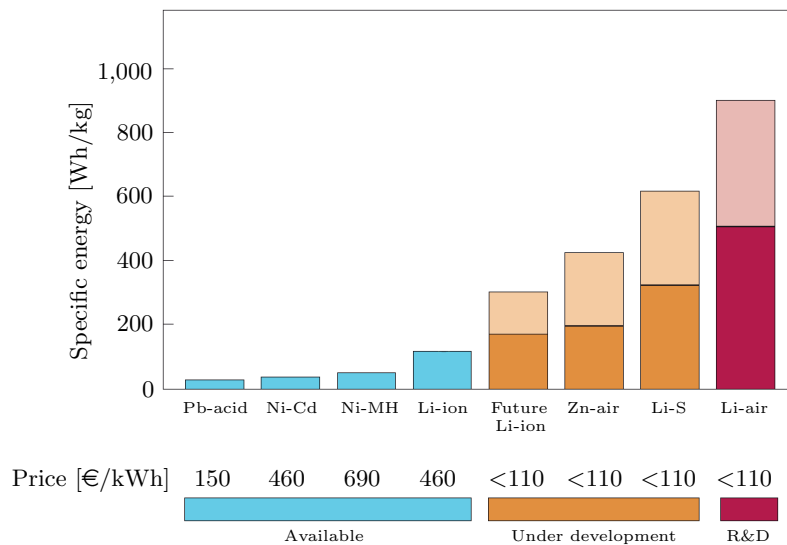


Figure 9.10: Practical specific energy of rechargeable batteries, along with estimated pack prices [Bruce et al., 2012]. The light shaded region on the bars in the chart represent a range of anticipated specific energies. The prices for technologies under development represent targets set by the U.S. Advanced Battery Consortium.

Neither of the batteries shown in Figure 9.10 are new. Recent advances in materials science, nano-materials in particular, mean the main barriers that have so far prevented these systems from being used practically are now somewhat closer to being overcome. Encouraging results have recently been obtained in the lab for Li-S batteries in particular, whereas the Li-air batteries appear more uncertain [Bruce et al., 2012]. It is impossible to predict if and when these batteries will become commercially available for use. Yet, it is reasonable to assume that Li-air batteries will not be available at scale before 2030 [Cluzel and Dougleas, 2012]. Therefore, until then, Superbus has to rely on advances made in the Li-ion technology to improve its performance. According to Figure 9.10, the maximal achievable energy density till 2030 will then be about 200 Wh/kg.

Although the effects of energy density on the environmental impact of Superbus can be easily calculated, it is unknown how future generation Li-ion batteries affect the specific environmental impact of the batteries as shown in Table A.1. As became clear from Chapter 4, the type of battery chemistry in general does not affect the results of a general LCA. For this reason, it is assumed that the environmental impact of future Li-ion batteries is equal to the current Li-ion generation.

Figure 9.11 shows how the carbon footprint of Superbus is reduced with increasing energy density. According to the figure, the carbon footprint is inversely proportional to the energy density. This can be verified by considering Equation 9.17 and recalling that the mass of the vehicle consist of the battery mass and the mass of the other components. Consecutively, the battery mass is calculated via $m_{batt} = \frac{E_{trip}}{E_{specific}}$. For a specific energy of 200 Wh/kg, the environmental impact of the system is reduced by about 10%. Considering the relative impact of the operational phase which amount to 79% for an UCTE mix and 20% for wind energy, this would yield an overall impact reduction of 8% and 2% respectively.

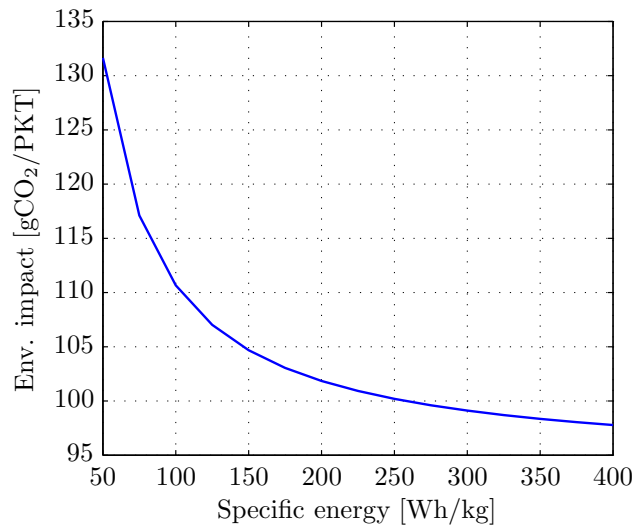


Figure 9.11: Sensitivity of the system carbon footprint to the specific energy of the battery.

9.3 Opportunities infrastructure

The contribution of the infrastructure to the total system impact is relatively small. Measures for reducing the environmental impact of the infrastructure will therefore not be very effective for reducing the system impact. However, it might be interesting from a safety or practical point of view to replace the asphalt top layer with concrete. Figure 9.12 shows the per kilometre carbon footprint for the two options. It can be seen that a concrete road surface increases the infrastructural impact by 66%. Hence, a concrete road surface negatively affects the environmental impact of the system.

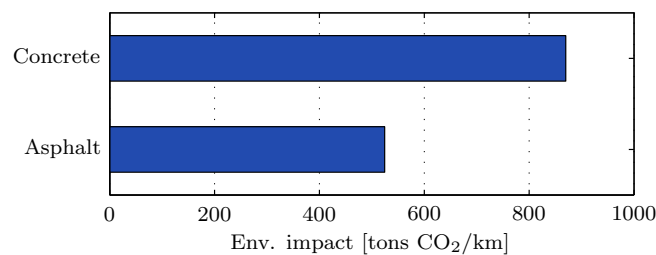


Figure 9.12: Carbon footprint comparison of a road with a concrete and asphalt top layer.

9.4 Opportunities operation

9.4.1 Decrease operational energy consumption

From Figure 9.1 it can be seen that the operational phase has the largest contribution to the environmental impact for the UCTE electricity mix. The contribution of the operational phase in case of wind energy is 20%. Hence, measures to reduce the environmental impact of Superbus will be very effective if applied to the operational phase.

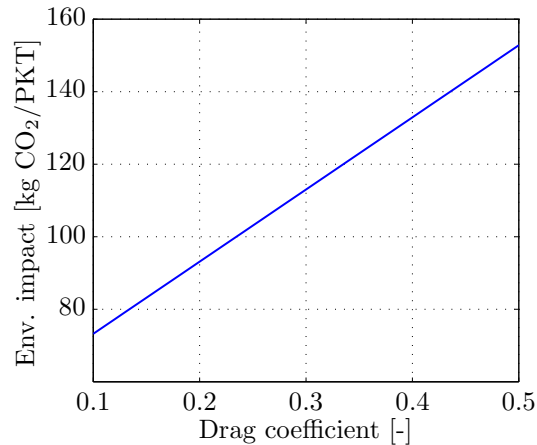


Figure 9.13: Effect of drag coefficient C_D on carbon footprint

As was already elaborated in Section 6.6.2 and shown by Figure 6.9, a simple measure to reduce the impact of the operational phase is by limiting the maximum Supertrack velocity. Other opportunities for reducing the impact of the operational phase include a reduction of vehicle mass, a reduction of the friction between the tyres and the road surface and a reduction of the vehicle drag. Of all measures, reduction of the aerodynamic drag is most effective. The influence of the drag coefficient on the carbon footprint of the Superbus system can be seen in Figure 9.13. According to this figure, a linear relationship exist between C_D and the environmental impact. This is in accordance with theory as the energy consumption of Superbus is defined by the equation $E = C_D k_1 + k_2$. Figure 9.13 shows that the drag coefficient has a large influence on the environmental impact of Superbus. Yet, the importance of the drag coefficient is of even more importance when taking into account head- and crosswinds.

Figure 9.14 shows which progress has been made regarding reduction in drag coefficient. According to this figure, drag coefficients as low as 0.23 can be achieved for well optimized sedans. According to Ir. J.A. Melkert [2013], these C_D values might also be feasible for Superbus after optimizing the aerodynamic design. If a drag coefficient of 0.28 is assumed, the system impact is reduced by 3% for an UCTE electricity mix and by about 1% for electricity from wind energy.

9.4.2 Regenerative braking

As was stated in Section 6.4, the energy consumption during the operational phase is calculated by assuming no intermediate acceleration or deceleration of the vehicle, i.e. the speed of the vehicle changes in accordance with the schematic speed profile shown by Figure 6.5. Hence, the speed instantaneously changes from v_i to v_e . Although a similar approach was used by Verduyckt et al. [2006], the approach does not allow an analysis of the possible benefits of regenerative braking. This section will asses the potential from regenerative braking with respect to the environmental impact of the operational phase of Superbus.

The energy consumption of the vehicle can be derived by considering the free body dia-

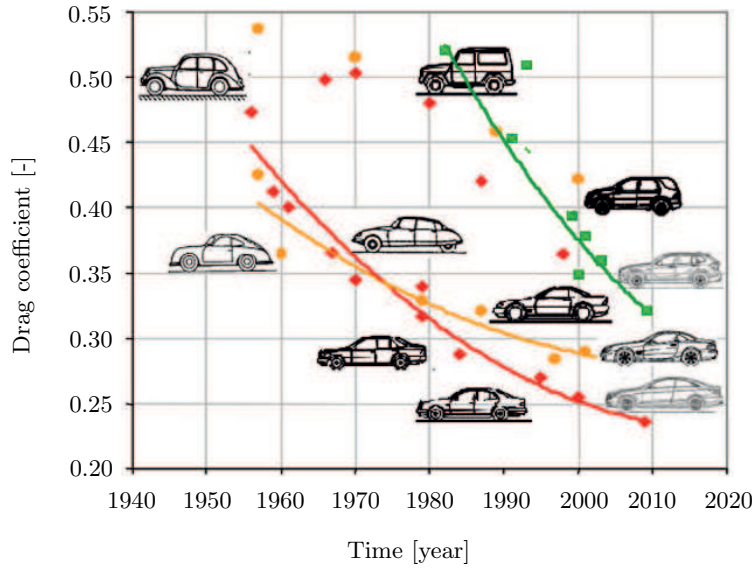


Figure 9.14: The development of C_D values for different car classes (red: sedan, yellow: sports car, green: SUV).

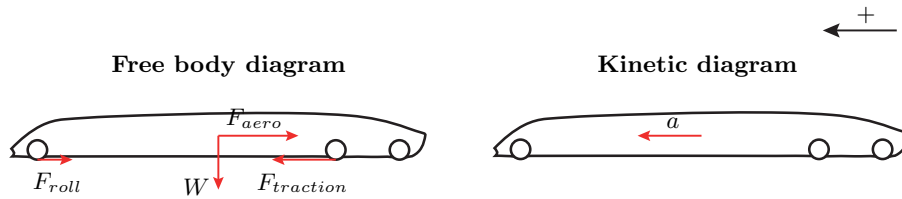


Figure 9.15: Superbus FBD and KD.

gram (FBD) and kinetic diagram (KD) of Superbus, see Figure 9.15.

Applying the second law of Newton, $\sum F = ma$, it can be derived that the motor force can be found from Equation 9.14. In Equation 9.14, F_{motor} can be either positive or negative. In the latter case, the motor force should be interpreted as the braking force.

$$F_{motor} - F_{rolling} - F_{aerodyn.} = ma \rightarrow F_{motor} = ma + F_{aerodyn.} + F_{rolling} \quad (9.14)$$

The work W done by the motor force can be found by integrating Equation 9.14 with respect to the differential displacement dx associated with the movement from x_1 to x_2 . Carrying out this integration and substituting the equations for the drag force, $F_{aerodyn.}$ and rolling force, $F_{rolling}$ gives:

$$\int_{x_1}^{x_2} F_{motor} dx = \int_{x_1}^{x_2} madx + \int_{x_1}^{x_2} 0.5C_D \rho v^2 A dx + \int_{x_1}^{x_2} \mu mg dx \quad (9.15)$$

Note that the first and second term on the right hand side can be modified using the relation $v dv = adx$. The velocity in the second term is hereby replaced by the term $v = \sqrt{2a\Delta x + v_1^2}$, see Equation 9.16.

$$E_{motor} = m \int_{v_1}^{v_2} v dv + 0.5 C_D \rho A \int_{x_1}^{x_2} \left(\sqrt{2a\Delta x + v_1^2} \right)^2 dx + \mu mg \int_{x_1}^{x_2} dx \quad (9.16)$$

By carrying out the integration, it can be found that the energy delivered by the motors for an acceleration or deceleration from v_1 to v_2 over a distance $x_2 - x_1$ equals:

$$E_{motor} = \underbrace{0.5m(v_2^2 - v_1^2)}_{\Delta E_{kin}} + \underbrace{0.5C_D\rho A \left(a(x_2^2 - x_1^2) + v_1^2(x_2 - x_1) \right)}_{\Delta E_{drag}} + \underbrace{\mu mg(x_2 - x_1)}_{\Delta E_{roll}} \quad (9.17)$$

From Equation 9.17, it can be seen that the energy delivered by the motors, as expected, is equal to the sum of the change in kinetic energy, drag energy and roll energy. Moreover, it can be shown that Equation 9.17 is similar to Equation 6.6 for a constant speed where $a = 0$ and $v_1 = v_2$ and by noting that $dx = v dt$.

Potential of regenerative braking

Equation 9.17 can be used to determine the required amount of energy for acceleration, see Table 9.2. The required braking energy shown in the rightmost column is the energy that can be recovered via regenerative braking. Table 9.2 also shows the required distance for the indicated speed change. This distance is obtained assuming a maximal acceleration of 1 m/s^2 and a deceleration of -0.8 m/s^2 .

Consecutively, it is required to determine when and how often the vehicle accelerates and decelerates. Referring to the schematic speed profile shown in Figure 6.5, it can be derived that most stops are made at a speed of 30 km/h to pick up or drop off passengers or to stop in front of traffic lights and road crossings. In some situations, traffic lights are also placed at provincial roads during which the vehicle drives at a speed of 80 km/h .

A representative 210 km trip might contain four stops at 30 km/h to pick up and drop off passengers, ten stops at 30 km/h for traffic lights and road crossings and two stops at 80 km/h for traffic lights. Using Table 9.2 and Equation 9.17, it can be calculated that during this trip, 36 MJ is converted into heat by the brakes. Assuming a generator and charge efficiency of 60% and 89% respectively, 19.2 MJ of this energy can be stored in the batteries via regenerative braking. Comparing this number with the total consumed trip energy of 910 MJ , it can be concluded that the recoverable energy is only about 2% of the total consumed energy. Assuming the same amount and type of stops, this number increases to 10% for a trip distance of 25 km .

In general, the efficiency gains vary greatly with driving conditions. In stop and go city travelling, regenerative braking is more effective compared to high speed travel. If it is assumed that the average efficiency is 5% (corresponding to the average trip distance of 90.6 km), the environmental impact reduction that can be obtained from regenerative braking is only 4% and 1% for an UCTE and wind energy electricity mix.

Above elaboration shows that compared to the total energy consumption, only a small amount of energy can be recovered via regenerative braking, mainly due to the small number of stops that usually take place at a low speeds of 30 km/h .

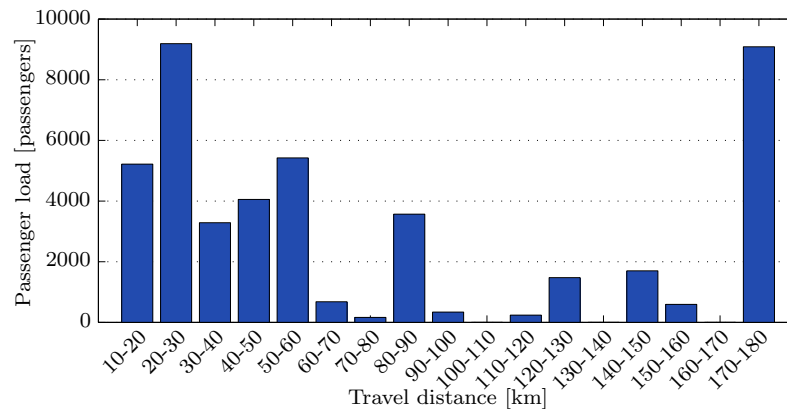
Table 9.2: Acceleration/deceleration distance and energy requirements.

ΔV [km/h]	Accelerating		Decelerating	
	Distance [m]	E_{motor} [MJ]	Distance [m]	$E_{braking}$ [MJ]
0 - 30	34.7	0.67	43.4	0.43
30 - 80	212	3.57	265	2.57
80 - 120	309	5.17	386	3.58
120 - 250	1856	33.1	2320	17.4

9.4.3 Battery swap schedule

As was elaborated in Section 6.2, the battery adds a considerable amount of mass to the vehicle resulting in a larger rolling friction. The large battery is required to enable large distance transport.

From Figure 9.16 it appears that the travel distance of the majority of the trips, i.e. 71%, covers a distance smaller than 60 kilometres. This implies that a smaller battery is sufficient in many cases. The positive side effect is that a lighter battery induces less rolling friction, resulting in lower energy consumption during the operational phase.

**Figure 9.16:** Travel distance distribution [Melkert and Ockels, 2006].

According to Equation 9.17, the energy consumption due to the rolling resistance scales with a factor v , whereas the energy consumption due to drag resistance scales with a factor v^3 . A reduction of battery mass will therefore be less effective for reducing the energy consumption of the vehicle compared to a reduction of aerodynamic drag. Besides, using a smaller battery requires an intermediate stop for long trips depending on the battery capacity. These intermediate stops are accompanied with additional energy consumption to accelerate to cruising speed after the swaps. As was elaborated in the previous section, only part of this energy can be recovered from the decelerating phase.

Assuming a maximum of one battery swap is allowed during a 210 km travel, implies that the battery can be half its original capacity. The reduction in environmental impact can now be calculated as follows.

Given the result from Figure 9.16, the amount of vehicle kilometres travelled during trips longer than 110 km, can be calculated by multiplying the bin centre C with the passenger load L , see Table 9.3. From this table, it can be derived that 62% of the vehicle kilometres are travelled during trips longer than 110 km. Using the average travel distance of 90.6 kilometre, it can be derived that during Superbus' lifetime, 10,430 battery swap stops are made. Moreover, the required energy to accelerate to cruising speed is 36.3 MJ.

Calculating the total energy consumption during Superbus' lifetime and adding the acceleration energy required during the battery swaps, it is found that the total energy consumption is reduced by 1.7% compared to the reference situation. The corresponding reduction in environmental impact is 1.3% and 0.3% for an UCTE and wind energy electricity mix respectively.

Table 9.3: Superbus trip characteristics.

Trip distance [km]	Bin centre (C) [km]	Pass. load (L) [%]	$C \cdot L$ [km]	$C \cdot L$ [%]
10 - 20	15	11.6	174	2.28
20 - 30	25	20.4	510	6.68
30 - 40	35	7.3	256	3.35
40 - 50	45	9.0	405	5.31
50 - 60	55	12.0	662	8.68
60 - 70	65	1.51	98.3	1.29
70 - 80	75	0.36	27.3	0.358
80 - 90	85	7.93	674	8.83
90 - 100	95	0.75	71.7	0.940
100 - 110	105	0	0	0
110 - 120	115	0.53	61.3	0.803
120 - 130	125	3.28	410	5.37
130 - 140	135	0	0	0
140 - 150	145	3.78	548	7.18
150 - 160	155	1.32	204	2.68
160 - 170	165	0	0	0
170 - 180	175	20.2	3532	46.3

9.5 Opportunities transport efficiency

9.5.1 Supertrack velocity

The sensitivity analysis that was performed in Section 6.6, assessed the effect of a change in the Supertrack velocity on the environmental impact of the Superbus system. During this analysis, all other parameters were kept constant. Yet, changing the maximum speed on the Supertrack will affect all results that were obtained from the LMS model. For example, an increase in velocity will reduce the overall travelling time, and thus increase the popularity of Superbus (thus increasing the required amount of vehicles). Moreover, it will increase the average passenger travel distance and, of course, increase the total

energy consumption. An analysis of the effects of Supertrack speed on the environmental performance should therefore also include an examination of related parameters.

The effect of velocity on transport demand D and average travel distance s_{trip} are normally indirectly defined in terms of the elasticity E with respect to travel time, see Equation 9.18 and 9.19. In Dutch studies, the elasticity of demand of a train is usually assumed between -0.5 and -0.6, while international studies use values up to -0.7 [Dr. Ir. R. van Nes, 2013]. In the present study, E_{demand} is set at -0.6, so reducing the travel time with 10% will increase traffic demand with 6%. The elasticity of travel distance can be obtained by considering the fact that the amount of time people daily devote to travel tends to remain constant. This *constant travel time budget hypothesis* implies that the elasticity of travel distance with respect to travel time is -1 [T. Litman, 2012].

$$E_{demand,time} = \frac{\partial D}{\partial t} = -0.6 \quad (9.18)$$

$$E_{distance,time} = \frac{\partial s_{trip}}{\partial t} = -1 \quad (9.19)$$

In order to be able to use the elasticities presented above, the impact of a change in maximum speed on the average travel time t should be determined first. This can be done by calculating the average trip time for a given maximum speed using Equation 9.20 and determine the relative increase in trip time with respect to the LMS reference situation, see Equation 9.21.

Table 9.4: Adapted results of the LMS model for different Supertrack speeds.

Supertrack speed [km/h]	Average speed [km/h]	Time increase [%]	Passenger-km [-]
120	88.3	18.9	4588432
130	91.6	14.6	4979379
140	94.7	10.8	5326156
150	97.6	7.58	5635416
160	100	4.74	5912660
170	103	2.23	6162437
180	105	0	6388512
190	107	-2.00	6594023
200	109	-3.79	6781592
210	111	-5.42	6953429
220	113	-6.70	7111402
230	114	-8.24	7257098
240	116	-9.48	7391879
250	117	-10.6	7516912

$$\bar{t}_{v,max} = \sum_{i=1}^3 \left(\frac{D_i s_{life}}{v_i} \right) + \frac{d_{v,max} s_{life}}{v_{max}} + t_{stop} \quad (9.20)$$

In Equation 9.20, i represents the various road types, i.e. municipal, provincial and state roads, D is the distribution of VKT along the different road types (see Table 6.4), s_{life}

is the VKT during Superbus's life and t_{stop} is the time required for bus stops and can be calculated from the LMS model results.

$$\Delta t = \frac{\bar{t}_{v,max}}{\bar{t}_{180}} - 1[\%] \quad (9.21)$$

The relative increase in trip time and the amount of passenger-kilometres that follows, can be found in Table 9.4. The table also shows the average velocity which is calculated from Equation 9.22.

$$v_{avg} = \frac{S_{life}}{\bar{t}} \quad (9.22)$$

It is unknown how passenger occupancy changes the required number of vehicles. This study therefore assumes that passenger numbers do not affect the required number of vehicles. The normalized vehicle manufacturing impact will therefore become smaller with increasing passenger numbers. This also applies to the Supertrack and existing infrastructure, i.e. the higher the number of passengers, the lower the normalized environmental impact.

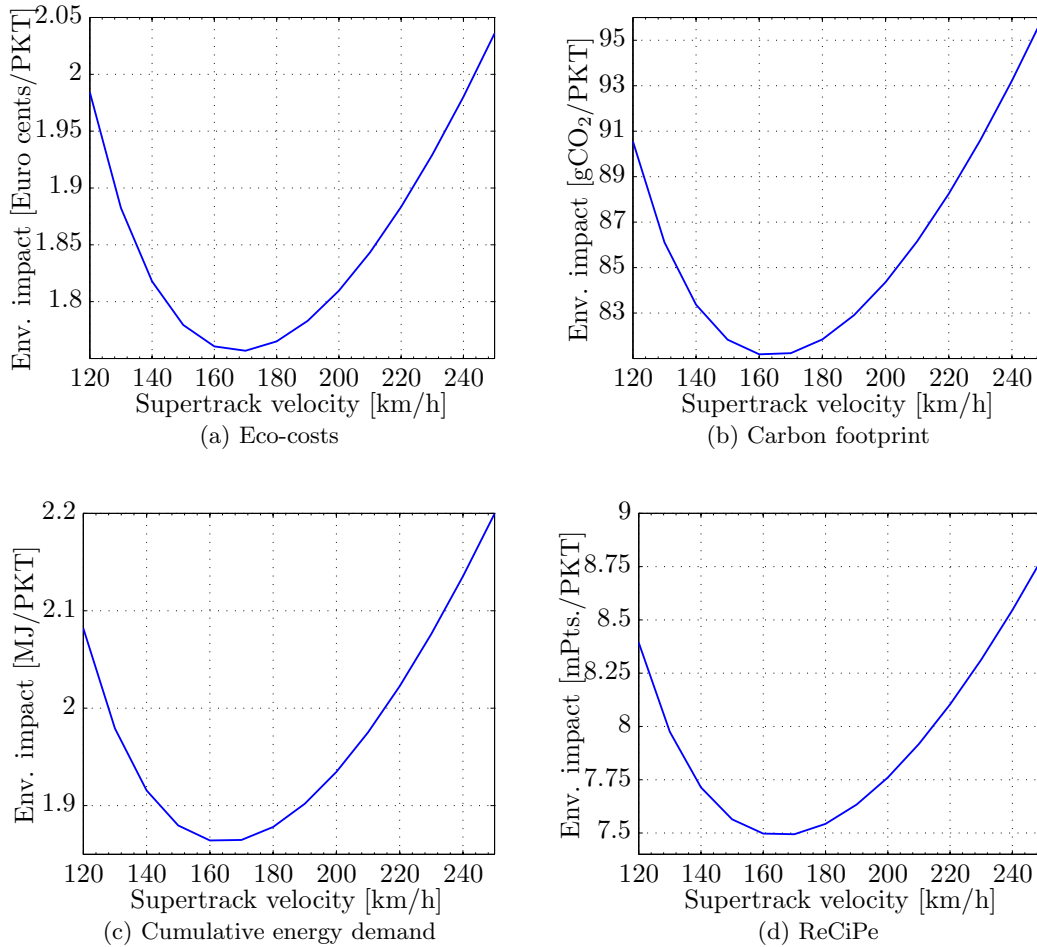


Figure 9.17: Effect of Supertrack velocity.

The total normalized environmental impact that can be obtained from the above calculations can be found in Figure 9.17. It can be seen that the figure resemble a parabola with its through located at a Supertrack velocity of about 165 km/h. The asymmetric shape of the plot is caused by the decreasing contribution of the vehicles and infrastructure to the normalized impact. It is determined from the figure that the total environmental impact is increased by about 16% if the speed is changed from 180 to 250 km/h. Decreasing the speed from 180 to 120 km/h increases the environmental impact with about 11%.

9.6 Summary environmental impact reduction opportunities

In this section, the effects of the various impact reduction measures are summarized. Table 9.5 shows an overview of the various reduction measures and their effect on the total environmental impact of the system.

Table 9.5: Overview of achievable system impact reductions. All values are rounded to nearest integer.

Reduction measure	Impact reduction	
	UCTE	Wind
Vehicle		
Chassis material	N/A	N/A
Recycling	0%	3%
Re-use	1%	4%
Vehicle length	N/A	N/A
Batteries		
Recycling	2%	17%
Battery type	8%	2%
Infrastructure		
Material top layer	N/A	N/A
Operation		
Decrease propulsion energy	3%	1%
Regenerative braking	4%	1%
Battery swap schedule	1%	0%
Transport efficiency		
Supertrack velocity	N/A	N/A
Total	19%	28%

It can be seen that a total reduction of 19% can be achieved for an UCTE electricity mix and a reduction of 28% for electricity from wind. Moreover, the different electricity mixes bring about a shift of the effectiveness of various reduction measures. For example, for the UCTE electricity mix, the most effective reduction measures are affecting the operational phase and the batteries. For wind energy, the most effective measure apply to the vehicles and the batteries.

Figure 9.18 shows the effect of the various reduction measures for the UCTE electricity mix and electricity obtain from wind. In Figure 9.18, the scenario including reduction measures has '+ red.' in its label.

Given the results, it can be concluded that the largest impact reduction can be obtained by utilizing electricity from sustainable energy sources like photovoltaic or wind energy. Hence, for Superbus as well as for other electric vehicles, this should be the number one priority.

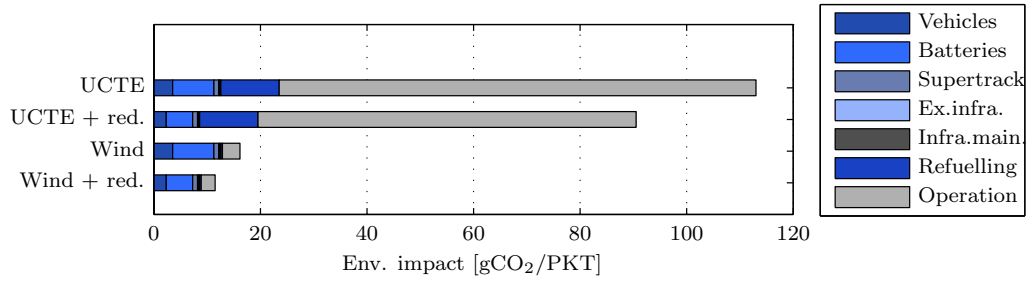


Figure 9.18: Environmental performance of Superbus public transport system including impact reduction measures.

Conclusion and recommendations

Environmental impact opportunities for the Superbus transport concept were assessed using the life cycle assessment methodology. Overall, the methodology provided the correct tools to establish the foundation of the present study.

In Chapter 6, an environmental impact assessment was performed on the Superbus transport concept to establish the contribution of the different life cycle components to the total environmental impact. With respect to the vehicles, the main contributor to the environmental impact is the CFRE chassis and the suspension system. Compared to literature, the total impact of 47.4 tons of CO₂ and 1005 GJ of energy is comparable to a 40-tons truck.

With respect to the Supertrack dedicated infrastructure, the main contributor to the environmental impact is the asphalt top layer. Compared to the total construction impact of an average Dutch road, the construction energy requirements of the Supertrack are 14% lower.

From a system point perspective, the operational and charging phase for an UCTE electricity mix account for 76-87% of the total impact. The 2nd and 3rd largest components are the batteries and the vehicles. Interesting is the large impact reduction that can be obtained by utilizing electricity from photovoltaic or wind, i.e. compared to the UCTE electricity mix, the reduction is 44-76% for photovoltaic and 51-84% for wind energy.

In Chapter 7, the electric powertrain was compared with a diesel and compressed natural gas powertrain. With regard to the total environmental impact of the vehicles, no large differences were determined. In contrast, the total system impact of the diesel and CNG alternatives are about 1.1-2.6 and 1.5-3.1 times larger respectively. Interestingly, in spite of the lower CO₂ emissions during the operational phase, the CNG powertrain is found to have a higher impact compared to the diesel powertrain, .

In Chapter 8, the Superbus system was compared to the high-speed train and Maglev transport modes for a speed of 250 km/h. For the given function, Superbus was found to have a total environmental impact that is about 2 and 2.6 times higher compared to

the high-speed train and Maglev respectively. This difference is mainly caused by the relatively high ratio of $C_D A/S$.

In Chapter 9, the opportunities for environmental impact reduction were discussed. A total reduction of about 19% and 28% can be achieved for a UCTE and wind energy electricity mix respectively. Of the different measures considered, increasing the specific energy of the battery has the largest effect for an UCTE electricity mix. In case of wind energy, recycling of the batteries is the most promising with a total achieved reduction of about 17%.

Considering the results of Chapter 6 and 9, it can be concluded that the largest impact reduction can be obtained from a shift towards sustainable electricity sources like photovoltaic or wind energy. Hence, for Superbus, as well as other electric vehicles, this should be the number one priority. In addition, efforts should be made to reduce the environmental impact of the batteries as this component has the largest contribution in case of electricity from wind energy.

The life cycle assessment that was conducted in the present study is based on the Ecoinvent v2.2 database that can be accessed via <http://www.ecocostsvalue.com/>. Although this database contains many materials and processes, characterisation and weighing is implicitly carried out. Hence, the performed assessment suffers from less transparency on which calculations are performed where. The present study might therefore be reworked to be more transparent and in line with the ISO methodological description. Moreover, results can be presented on midpoint level to investigate the effects of the different measures and alternatives on more impact categories.

In addition, the current study adopts the results from Melkert and Ockels [2006], which lacks the results for several important transport scenarios. For example, the study did not include the effect of travelling velocity on the amount of passenger kilometres. Besides, because of the large impact of the operational phase for an UCTE electricity mix, more detailed calculation might be performed to determine the energy consumption of the vehicles. More (practical) data is essential in this respect.

References

- ABB. Environmental Product Declaration: ACS 600 Frequency Converter, 250 kW Power. <http://goo.gl/xQnCe>, 2001.
- ABB. Environmental Product Declaration: Drive Low Voltage AC Drive, ACS 800 Frequency Converter, 250 kW Power. <http://goo.gl/75ABR>, 2002a.
- ABB. Environmental Product Declaration: AC Low Voltage Cast Iron Motor, Type M3BP 315. <http://goo.gl/oxmgQ>, 2002b.
- ABB. Environmental Declaration: AC 800M Controller. <http://goo.gl/v5QP0>, 2005.
- A.Dinger, R. Martin, X. Mosquet, M. Rabl, D. Rizoulis, M. Russo, and G. Sticher. Batteries for Electric Cars: Challenges, Opportunities, And the Outlook to 2020, 2010.
- J. Ally and T. Pryor. Life-cycle Assessment of Diesel, Natural Gas and Hydrogen Fuel Cell Bus Transportation Systems. *Journal of Power Sources*, 170:401–411, Apr 2007.
- Auto Recycling Nederland. ARN Coördineert inzameling en verwerking Lithium Ion Accu's. <http://goo.gl/AxkEL>, 2010. Date accessed: May 2013.
- Better Place. Behind the Scenes at a Battery Switch Station. <http://goo.gl/a7Qpo>, 2012. Date accessed: February 2013.
- A.J.M. Bos. *Direction Indirect: the Indirect Energy Requirements and Emissions from Freight Transport*. PhD thesis, Rijksuniversiteit Groningen, May 1998.
- P.G. Bruce, S.A. Freunberger, L.J. Hardwick, and J.-M. Tarascon. Li-O₂ and Li-S Batteries with High Energy Storage. *Nature*, 11, Jan 2012.
- A. Burnham, M. Wang, and Y. Wu. Development and Applications of GREET 2.7 - The Transportation Vehicle-Cycle Model, Nov 2006.
- CEMEP. Electric Motors and Variable Speed Drives. <http://goo.gl/LKkd8>, Feb 2011.
- Centraal Bureau voor de Statistiek (CBS). Mobiliteit Per Regio, Naar Motief, en Algemene Kenmerken. Statline, 2007.

- Centraal Bureau voor de Statistiek (CBS). Energiebalans; Kerncijfers. Statline, 2011a.
- Centraal Bureau voor de Statistiek (CBS). Lengte van Wegen; naar Wegkenmerken en Gemeente. Statline, 2011b.
- Centraal Bureau voor de Statistiek (CBS). Luchtverontreiniging, Feitelijke Emissies door alle Bronnen. Statline, 2011c.
- Centraal Bureau voor de Statistiek (CBS). Mobiliteit in Nederland; Mobiliteitskenmerken en Vervoerswijzen, Regio's. Statline, 2011d.
- Centraal Bureau voor de Statistiek (CBS). Verkeersprestaties; Kilometers naar Voertuigtype en Grondgebied. Statline, 2011e.
- Centraal Bureau voor de Statistiek (CBS). Nabijheid voorzieningen: Afstand Tot Locatie, Regionaal. Statline, 2012.
- C.C. Chan. The State of the Art of Electric, Hybrid, and Fuel Cell Vehicles. *Proceedings of the IEEE*, 95:704–718, Apr 2007.
- M.V. Chester. *Life-cycle Environmental Inventory of Passenger Transportation Modes in the United States*. PhD thesis, University of California, 2008.
- M.V. Chester and A. Horvath. Environmental Assessment of Passenger Transportation Should Include Infrastructure and Supply Chains. *Environmental Research Letters*, 4, Jun 2009a.
- M.V. Chester and A. Horvath. Life-cycle Energy and Emissions Inventories for Motorcycles, Diesel Automobiles, School Buses, Electric Buses, Chicago Rail and New York City Rail. Working Paper, Jan 2009b.
- M.V. Chester and A. Horvath. Life-cycle Assessment of High-Speed Rail: the Case for California. *Environmental Research Letters*, 5, Jan 2010.
- M.V. Chester, A. Horvath, and S. Madanat. Comparison of Life-cycle Energy and Emissions Footprints of Passenger Transportation in Metropolitan Regions. *Atmospheric Environment*, 44, Mar 2010.
- C. Cluzel and C. Dougleas. Cost and Performance of EV Batteries, Mar 2012.
- M. Connel, D. Jones, A. Lake, B. Magee, and T. Parry. Sustainable Benefits of Concrete Step Barrier, September 2008.
- G.A. Cooney. Life Cycle Assessment of Diesel and Electric Public Transport Buses. Master thesis, University of Pittsburgh, June 2011.
- Detroit. DT12 Transmission. <http://goo.gl/M2Nws>, 2008.
- Dienst Weg- en Waterbouwkunde. *Handleiding Wegbouw: Ontwerp Verhardingen*. Ministerie van Verkeer en Waterstaat, Jun 1994.
- Dr. Ing. A. Terzi. Sustainable Mobility and Vehicle Design, 2010. Course AE4-T39, lecture 1.

- Dr. Ir. J.G. Vogtländer. Personal Interview, May 2013.
- Dr. Ir. R. van Nes. Personal Interview, Feb 2013.
- J.R. Duflou, J. de Moor, I. Verpoest, and W. Dewulf. Environmental impact analysis of composite use in car manufacturing. *CIRP Annals - Manufacturing Technology*, 58: 9–12, 2009.
- End of Life Vehicle Directive. 2000/53/EC, Aug 2000.
- Energie Nederland. Energie in Nederland 2011, Aug 2011.
- R. Frischknecht. Life Cycle Assessment of Driving Electric Cars and Scope Dependent LCA Models. In *43th LCA Discussion Forum: Life Cycle Assessment Of Electromobility*, Apr 2011.
- G. W. Schweimer and M. Levin. Life Cycle Inventory for the Golf A4, 2000.
- Grindex. Environmental Product Declaration: Matador 8106.180. <http://goo.gl/Eo0ia>, 2009.
- J.B. Guiné, R. Heijungs, and G. Huppes. Economic Allocation: Examples and Derived Decision Tree. *The International Journal of Life Cycle Assessment*, 9:23–33, 2003.
- J.B. Guinee, M. Gorree, R. Heijungs, G. Huppes, R. Kleijn, A. de Koning, L. van Oers, A. Wegener Sleeswijk, S. Suh, H.A. Udo de Haes, H. de Bruijn, R. van Duin, and M.A.J. Huijbregts. *Handbook on Life Cycle Assessment. Operational Guide to the ISO Standards: III: Scientific Background*.
- T.R. Hawkins, O.M. Gausen, and A.H. Strømman. Environmental Impacts of Hybrid and Electric Vehicles - a Review. *The International Journal of Life Cycle Assessment*, 17, Sep 2012a.
- T.R. Hawkins, B. Singh, G. Majeau-Bettez, and A.H. Strømman. Comparative Environmental Life Cycle Assessment of Conventional and Electric Vehicles. *Journal of Industrial Ecology*, 17, Feb 2012b.
- R. Heijungs and R. Kleijn. Numerical Approaches Towards Life Cycle Interpretation. *International Journal of LCA*, 6:141–148, May 2001.
- M. Held. LCA E-Mobility: Current Results of the Fraunhofer System Research for Electromobility (FSEM) and Need for Further Research. In *43th LCA Discussion Forum: Life Cycle Assessment Of Electromobility*, Apr 2011.
- Ir. J.A. Melkert. Personal Interview, Jan 2013.
- ITT. Environmental Product Declaration: Flygt 2640.180. <http://goo.gl/6BBKe>, 2009.
- M. Jakob. Methodological Approaches for Determining Marginal Electricity Mixes. In *43th LCA Discussion Forum: Life Cycle Assessment Of Electromobility*, Apr 2011.
- S. Jorritsma. Ketenanalyse Asfalttransport: Optimalisatie Inzet Asfalttransport. <http://goo.gl/XeEVV>, Sep 2010.

- F.R. Kalhammer, B.M. Kopf, D.H. Swan, V.P. Roan, and M.P. Walsh. Status and Prospects for Zero Emissions Vehicle Technology, Apr 2007.
- J. Kartanegara. Project Superbus: Aanbiedingsdocument, Augustus 2011.
- H. Kato, N. Shibahara, M. Osada, and Y. Hayashi. A Life Cycle Assessment for Evaluating Environmental Impacts of Inter-Regional High-Speed Mass Transit Projects. *Journal of Eastern Asia Society for Transport Studies*, 217, 2003.
- S. Kromer, E. Kreipe, D. Reichenbach, and R. Stark. Life Cycle Assessment of a Car Tire, 1999.
- K. Lindquist and M. Wendt. Retreaded Tire Use and Safety: Synthesis, Sep 2009.
- H.L. Maclean and L.B. Lave. Life Cycle Assessment of Automobile/Fuel Options. *Environmental Science And Technology*, 37:5445–5452, 2003.
- G. Majeau-Bettez, T.R. Hawkins, and A.H. Stromman. Life Cycle Environmental Assessment of Lithium-ion and Nickel Metal Hydride Batteries for Plug-In Hybrid and Battery Electric Vehicles. *Environmental Science and Technology*, 45:4548–4554, Apr 2011.
- J. Matheys, J. van Mierlo, J. Timmermans, and P. van den Bossche. Life-Cycle Assessment of Batteries in the Context of the EU Directive on End-of-life Vehicles. *International Journal of Vehicle Design*, 46:189–203, 2008.
- E.C. McKenzie and P.L. Durango-Cohen. Environmental Life-cycle Assessment of Transit Buses with Alternative Fuel Technology. *Transportation Research Part D*, 17, Jan 2012.
- J. Melkert and W. Ockels. Modelling van de Superbus in het Landelijk Model Systeem en bepaling van de uitgangspunten van de exploitatieberekening. Supporting Information LMS Calculations, Version B, March 2006.
- Ministerie van Infrastructuur en Milieu. Structuurvisie Zuiderzeelijn. <http://goo.gl/KZYDD>, Aug 2009.
- Ministerie van Verkeer en Waterstaat. Strategische Milieubeoordeling Structuurvisie Zuiderzeelijn, Apr 2006.
- H. Uedmand T. Miyauchi and T. Tsujimura. Application of Life Cycle Assessment to Shinkansen Vehicles and Cross Ties in Japan. *Journal of Rail and Rapid Transit*, 6, Jul 2005.
- A.A.A. Molenaar and L.J.M. Houben. CT2800: Wegen en Spoorwegen. Collegedictaat, Nov 2011.
- Nissan Europe - France. Nissan Leaf. <http://goo.gl/r4Nd7>, 2012. Date accessed: February 2013.
- D.A. Notter, M. Gauch, R. Widmer, P. Wager, A. Stamp, R. Zah, and H.J. Althaus. Contribution of Li-Ion Batteries to the Environmental Impact of Electric vehicles. *Environmental Science and Technology*, 44:6550–6556, Aug 2010.

- Centraal Planbureau. Economisch effecten van de betuweroute op basis van recente informatie, Apr 1995.
- Ragasco. Lightstore: All Composite Type 4 CNG Cylinder. <http://goo.gl/dozm5>. Date accessed: February 2013.
- G. Rebitzer, U. Schiller, and W. Schmidt. *Methode euroMat '98 - Grundprinzipien und Gesamtmethode*. Springer, Berlin, 2000.
- G. Rebitzer, T. Ekvall, R. Frischknecht, D. Hunkeler, G. Norris, T. Rydberg, W.-P. Schmidt, S. Suh, B.P. Weidema, and D.W. Pennington. Life Cycle Assessment - Part 1: Framework, Goal and Scope Definition, Inventory Analysis, and Applications. *Environmental International*, 30:701–720, Nov 2004.
- J.A. Schetz. Aerodynamics of high-speed trains. *Annual Review of Fluid Mechanics*, 33, Jan 2001.
- W.P. Schmidt, E. Dahlqvist, M. Finkbeiner, S. Krinke, S. Lazzari, D. Oschmann, S. Pichon, and C. Thiel. Life Cycle Assessment of Lightweight and End-of-Life Scenarios for Generic Compact Class Passenger Vehicles. *The Internal Journal for Life Cycle Assessment*, 9:405–416, 2004.
- Shenzen Kaisai Electric Motor Co. Ltd. N-Type KCM-SK100 NB112Z Diesel Fuel Injection Pump. <http://goo.gl/zKJrp>, 2010. Date accessed: June 2013.
- H. Sockel. *Handbook of Fluid Dynamics and Fluid Machinery*, chapter 8, pages 1721–1741. Wiley & Sons, 1996.
- M. Spielman, C. Bauer, R. Dones, P. Scherrer, and M. Tuchschnid. 14. Transport Services, Data V2.0, Dec 2007.
- R. Spotnitz. Simulation of Capacity Fade in Lithium-ion Batteries. *Journal of Power Sources*, 113, Jan 2003.
- L. Stankevičiūtė. Energy Use and Energy Management in Tyre Manufacturing: the Trelleborg 1 Case. Master's thesis, Lund University, Nov 2000.
- R. Birgitte Svånå. A Methodology for Environmental Assessment - Norwegian High Speed Railway Project Phase 2, Mar 2011.
- T. Litman. Understanding Transport Demands and Elasticities: How Prices and Other Factors Affect Travel Behavior. <http://goo.gl/sqSpu>, September 2012.
- O. van Boggelen and B. Tijssen. Ontwikkeling van het Fietsgebruik in Voor- en Natransport van de Trein, Ma 2007.
- N.W. van den Berg, C.E. Dutilh, and G. Huppes. *LCA voor beginner: Handleiding milieugerichte levenscyclus analyse*. NOH, 1995.
- R.M.M. van den Brink, H. Nijland, and G.P. van Wee. Nieuwe Snelle Treinverbindingen Tussen de Randstad en Noord Nederland, Jul 2001.
- D. van der Wall Bake and R. Spriensma. CO₂ Ketenanalyse Spoorstaven, Nov 2010.

- A. van der Woud. *Een Nieuwe Wereld: Het Ontstaan van het Moderne Nederland*. Bert Bakker Amsterdam, 8 edition, 2010.
- J. van Mierlo and Y. Marenne. Energy Consumption, CO₂ emissions and Other Consideration Related to Battery Electric Vehicles, Apr 2009.
- van Ooijen B.V. Scope-3 Emissie Ketenganalyse. Waardeketen: Aanbrengen van Diverse Soorten Asfalt. <http://goo.gl/h8P9k>, Maart 2012.
- O. van Vlijmen. Brandstoffen: Calorische Waarden. <http://goo.gl/w8eWg>, 2011.
- VBW Asfalt. De Toekomst van Wegverhardingen met Asfalt tot 2010, Mar 1989.
- T. Verduyckt, J. Melkert, and W. Ockels. Bijdragen voor de Strategische Milieuboordeling van de Superbus. Supporting Information Strategische Milieubeoordeling, Versie A, January 2006.
- J.G. Vogtländer, B. Baetens, A. Bijma, E. Brandjes, E. Lindeijer, M. Segers, F. Witte, J.C. Brezet, and Ch. F. Hendriks. *LCA-Based Assessment of Sustainability: the Eco-Costs / Value Ratio EVR*, chapter 9, pages 155–166. VSSD, 2010.
- C. von Rozycki, H. Koeser, and H. Schwarz. Ecology profile of the German High-speed Rail Passenger Transport System. *The International Journal of Life Cycle Assessment*, 8, Mar 2003.
- M.Q. Wang and H.-S. Huang. A Full Fuel-Cycle Analysis of Energy and Emissions Impacts of Transportation Fuels Produced from Natural Gas, Dec 1999.
- M.A. Weiss, J.B. Heywood, E.M. Drake, A. Schafer, and F.F. AuYeung. On the Road in 2020: A Life Cycle Analysis of New Automobile Technologies, Oct 2000.
- R.A. Witik, J. Payet, V. Michaud, C. Ludwig, and J.-A.E. Manson. Assessing the Life Cycle Costs and Environmental Performance of Light-weight Materials in Automobile Applications. *Composites: Part A*, 42:1694–1709, Aug 2011.
- X.O., X. Zhang, and S. Chang. Alternative Fuel Buses Currently in Use in China: Life-Cycle Fossil Energy Use, GHG Emissions and Policy Recommendations. *Energy Policy*, 38:406–418, 2010.
- Xylem. Environmental Product Declaration: Flygt 3153.181. <http://goo.gl/NMFfT>, 2009.
- M. Zackrisson, L. Avellan, and J. Orlenius. Life Cycle Assessment of Lithium-ion Batteries for Plug-in Hybrid Electric Vehicles - Critical Issues. *Journal of Cleaner Production*, 18:1519–1529, 2010.
- Yancheng Zhang and Chao-Yang Wang. Cycle-life Characterization of Automotive Lithium-Ion Batteries with LiNiO₂ Cathode. *Journal of the Electrochemical Society*, 156, May 2009.

Appendix A

Impact database

Table A.1: Impact database life cycle assessment data on products and services.

	Eco-costs	Carbon footprint	CED	ReCiPe
Material	(€/kg)	(kg CO ₂ equiv./kg)	(MJ/kg)	(Pt./kg)
Sand	0.00303	0.00677	0.0981	0.000696
Crushed concrete aggregate	0.00268	0.00822	0.127	0.000725
Bitumen	0.818	0.430	52.0	0.162
Asphalt	0.0435	0.0288	2.71	0.00879
Concrete	0.0277	0.133	0.939	0.00940
Steel (21% secondary)	0.595	1.61	23.3	0.170
Copper (primary)	4.14	1.85	34.5	0.462
Copper (44% secondary)	2.70	1.82	31.7	0.397
Aluminium (primary)	4.26	12.2	1.94	1.12
Aluminium (55% secondary)	2.12	6.26	100	0.583
Cast iron	0.172	0.646	10.8	0.0670
Styrene butadiene rubber (SBR)	0.991	2.00	87.3	0.310
Natural rubber	0.0977	0.158	2.47	0.0181
Carbon fibre	3.18	12.5	339	1.55
Epoxy resin	2.11	6.73	135	0.734
CFRE	2.84	10.7	273	1.29
Crude oil	0.766	0.232	49.3	0.140
Carbon black	0.340	1.89	99.2	0.349
Nylon	2.16	9.27	122	0.760
Li-ion battery (99 Wh/kg)	3.29	8.09	323	1.28
Electronics for control units	9.93	26.0	462	4.05
Leather	0.418	2.34	52.4	0.40
PUR flexible foam	1.68	4.96	111	0.514
Polyethylene, high density	1.06	1.93	77.3	0.278
Polycarbonate (PC)	2.05	7.78	107.5	0.674
Polyvinylchloride (PVC)	0.702	2.01	60.9	0.224
Recycling	(€/kg)	(kg CO ₂ equiv./kg)	(MJ/kg)	(Pt./kg)
Polycarbonate	-1.58	-5.32	-55.3	-0.465
Steel	-0.224	-0.865	-11.2	-0.0849
Copper	-1.82	-0.0317	-3.59	-0.0834
Aluminium	-1.75	-4.88	-76.4	-0.442
Natural rubber	-0.516	-2.77	-59.6	-0.236
Leather (co-firing)	-0.202	-1.08	-2.70	-0.0920
Polyvinylchloride	-0.484	-0.913	-38.0	-0.131
Process	(€/kg)	(kg CO ₂ equiv./kg)	(MJ/kg)	(Pt./kg)
Aluminium machining	15.4	82.9	1.78	7.04
Extrusion, plastics	0.109	0.422	7.15	0.0404
Injection moulding, plastics	0.264	1.33	28.7	0.131
Thermo forming, plastics	0.155	0.530	12.2	0.0573
Weaving	0.281	1.49	32.1	0.124
Rolling, steel	0.106	0.0514	0.814	0.00452
Deep drawing, steel	0.0650	0.316	3.82	0.0278
Energy	(€/MJ)	(kg CO ₂ equiv./MJ)	(MJ/MJ)	(Pt./MJ)
Electricity, UCTE mix	0.0264	0.141	3.04	0.120
Electricity, PV	0.00496	0.0167	1.37	0.0183
Electricity, wind	0.00263	0.00396	1.13	0.000408
Diesel incl. combustion	0.0296	0.0865	1.27	0.00747
Heat, natural gas	0.0284	0.0817	1.40	0.00738
Heat, industrial	0.0119	0.0637	1.37	0.00541
Transport	(€/tkm)	(kg CO ₂ equiv./tkm)	(MJ/tkm)	(Pt./tkm)
Truck + trailer 24 tons	3.90·10 ⁻⁶	8.06·10 ⁻⁶	0.000127	9.53·10 ⁻⁷
Container ship	0.0287	0.082	1.18	0.00729

Appendix B

Battery specifications

Table B.1: SE100AHA battery specifications.

Property	
Nominal capacity	100 Ah
Energy density	116 Wh/kg @ 0.1C
Float voltage	3.4 V
Inner resistance	<1.0 m Ω
Operating voltage	3.6 V (charge) 2.0 V (discharge)
Max. charge current	≤ 3 CA
Max. discharge current	≤ 4 CA (30s) ≤ 12 CA (5ms)
Standard charge/discharge current	0.3 CA
Cycle life	≥ 2000 times (80% DoD) ≥ 3000 times (70% DoD)
Max. transient temp. resistance shell	180 °C
Long term shell temp. resistance	≤ 130 °C
Operating temperature	0 °C ~ 55 °C (charge)
Low temperature discharge efficiency	$\geq 90\%$
Self-discharge rate	$\leq 3\%$ /month
Mass	3.1 kg \pm 0.1 kg

